

Low energy physics for the high energy physicist

Effective theories, holographic duality and all that

Angelo Esposito

Submitted in partial fulfillment of the
requirements for the degree of
Doctor of Philosophy
in the Graduate School of Arts and Sciences

COLUMBIA UNIVERSITY

2018

©2018
Angelo Esposito
All rights reserved

ABSTRACT

Low energy physics for the high energy physicist

Angelo Esposito

In this work we discuss the application of high energy theory methods to the study of condensed matter problems. We focus in particular on the effective field theory (EFT) approach and on the holographic duality. We show that, in certain contexts, both techniques present some relevant advantages with respect to more standard approaches. In particular, we will study holographic superfluids, and make explicit connection between the holographic picture and the EFT one. We also determine for the first time the gravity dual of a solid, and show that it undergoes a first order phase transition, a “holographic melting”. On a more phenomenological ground, we study the motion of vortex lines in a confined superfluid. Using a suitable EFT we successfully reproduce the experimental results, and perform a number of steps forward with respect to traditional methods. Finally, we also discuss possible exciting directions for the future of EFTs and condensed matter.

Contents

List of conventions	iii
Acknowledgements	iv
Introduction	1
1 An unconventional approach to condensed matter	5
1.1 To be or not to be (broken)	6
1.2 The eight states of matter	11
1.3 An EFT language for condensed matter: why bother?	21
1.4 Superfluids	23
1.5 Solids	26
2 The holographic duality	29
2.1 Weak coupling is strong coupling	30
2.2 Bulk fields and boundary operators	33
2.3 Which symmetry?	40
2.4 Finite temperature	42
2.5 Summary	44
3 Holographic superfluids	45
3.1 On the previous episodes	46

3.2	From bulk fields to boundary phonons	50
3.3	Summary	59
4	Holographic solids	61
4.1	Conformal solids and solids on a sphere	62
4.2	Meet the solidon	66
4.3	Phonons of the boundary theory	72
4.4	Melting the solidon	78
4.5	Summary	82
5	Vortex lines in superfluids	84
5.1	Vortices and their precession	85
5.2	One more EFT: vortex lines in superfluids	88
5.3	Trapping the superfluid	94
5.4	Vortex precession in 2D	98
5.5	Summary	105
Conclusion		107
Bibliography		110
Appendix A: From bulk equations to RG flow		121
Appendix B: Linear representations of the Euclidean group		123
Appendix C: How to go from the scalar to the 2-form and back		125
Appendix D: Relativistic corrections to the vortex action		126

List of conventions

QFT	Quantum Field Theory.
EFT	Effective Field Theory.
AdS	Anti-de Sitter spacetime.
Metric	We use the “mostly plus” convention for the spacetime metric. In particular, the Minkowski metric is $\eta_{\mu\nu} = \text{diag}(-, +, \dots, +)$.
M, N, \dots	We indicate with capital latin letters spacetime indices that run over all the coordinates of the bulk of AdS, i.e. $M, N, \dots = 1, \dots, d+1$.
μ, ν, \dots	We indicate with greek letters the spacetime indices that run over all the coordinates of the boundary theory, i.e. $\mu, \nu, \dots = 1, \dots, d$.
i, j, \dots	We indicate with small latin letters the indices that run over spatial coordinates, i.e. $i, j, \dots = 1, \dots, d-1$.

Acknowledgements

I am not sure whether these acknowledgments will be original or entertaining. I can however promise that they will be sincere.

In my (short) academic career I have been lucky enough to learn from the experience, understanding and passion of many giants. Hence, my first thank-yous go to my advisors, both the official and unofficial ones. Get ready, because I have several of them.

I am extremely grateful to Alberto Nicolis for taking me with him, despite my lack of experience in the field, and for sharing with me his rare abilities. The passion he has for new ideas and for physics in general is contagious, and if I managed to inherit only a fraction of it I know that I will be fine.

I would also like to thank Lam Hui. I am always amused by the variety of his understandings, and I am grateful for the patience he showed in teaching them to me. Moreover, teaching little children with him has been one of the most fun and enriching experiences of my years in New York.

A very special thanks also goes out to Antonello Polosa, for being with me since my very first day of research. I will never stop learning from his unconventional approach to physics and physicists. Most of all, thank you for pushing me towards this adventure. It was the right thing to do.

Lastly, I am deeply grateful to the youngest of my advisors: Riccardo Penco. His attitude towards physics is enlightening. Riccardo is patient and humble, despite

being one of the best scientists I have met. If there is a path that I would like to follow, that is his.

I would also like to really express my gratitude to Andrea Guerrieri, Danilo Latini, Matteo Lotito and Alessandro Pilloni, my scientific brothers. Every interaction with them allowed me to learn new things and improve myself as a physicist. Our nights together helped putting everything under the right perspective.

Science has a peculiar way of proceeding. Every contamination with other people, no matter how small, can surprisingly lead to new ideas. I am therefore grateful to all those people that shared even a bit of their knowledge with me (in strict alphabetical order): Erick Andrade, Niccolò Bigagli, Giuliano Chiriacò, Felix Clark, Brian Cole, Frederik Denef, Jeremy Dodd, Drew Edelberg, Sebastian Garcia-Saenz, Miklos Gyulassy, Geoff Iwata, Austin Joyce, Alex Kerelsky, Rafael Krichevsky, Giacomo Lovat, Rees McNally, Andrea Morales, Andrea Petri, Fulvio Piccinini, Rachel Rosen, Roman Scoccimarro, Evan Telford, Chiara Toldo, Claire Warner, Konrad Wenz, Sebastian Will and Bill Zajc.

Finally, none of this could have been possible without the continuous and unconditional love and support of my family: Mamma, Papà, Lella, Antonio, Michelangelo, Angelica, Riccardo, Andrea, Edoardo, Paolo, Federico, Tilli, Stefano, Luca E., Luca T., Ela, Melania, and many others. All of them showed me, beyond any rhetoric, that distance really does not matter.

This thesis goes to all the people I mentioned above, and to those that I mistakenly forgot.

Grazie.

*La sua forma è la mia forma,
la Roma di chi se ne va ma che tanto poi ritorna.*

Colle der Fomento — Il Cielo su Roma

Introduction

The regime of validity of high energy theory and the regime of existence of nonrelativistic matter could not seem more separated. The first one deals with phenomena at very high energy scales, with experiments that probe either the smallest constituents of matter or the largest scales known to us. On the other hand, the condensed matter world is characterized by low energy processes and by typical velocities that are much smaller than the speed of light. Experiments in this branch of physics aim at understanding the complicated behavior of collective, macroscopic systems, rather than discovering the fundamental bricks of our world.

Nevertheless, these two corners of physics recently found an unexpected common ground in the use of relativistic effective field theories (EFTs) for the description of several states of matter (fluids, solids, superfluids, and so on).

The basic idea behind this approach is surprisingly simple. To the best of our knowledge, the Poincaré invariance (rotations, spacetime translations and boosts) of fundamental interactions is a symmetry of our whole Universe, including the condensed matter world. Despite that, macroscopic systems like a solid, a fluid and many others manifestly violate it. It then follows that Poincaré symmetry must be *spontaneously* broken: the underlying theory is symmetric but the particular state under consideration is not.

It is very well known that the spontaneous breaking of a symmetry comes with some powerful consequences. As we will see, this is the starting point of our approach.

It will allow us to classify different states of matter solely in terms of their symmetry breaking pattern, as well as to determine the interactions of their low energy modes in a universal way, up to a few effective parameters.

But this will not be the end of our story. In the last two decades the high energy community devoted huge attentions towards a new, powerful tool: the so-called holographic principle (also known as AdS/CFT correspondence or gauge/gravity duality). Such a conjecture relates a gravitational theory on an asymptotic anti-de Sitter (AdS) spacetime to a (possibly) strongly coupled theory without gravity on the boundary of AdS. We will later explain how this correspondence allows to obtain physical results in a nonperturbative regime, which is hardly accessible with more traditional techniques.

For this reason, among many other applications, holography has been extensively employed to study different states of matter. In particular, this line of research took essentially two roads. On the one hand, one can search for the gravity dual of the systems observed so far, with the hope of understanding better their strong dynamics. On the other hand, given a gravity dual, one can investigate the corresponding boundary theory. In this way one might be able to identify new possible states of matter, and determine whether or not they can be realized by Nature.

In this thesis we employ both the tools presented above to investigate different systems. There will be two distinct goals. From a more formal viewpoint we will make explicit connection between the standard approach used in AdS/CFT and the low energy EFT formulation of the problem. This connection is rather crucial to understand known holographic systems as well as to identify new ones. On a more phenomenological ground, we will show how the EFT methods for condensed matter are now mature enough to become more than an interesting exercise for high energy physicists. We will show how they can be used as a powerful tool to describe real experimental data or probe novel phenomena.

This thesis is organized as follows. In Chapter 1 we give an introduction to the effective theory approach to condensed matter. We will classify several systems based on their symmetry breaking pattern, and present a detailed description of the EFT for superfluids and solids, which are very relevant for the present work. In Chapter 2 we instead present the holographic duality. In particular, we will build the relevant pieces of the holographic dictionary using concrete examples. Both these chapters serve as a quick review of the background material.

From Chapter 3 we start presenting novel results. We will discuss holographic superfluids and provide an analytical proof of their duality with a theory of scalar quantum electrodynamics (QED) on asymptotically AdS background. Beside being an interesting result, the technique used to give the proof will be the crucial ingredient of the analysis of Chapter 4. There we first write down the effective theory for solids on a sphere, and then determine the gravity dual of a solid. In the bulk of AdS this will be an $SO(d)$ magnetic monopole coupled to a scalar field in the fundamental representation. We also study the phase transition of our solution, exhibiting an example of holographic melting.

In Chapter 5 we instead switch gears considerably and focus on more phenomenological aspects. We introduce the effective theory for vortex lines in superfluids, and employ it to correctly reproduce the experimental results on vortex precession in ultra cold atom gases. Finally in the Conclusions we will discuss what have been achieved in this work, as well as some interesting work in progress and directions for the future.

It should be mentioned that, in order to keep the present thesis self-contained, some part of the author's work has been left out. This includes the study of the so called *exotic mesons*, i.e. experimentally observed resonances that do not fit the standard quark-antiquark picture. Such particles are likely composed by two quarks and two antiquarks, but their internal configuration is still unknown. The two main

models are the compact tetraquark (where the four constituents are tightly bound together inside the hadron) and the meson molecule (where two quark-antiquark pairs are separated in space and interact via residual strong forces). In particular, we have shown how the molecular interpretation is at odds with Monte Carlo simulations [1] as well as experimental data [2]. We have also discussed possible experimental signatures that could uniquely determine the nature of these particles [3, 4], and put forward a model based on the Feshbach resonance mechanism that aims at providing a unified picture of all the exotic mesons [5] (see also [6]). A broader picture of this puzzle has been presented in two review articles [6, 7].

Another work concerned the study of the effects of hadronization on initial state correlations in proton-nucleus collisions [8]. Although, as we showed, hadronization severely modifies the initial partonic angular distribution, its effects are surprisingly often neglected in theoretical studies.

Lastly, there is some ongoing work on the application of the so called *consistency relations* (see e.g. [9]) to the study of primordial nongaussianities [10]. The main idea is that, being consistency relations a nonperturbative statement, they could be applied to data on large scale structures at *all* scales. The dramatic increase in the available statistics might allow to measure primordial nongaussianities and hence constrain the available inflationary models.

An unconventional approach to condensed matter

All condensed matter systems¹ share one feature that makes them apparently incompatible with a Poincaré invariant formalism: they naturally single out a particular reference frame. Moreover, the states of matter that have been produced in the lab so far are all characterized by typical velocities (e.g. the speed of sound) that are much smaller than the speed of light. For this reason, the standard descriptions of such systems never invoke Poincaré symmetry as a guiding principle.

Nevertheless, as already mentioned in the Introduction, condensed matter systems emerge as particular symmetry breaking states of an underlying Poincaré invariant theory. Consider for example an ordinary solid. Its properties are essentially determined solely by electromagnetic interactions. These can generate, for example, a lat-

¹It should be noted that the term “condensed matter” is typically not used to refer to systems as, for example, ultra cold gases of atoms or molecules. Nevertheless, in our language, condensed matter is any state of matter that spontaneously breaks the Poincaré group and is isotropic and homogeneous at long distances. I will collect all these systems under the same umbrella. I hope the true experts in the field will find the compassion to forgive me.

tice structure which is in general neither symmetric under rotations nor translations. However, we know that the fundamental theory behind electromagnetism is quantum electrodynamics (QED), which is instead invariant under the whole Poincaré group. Therefore the solid under consideration emerges as a particular symmetry-violating state subject to fundamentally relativistic laws. This means that the Poincaré group is broken spontaneously.

In the EFT approach to this problem the spontaneous breaking of the Poincaré group is taken as the defining feature of a condensed matter system. In other words, we consider any state of matter as being defined by which symmetries it spontaneously breaks and which ones it instead preserves. As it will be clear soon, for every symmetry breaking pattern, the well known Goldstone theorem strongly constrains the possible interactions of the low energy modes of the systems. In particular, they will be much less general than what is admitted in a system with no underlying Poincaré invariance.

It should be pointed out that in this thesis we will only deal with the low energy bosonic excitations and we will not treat the case of fermionic ones. A large portion of the interesting phenomena observed experimentally are actually due to the latter ones. The approach presented here will not focus on these aspects.

1.1 To be or not to be (broken)

The allowed states of matter have been systematically classified in [11]. The authors studied the possible ways of breaking the Poincaré group, while still preserving spatial homogeneity, time-translational invariance and (although not necessary) isotropy².

The generators of the Poincaré group are those of spacetime translations, P_μ ,

²It is in principle conceptually straightforward, although tedious, to lift the requirement of isotropy. This would allow to describe, for example, systems with a discrete rotational symmetry. We will not consider these cases for simplicity.

rotations, J_i and boosts, K_i . We remind the reader that their Lie algebra is given by

$$\begin{aligned} [J_i, P_j] &= i\epsilon_{ijk}P^k, & [K_i, P_j] &= i\delta_{ij}P_0, & [K_i, P_0] &= -iP_i, \\ [J_i, J_j] &= i\epsilon_{ijk}J^k, & [J_i, K_j] &= i\epsilon_{ijk}K^k, & [K_i, K_j] &= -i\epsilon_{ijk}J^k. \end{aligned} \tag{1.1}$$

In addition to this spacetime Poincaré group we will also allow for some *internal* symmetries, whose generators commute with those presented above. As already mentioned, we also assume the existence of some unbroken spacetime translations and spatial rotations generators, \bar{P}_0 , \bar{P}_i and \bar{J}_i . These ensure that our system (at large enough distances) is homogeneous, isotropic and time-translational symmetric.

It is crucial to notice that the \bar{P} s and \bar{J} s need not to correspond to the same generators as the original Poincaré group, as long as they satisfy the algebra (1.1) among themselves. They can be a linear combination of the latter ones together with the generators of the internal symmetries. Indeed we classify condensed matter systems precisely on the basis of which of the unbroken generators presented above involve or not internal symmetries. It is however important to keep in mind that, as explained already, all condensed matter systems spontaneously break Lorentz boosts.

It is clear that one could always introduce additional internal symmetries, both broken and unbroken. This would realize the same symmetry breaking pattern but introduce additional Goldstone modes, that transform nonlinearly under the broken symmetries. In this work we will focus on those systems that present the minimum number of Goldstones. In particular, it turns out that only eight different states of matter are possible [11].

Counting the Goldstone bosons

Before going into the details of the different condensed matter systems it is important to comment on the number of Goldstone modes expected for each of them. Most of the readers will probably be familiar with the Poincaré invariant version of the Goldstone

theorem. In particular, in that context it is stated that given a certain symmetry group G broken to some subgroup H , the spectrum of the theory will present a massless mode (the Goldstone boson) for each broken generator of G (see e.g. [12]).

This is not true anymore when the set of broken generators includes spacetime ones. One famous example is that of a 2-dimensional brane in a 4-dimensional spacetime (e.g. a sheet in your office) [13]. The brane breaks four spacetime symmetries: translations and boosts perpendicular to it, as well as the two rotations that are not contained on its plane. Nevertheless, at low energies, the brane can be described solely in terms of its local position in the transverse direction, i.e. just one degree of freedom.

Where are the additional Goldstones hiding? The reason for the mismatch between the number of broken generators and the number of gapless modes is due to the fact that, when broken spacetime symmetries are involved, one can impose the so-called *inverse Higgs constraints* and remove some of the Goldstone modes in favor of the others [11, 13–16].

The criterion for when such constraints can be imposed is the following. Let us label with Q_a the broken generators of the group G , with \bar{P}_μ the unbroken spacetime translations and with T_A all the other unbroken generators. Whenever the commutator between the unbroken spacetime translations and one multiplet of broken generators Q_a contains another multiplet of broken generators Q'_a , i.e.

$$[\bar{P}_\mu, Q_a] = i f_{\mu a}{}^b Q'_b + \text{other generators}, \quad (1.2)$$

one can impose inverse Higgs constraints and express the Goldstones associated with Q_a in terms of derivatives of those associated with Q'_a .

Let us show it with a simple example [16, 17]. Consider a point particle moving in a $(1+1)$ -dimensional spacetime. In this case the Poincaré algebra has only three

generators, P_0 , P_1 and K , associated with the time translation, the spatial translation and the boost. Their algebra is simply

$$[K, P_0] = -iP_1, \quad [K, P_1] = -iP_0, \quad [P_0, P_1] = 0. \quad (1.3)$$

The position of the particle can be described as a field, $x(t)$, in a (0+1)-dimensional spacetime. In this case P_0 generates a spacetime symmetry while P_1 has to be regarded as the generator of an internal shift symmetry, $x(t) \rightarrow x(t) + a$. Let us consider the background where the particle is at rest, say at the origin. This means

$$\langle x(t) \rangle = 0. \quad (1.4)$$

This vev clearly breaks the spatial translation and the boost (the particle is here and not there and its velocity is zero and not something else), but leaves the time translation unbroken. In the language described above $\bar{P}_0 = P_0$.

The most general element of the group can be parametrized as³

$$g = e^{itP_0+ix(t)P_1} e^{i\omega(t)K}, \quad (1.5)$$

where $x(t)$ and $\omega(t)$ play the role of “Goldstone bosons”. One might therefore expect for both of them to appear in the action. However, it is well known that the action for a point particle only involves the first one, i.e.

$$S_{\text{p.p.}} = -m \int dt \sqrt{1 - \left(\frac{dx}{dt} \right)^2}. \quad (1.6)$$

Indeed, since $[K, \bar{P}_0] \supset P_1$, we can impose an inverse Higgs constraint. To do that

³Note that it is actually rather crucial to parametrize g this way. An alternative parametrization could have been $g = e^{itP_0+ix(t)P_1+i\omega(t)K}$, in which case imposing the inverse Higgs constraint becomes much less trivial.

one has to write the so-called Maurer-Cartan form, $-ig^{-1}dg$. In this particular case we have

$$\begin{aligned}
-ig^{-1}dg &= e^{-i\omega K} P_0 e^{i\omega K} dt + e^{-i\omega K} P_1 e^{i\omega K} dx + K d\omega \\
&= (\cosh \omega dt - \sinh \omega dx) P_0 + (\cosh \omega dx - \sinh \omega dt) P_1 + d\omega K \\
&\equiv dt \mathcal{L} (P_0 + \mathcal{D}_0 x P_1 + \mathcal{D}_0 \omega K).
\end{aligned} \tag{1.7}$$

The inverse Higgs constraint corresponds to finding a non-trivial solution to the equation $\mathcal{D}_0 x = 0$. In particular this is given by

$$\omega(t) = \tanh^{-1} \left(\frac{dx}{dt} \right). \tag{1.8}$$

The equation above indeed allows to eliminate $\omega(t)$ in favor of $x(t)$. Moreover, it is easy to show that the other constraint, $\mathcal{D}_0 \omega = 0$, simply corresponds to the equation of motion of a relativistic particle, and that \mathcal{L} corresponds to its lagrangian.

It should be noted that the interpretation of the inverse Higgs constraints is still somewhat obscure. In particular, it can be shown that in certain circumstances where some redundancy is present (see Section 1.4 for an example) they correspond to a gauge fixing [13]. On the other hand, in other instances they correspond to integrating out gapped Goldstones [13, 18, 19].

In general, it is not mandatory to impose the inverse Higgs constraints. However, in those instances where the gap of the gapped Goldstones is comparable to the strong coupling scale, one would need to also include all the other gapped modes present in the theory. If these are not known, then the inverse Higgs constraints must be imposed for consistency with the low energy expansion.

1.2 The eight states of matter

In this section we list the possible symmetry breaking patterns of the Poincaré group and briefly comment on the properties of the associated condensed matter systems. Six of these states will be realizable solely postulating the presence of internal symmetries, while two will require additional symmetries, whose generators do not commute with those of the Poincaré group. In all cases, we will represent the additional generators as Q . The “eightfold way” of condensed matter is given by the following states.

Type-I framid

$$\bar{\mathbf{P}}_0 = \mathbf{P}_0, \quad \bar{\mathbf{P}}_i = \mathbf{P}_i, \quad \bar{\mathbf{J}}_i = \mathbf{J}_i$$

This is the simplest possible scenario, the one where the only broken symmetries are the three Lorentz boosts. We will call this system a *type-I framid*. The minimal way to implement this symmetry breaking pattern is through a single vector field that acquires a vacuum expectation value (vev) along its time component, $\langle A_\mu(x) \rangle = \delta_\mu^0$.

As usual, the Goldstone bosons can be parametrized as the coefficients of a broken symmetry acting on the vacuum [12]. We can then write

$$A_\mu(x) = \left(e^{i\vec{\eta}(x) \cdot \vec{K}} \right)_\mu^\nu \langle A_\nu(x) \rangle, \quad (1.9)$$

where the K s are taken in the suitable representation, and the associated Goldstone modes, $\vec{\eta}$, are called *framons*.

Note that a framid is an extremely peculiar system. Since boosts are the only broken symmetries, it cannot be rotated nor translated. The language itself of “volume element” is absent and one can only talk about the local velocity of the system. The framons correspond to fluctuations of this local velocity. Surprisingly, even though

they represent the cheapest way of breaking the Poincaré group, framids do not seem to be realized by Nature.

Another peculiarity is that the infinitely many interactions of the framons are, at lowest order in derivatives, completely determined solely in terms of their speeds [11]. Indeed, the most general lagrangian for A_μ that is Poincaré-invariant, compatible with $A_\mu A^\mu = -1$ and with at most two derivatives is

$$\mathcal{L} = -\frac{M^2}{2} \left\{ (c_L^2 - c_T^2) (\partial_\mu A^\mu)^2 + c_T^2 (\partial_\mu A_\nu)^2 + (c_T^2 - 1) (A^\rho \partial_\rho A_\mu)^2 \right\}, \quad (1.10)$$

where M is some overall mass scale and c_L and c_T are the longitudinal and transverse speeds of the framons. Indeed, given the parametrization (1.9), the action above contains all the possible interactions for the $\vec{\eta}$ field.

Type-I superfluid

$$\bar{P}_0 = P_0 - \mu Q, \quad \bar{P}_i = P_i, \quad \bar{J}_i = J_i$$

In this case, the operator Q is simply the conserved charge associated with an internal $U(1)$ symmetry. This is the symmetry breaking pattern corresponding to a *type-I superfluid*, as we will discuss more in detail in Section 1.4. The number of broken generators here is four, i.e. time translations and three boosts. However, it is well known that the low energy dynamics of a superfluid can be described by only one Goldstone mode, the superfluid phonon [20–22]. Indeed from the algebra (1.1) we find that $[K_i, \bar{P}_j] = i\delta_{ij}(\bar{P}_0 + \mu Q)$, which indicates that there are three available inverse Higgs constraints.

Indeed the simplest realization of such a pattern is through a single, real scalar field whose vev is proportional to time, $\langle \phi(x) \rangle = \mu t$, which clearly breaks both time translations and boosts. To recover time-translational invariance one postulates a shift symmetry, $\phi \rightarrow \phi + a$, such that a linear combination of time translations and shifts

leaves the vev unaltered. The $U(1)$ symmetry generated by Q acts nonlinearly on ϕ .

Very similarly to what we have done for the framid, the Goldstone mode can be written as the (spacetime dependent) parameter of the symmetry under consideration, i.e. $\phi(x) = \mu(t + \pi(x))$. Moreover, the physical interpretation of the parameter μ is that of a chemical potential.

Type-I galileid

$$\bar{P}_0 = P_0, \quad \bar{P}_i = P_i - \beta Q_i, \quad \bar{J}_i = J_i$$

For reasons that will soon be clear such a system is dubbed *type-I galileid*. The unbroken generators must follow the same algebra as in Eq. (1.1), i.e. it must be $[\bar{J}_i, \bar{P}_j] = i\epsilon_{ijk}\bar{P}^k$. From this it follows that the Q_i 's must obey the following commutation relation

$$[J_i, Q_j] = i\epsilon_{ijk}Q^k, \quad (1.11)$$

and hence they cannot be the generators of an internal symmetry, since they do not commute with the original Poincaré group.

The field theory implementation of a type-I galileid is very non trivial and apparently plagued by pathologies. One possibility is that of realizing the symmetry breaking pattern via a reducible representation of the Lorentz group involving a scalar field φ and a vector field B_μ , that transform under the action of Q_i as

$$\varphi \rightarrow \varphi + 2b^j B_j, \quad (1.12a)$$

$$B_i \rightarrow B_i + b^j(\partial_i B_j + \partial_j B_i) - \frac{1}{2}b^j\partial_j\partial_i\varphi, \quad (1.12b)$$

and with a background given by

$$\langle \varphi(x) \rangle = \beta |\vec{x}|^2 \quad \text{and} \quad \langle B_i(x) \rangle = x_i. \quad (1.13)$$

A system like this one breaks six generators but also presents three inverse Higgs constraints since $[K_i, \bar{P}_0] = i(\bar{P}_i + \beta Q_i)$. Hence it will feature three independent Goldstone modes. Nevertheless, one can show that it is impossible to write a standard kinetic term for the fluctuations, and that therefore the system must come with ghost instabilities [11].

To find a way out of this issue one can modify the algebra by introducing an additional generator, D , that satisfies the following commutation relations:

$$[Q_\mu, P_\nu] = 2i\eta_{\mu\nu}D. \quad (1.14)$$

Here we have defined the four-vector $Q_\mu = (Q, Q_i)$, anticipating what will be needed to describe a type-II galileid. In the case of type-I galileids there is no Q . This is the algebra of galileon theories [23], hence the name of our system. Such theories only involve a single scalar degree of freedom, $\phi(x)$, that enjoys a generalized shift symmetry given by

$$\phi \rightarrow \phi + c + b_\mu x^\mu, \quad (1.15)$$

where the shift c is generated by D , while $b_\mu x^\mu$ by Q_μ .

For our type-I we are after an expectation value that only breaks spatial translations, while preserving rotations and time translations. This is given by

$$\langle \phi(x) \rangle = \frac{1}{2}\beta |\vec{x}|^2, \quad (1.16)$$

where β is a constant free parameter. Since we can describe our symmetry breaking pattern through a single scalar, its fluctuation will correspond to the single Goldstone mode present in the system.

Although a theory like this one is free of instabilities, it still does not satisfy our requirements. In fact, the stress energy tensor can be found to be $\langle T_{\mu\nu}(x) \rangle \sim x^2$ [11], which is not translationally invariant.

Type-II framid

$$\bar{P}_0 = P_0, \quad \bar{P}_i = P_i, \quad \bar{J}_i = J_i + \tilde{Q}_i$$

Similarly as before, requiring that $[\bar{J}_i, \bar{J}_j] = i\epsilon_{ijk}\bar{J}^k$ implies

$$[\tilde{Q}_i, \tilde{Q}_j] = i\epsilon_{ijk}\tilde{Q}^k. \quad (1.17)$$

This means that the \tilde{Q}_i 's are the generators of an internal $SO(3)$ symmetry.

Indeed, its minimal implementation is through a triplet of vector fields, with a vev given by $\langle A_\mu^a(x) \rangle = \delta_\mu^a$, with $a = 1, 2, 3$. Since there are no inverse Higgs constraints and we are breaking six generators (boosts and rotations) we expect an equal number of Goldstone modes. Indeed, the corresponding framons and phonons can be parametrized by

$$A_\mu^a(x) = \left(e^{i\vec{\eta}(x) \cdot \vec{K}} \right)_\mu^\nu \left(e^{i\vec{\pi}(x) \cdot \vec{Q}} \right)_b^a \langle A_\nu^b(x) \rangle. \quad (1.18)$$

Since this implementation resembles closely that of a type-I framid, we refer to this system as *type-II framid*.

Type-II galileid

$$\bar{P}_0 = P_0 - \alpha Q, \quad \bar{P}_i = P_i - \beta Q_i, \quad \bar{J}_i = J_i$$

Similarly to what happens for the type-I galileid, the commutation relations between the unbroken spacetime generators imply that the Q_i 's transform as a vector under rotations (see Eq. (1.11)) and hence they cannot be generators of an internal symmetry as well. We can therefore dub this system a *type-II galileid*.

To implement this symmetry breaking pattern is slightly less cumbersome than for a type-I galileid. In fact we can introduce a simple vector field, $C_\mu(x)$, that shifts under the action of the Q_μ 's as $C_\mu \rightarrow C_\mu + c_\mu$, and acquires the following vev:

$$\langle C_\mu(x) \rangle = \alpha t \delta_\mu^0 + \beta x_i \delta_\mu^i. \quad (1.19)$$

The number of broken generators is seven but we can impose four inverse Higgs constraints. Indeed, it is easy to prove that

$$[K_i, \bar{P}_0] = -i\bar{P}_i + i(\alpha + \beta)Q_i, \quad (1.20a)$$

$$[K_i, \bar{P}_j] = i\delta_{ij}\bar{P}_0 + i\delta_{ij}(\alpha - \beta)Q, \quad (1.20b)$$

where we used the fact that Q_μ transforms as a four vector. Nevertheless, just like before, this system also presents pathologies. In particular, it can be seen that if the Goldstone associated to P_0 is not ghost-like then the ones associated with P_i suffer from gradient instabilities, and viceversa [11].

Introducing again the generator D as in Eq. (1.14), we can realize the symmetry breaking pattern also in terms of a galileon field, but now with a vacuum expectation value given by

$$\langle \phi(x) \rangle = \frac{1}{2}(\beta|\vec{x}|^2 - \alpha t^2). \quad (1.21)$$

However, this state as well features a nonhomogeneous stress energy tensor.

Type-II superfluid

$$\bar{P}_0 = P_0 - \mu Q, \quad \bar{P}_i = P_i, \quad \bar{J}_i = J_i + \tilde{Q}_i$$

Just like in the case of type-II framids, the \tilde{Q} s must be the generators of an internal $SO(3)$ symmetry. Since they commute with Q , the simplest implementation of this symmetry is via an $SO(3) \times U(1)$ group. Given that $[\bar{P}_i, K_j] = -i\delta_{ij}(\bar{P}_0 + \mu Q)$, we can impose three inverse Higgs constraints and reduce the number of Goldstone modes to four. This is a so called *type-II superfluid*.

Its nonrelativistic version is nothing but the B -phase of superfluid He-3 [24]. Indeed He-3 has three degrees of freedom: atomic spin and orbital angular momentum, as well as the phase of its order parameter. The broken phase associated with the $U(1)$ subgroup is just like that of an ordinary type-I superfluid. However, rotations in the spin and orbital spaces are both broken but a linear combination of them is preserved⁴. Since in a nonrelativistic system the spin can be thought of as an internal $SO(3)$ degree of freedom, the structure just described indeed corresponds to a type-II superfluid.

A relativistic realization of this symmetry breaking pattern is presented in [18], via a triplet of vector fields acquiring the following vev:

$$\langle A_\mu^a(x) \rangle = e^{i\mu t} \delta_\mu^a, \quad (1.22)$$

where a is an internal $SO(3)$ index. The interesting property of this field theory is that this is one of the cases where the application of inverse Higgs constraints cannot be regarded as a gauge fixing but it corresponds to integrating out massive

⁴A nice visual representation of this symmetry breaking pattern is given in [24]. In particular, one can imagine the B -phase as a state where the orientations of spins and orbital momenta are randomly distributed but always with a fixed relative angle. Separate rotations of them clearly change the state of the system but a simultaneous rotation that preserves the relative orientation does not. In our language this is exactly the breaking of two separate $SO(3)$ groups down to the diagonal subgroup.

Goldstones [18].

Solid

$$\bar{P}_0 = P_0, \quad \bar{P}_i = P_i - \alpha Q_i, \quad \bar{J}_i = J_i - \tilde{Q}_i$$

It is very easy to show that the Q s and \tilde{Q} s must be the generators of an internal $ISO(3)$ group, i.e. the three-dimensional Euclidean group. Indeed their algebra is given by

$$[Q_i, Q_j] = 0, \quad [\tilde{Q}_i, \tilde{Q}_j] = -i\epsilon_{ijk}\tilde{Q}^k, \quad [\tilde{Q}_i, Q_j] = -i\epsilon_{ijk}Q^k, \quad (1.23)$$

with Q_i being the generator of translations and \tilde{Q}_i (minus) those of rotations. In this case we have a total of nine broken generators but also six inverse Higgs constraints, given that $[\bar{P}_0, K_i] = i(\bar{P}_i + \alpha Q_i)$ and $[\bar{P}_i, \tilde{Q}_j] = -i\alpha\epsilon_{ijk}Q^k$. It then follows that the system will be described, at low energies, by just a set of three Goldstone modes.

The simplest implementation of this symmetry breaking pattern is through a triplet of scalar fields $\phi^I(x)$ (with $I = 1, 2, 3$). These fields will shift and rotate under the internal $ISO(3)$ group, i.e.

$$\phi^I \rightarrow \phi^I + R^I_J \phi^J + a^I. \quad (1.24)$$

Their vacuum expectation value is instead given by $\langle \phi^I(x) \rangle = \alpha x^I$, and the Goldstone modes can be parametrized as $\phi^I(x) = \alpha(x^I + \pi^I(x))$.

From the properties above one easily realizes that such a system corresponds to a *solid*. In particular, the fields $\phi^I(x)$ correspond to nothing but the well known comoving coordinates, and the $\pi^I(x)$ are the acoustic phonons. The constant α is a free parameter of the theory and it represents the stretchability and compressibility of the solid. More details on this construction will be given in Section 1.5.

Interestingly, in this language solids and *fluids* are actually described by the same symmetry breaking pattern [25–27]. In particular, for a fluid one can actually postulate an infinitely larger internal symmetry for the scalar fields. This is given by

$$\phi^I \rightarrow \xi^I(\phi), \quad \text{with} \quad \det \frac{\partial \xi(\phi)}{\partial \phi^I} = 1, \quad (1.25)$$

which is the set of all possible volume preserving diffeomorphism (diffs). Physically this corresponds to the fact that, while for a solid we are only allowed to translate or rotate the volume elements, for a fluid we can also deform them, as long as their volume remains constant. It follows that, in our language, a fluid is nothing but a very special type of solid, one with an enhanced symmetry.

Moreover, it turns out that in this case there is an infinite number of inverse Higgs constraints that still allow to retain just three Goldstone modes [11]. Nevertheless, only the longitudinal fluid phonon will feature wave solutions as expected.

Lastly, given that framids and solids exhibit the same number of Goldstone modes one might wonder whether they are actually the same system, with the above implementation simply being more redundant. It should already be evident that this is not the case given the universality of framon interactions described by the lagrangian (1.10). Nevertheless, one can also compute any physical observable and check if the two cases match. It can be shown that the $2 \rightarrow 2$ scattering amplitude for framons and phonons at low momenta scales with energy respectively as E^2 and E^4 [11], hence showing that framids are physically distinct from solids and fluids.

Supersolid

$$\bar{\mathbf{P}}_0 = \mathbf{P}_0 - \mu \mathbf{Q}, \quad \bar{\mathbf{P}}_i = \mathbf{P}_i - \alpha \mathbf{Q}_i, \quad \bar{\mathbf{J}}_i = \mathbf{J}_i - \tilde{\mathbf{Q}}_i$$

In this last case it is easy to show that the Q_i 's and \tilde{Q}_i 's obey the same algebra as in Eq. (1.23), while Q commutes with all the generators. The additional internal group

will hence be $ISO(3) \times U(1)$. This symmetry breaking pattern features ten broken generators but also six inverse Higgs constraints (the same as in the case of a solid). It follows that we expect a total of four Goldstone modes.

The symmetry breaking pattern presented above is that of a *supersolid* [28], whose experimental observation was made feasible only recently [29, 30]. Indeed a simple field theory implementation of such a system is essentially a combination of that for a superfluid and that for a solid, i.e. introducing four scalars, $\psi(x)$ and $\phi^I(x)$, such that

$$\langle \psi(x) \rangle = \mu t \quad \text{and} \quad \langle \phi^I(x) \rangle = \alpha x^I. \quad (1.26)$$

The ψ field transforms under the $U(1)$ but it is a singlet under the $ISO(3)$ group, while the opposite is true for the ϕ^I field. Fluctuations around this background parametrize the four Goldstones.

Summary

In Table 1.1 we summarize the scheme presented in this section. In particular, we have presented the eight possible states of matter, classified based on which of the unbroken generators, \bar{P}_0 , \bar{P}_i and \bar{J}_i , are different from the original spacetime ones. In other words, we distinguish different states of matter depending on whether or not they need additional internal symmetries to recover spacetime isotropy and homogeneity at long distances. We also limited our analysis to those systems that feature the minimum number of Goldstone modes.

System	Modified generators			N_G	Internal symmetries	Extra spacetime symmetries
	P_0	P_i	J_i			
type-I framid				3		
type-I superfluid	✓			1	$U(1)$	
type-I galileid		✓		1		$\text{Gal}(3 + 1, 1)$
type-II framid			✓	6	$SO(3)$	
type-II galileid	✓	✓		1		$\text{Gal}(3 + 1, 1)$
type-II superfluid	✓		✓	4	$SO(3) \times U(1)$	
solid		✓	✓	3	$ISO(3)$	
supersolid	✓	✓	✓	4	$ISO(3) \times U(1)$	

Table 1.1: Summary of the classification of condensed matter systems. N_G represents the minimal number of Goldstone bosons. For the definition of the galileon group, $\text{Gal}(3 + 1, 1)$, see for example [31].

1.3 An EFT language for condensed matter: why bother?

As we will see in the next two sections, a classification of the states of matter in terms of their symmetry breaking pattern allows to describe them with relativistic, Poincaré invariant, low energy effective theories. Although unusual, this approach presents some very relevant advantages [32]. Some of them are:

- Our system is described by a local action, which can be written in a Lorentz invariant way almost trivially, without having to rely on any smart trick to implement Poincaré invariance. Once the action is given, questions as, for example, the derivation of the hydrodynamical equations or the calculation of density and pressure become straightforward.
- The degrees of freedom are simple bosonic fields that describe the low energy Goldstone modes. Their interactions are not engineered ad-hoc to reproduce the observed phenomenology, but are forced by the symmetries of the system.

- Relativistic field theories are easily treated in perturbation theory. In particular, our low energy EFTs are systematically organized in a derivative expansion. Once this is done it is possible to borrow a vast set of tools (Feynman diagrams, amplitude analysis, etc.) that have been developed over several decades of particle physics.
- This approach does not require thermodynamics⁵. It is a priori possible to never mention thermodynamical quantities and simply carry on the EFT procedure all the way to the final computation of physical observables. The intermediate steps will never invoke thermodynamical principles, but just fields, couplings, and so on. A dictionary that translates our language to thermodynamics is not necessary, but it is useful for the sake of comparison with experiments and to constrain the free parameters of the theory.

The above considerations explain why the EFT approach can be a powerful instrument to add to the theorist’s toolbox. Of course, it is not the Holy Grail of condensed matter and it comes with some drawbacks. Most notably:

- Being a low energy EFT it is valid in the regime where the Goldstone modes are weakly coupled and it breaks down at some ultraviolet (UV) scale. In particular, this means that this approach is unable to move away from perturbation theory. Phenomena that are intrinsically nonlinear and/or due to small distance physics (e.g. the formation of defects or phase transitions) are therefore outside the reach of these methods.
- As any EFT it is simply formulated in terms of few effective parameters. However, these parameters cannot be deduced from the EFT alone. They must be taken either as an input coming from some microscopic theory or fitted from experimental data.

⁵Here typically the “booing” starts.

Lastly, it should be noted that the EFT formulation does not necessarily requires relativistic invariance, since one could as well impose Galilean symmetry. Nevertheless, we see no reason not to require the full Poincaré invariance, and therefore write a theory for relativistic matter. The nonrelativistic limit can in fact be taken at any step of the process. This is done by formally taking the limit of large speed of light, $c \rightarrow \infty$ (see e.g. Chapter 5).

1.4 Superfluids

Let us now give a more detailed presentation of the effective theories for superfluids and solids, which will be the main focus of this thesis. We will also extend the treatment to a generic d -dimensional spacetime, to pave the road for the holographic analysis done in Chapter 3.

As already mentioned, a superfluid is a finite density system that carries a spontaneously broken $U(1)$ charge. The prototypical (weakly coupled) example is that of a free Bose-Einstein condensate. Such a system is clearly at finite density and, below the critical temperature, its ground state has a macroscopical occupation number. In field theory language this means that the ground state spontaneously breaks the $U(1)$ symmetry associated to number density via the vev $\langle 0 | \hat{N}_{\vec{k}=0} | 0 \rangle \neq 0$, where $\hat{N}_{\vec{k}}$ is the number operator for particles with momentum \vec{k} .

The simplest implementation of the desired symmetry breaking pattern is arguably the one involving a single real scalar field ϕ , that acquires a vev $\langle \phi(x) \rangle = \mu t$, and shifts under the $U(1)$ symmetry, $\phi \rightarrow \phi + a$ [21]. The superfluid phonon corresponds to small fluctuations around this background, $\phi(x) = \mu(t + \pi(x))$.

We therefore need to write down the most general action that is (i) Poincaré invariant, (ii) shift invariant and (iii) lowest order in energy. The most general low

energy action is easily found to be

$$S = \int d^d x P(X), \quad \text{with} \quad X = -\partial_\mu \phi \partial^\mu \phi. \quad (1.27)$$

The function $P(X)$ is a priori completely general. We will see that it can be determined if the equation of state of the superfluid is given. The quantity X is the square of the *local* chemical potential.

The Noether current associated with the $U(1)$ shift can be easily found to be

$$j^\mu = \frac{\partial P}{\partial(\partial_\mu \phi)} = -2P_X(X)\partial^\mu \phi. \quad (1.28)$$

With P_X we denote the derivative of the P with respect to X . If now we recall that j^0 is nothing but the number density, we see that the vev $\langle \phi(x) \rangle = \mu t$ is indeed the time dependence needed to implement a nonzero constant density on the ground state.

The stress energy tensor is instead given by

$$T_{\mu\nu} = -\frac{2}{\sqrt{-g}} \frac{\delta S}{\delta g^{\mu\nu}} \bigg|_{g=\eta} = 2P_X(X)\partial_\mu \phi \partial_\nu \phi + \eta_{\mu\nu}P(X). \quad (1.29)$$

On the equilibrium configuration it reduces to

$$\langle T_{\mu\nu} \rangle = 2XP_X\delta_\mu^0\delta_\nu^0 + \eta_{\mu\nu}P, \quad (1.30)$$

where P and its derivatives are now computed on the background, $X = \mu^2$. Since the stress tensor is related to the energy density and pressure of the system, the above equations allow to determine the lagrangian of our theory once the equation of state of the superfluid is known.

This is a good moment to give an explicit example of the application of inverse Higgs constraints [13]. Given the present ground state, the *physical* fluctuation of

the field is parametrized via the action of the broken generators (i.e. the $U(1)$ charge and boosts) as

$$\delta\phi(x) = i \left(\pi(x)Q + \vec{\eta}(x) \cdot \vec{K} \right) \langle \phi \rangle = i \left(\pi(x) \frac{P_0 - \bar{P}_0}{\mu} + \vec{\eta}(x) \cdot \vec{K} \right) \langle \phi \rangle. \quad (1.31)$$

Recall that the action of the generators is given by $P_0 = i\partial_0$ and $K_i = i(t\partial_i - x_i\partial_0)$, and that \bar{P}_0 is unbroken. Therefore

$$\delta\phi(x) = \left(\frac{\pi(x)}{\mu} - \vec{\eta} \cdot \vec{x} \right) \langle \dot{\phi} \rangle. \quad (1.32)$$

This parametrization features a gauge redundancy. Indeed if $\vec{\eta}(x) \rightarrow \vec{\eta}(x) + \vec{\epsilon}(x)$ and $\pi(x) \rightarrow \pi(x) + \mu \vec{x} \cdot \vec{\epsilon}(x)$, the above fluctuation remains unchanged. The three inverse Higgs constraints available in this context are found to be

$$\mathcal{D}_i \pi = \partial_i \pi - \mu \eta_i = 0. \quad (1.33)$$

They allow to express the framons in terms of derivatives of the phonon, and indeed they correspond to picking a particular gauge.

Let us now resume our general discussion. To study the behavior of the superfluid phonon one can expand the action (1.27) in small fluctuations. To illustrate the concept we will present it here up to cubic order in the Goldstone modes. In particular, one gets

$$S^{(3)} = (X P_X + 2X^2 P_{XX}) \int d^d x \left\{ \dot{\pi}^2 - c_s^2 (\vec{\nabla} \pi)^2 + g_3 \dot{\pi} (\vec{\nabla} \pi)^2 - \tilde{g}_3 \dot{\pi}^3 \right\}. \quad (1.34)$$

The speed of sound and the cubic couplings are given in terms of derivatives of the

lagrangian computed at equilibrium. In particular

$$c_s^2 = \frac{P_X}{P_X + 2XP_{XX}}, \quad g_3 = \frac{2XP_{XX}}{P_X} c_s^2, \quad \tilde{g}_3 = 2 \frac{XP_{XX} - \frac{2}{3}X^2P_{XXX}}{P_X} c_s^2. \quad (1.35)$$

Again, either the equation of state is known or these couplings must be extracted from data.

Finally, the effective theory presented above describes a zero temperature superfluid, for which a single phonon is present. At finite temperature, superfluids can be well described by the so called *two-fluid model* [33]. In that case, the system is seen as a superposition of a superfluid component and a normal fluid one, hence presenting also the phonons associated with the latter one. The EFT for relativistic superfluids at finite temperature has been written down in [32].

1.5 Solids

Let us now focus on the EFT for solids and fluids. In a d -dimensional spacetime the internal symmetry group is $ISO(d - 1)$ and the solid is described by $d - 1$ comoving coordinates that transform under the symmetry group as

$$\phi^I \rightarrow \phi^I + R^I_J \phi^J + a^I, \quad (1.36)$$

where $I, J = 1, 2, \dots, d - 1$. Their vev is instead given by $\langle \phi^I(x) \rangle = \alpha x^I$.

To lowest order in derivatives, the only object that is both Poincaré and shift invariant is the matrix $B^{IJ} = \partial_\mu \phi^I \partial^\mu \phi^J$. We now need to construct $SO(d - 1)$ invariants. For a $(d - 1) \times (d - 1)$ symmetric matrix the independent invariants are given by $\text{tr}B$, $\text{tr}(B^2)$, and so on, up to $\text{tr}(B^{d-1})$. For future convenience we decide to

collect them in the following way:

$$X = \text{tr}B, \quad \text{and} \quad Y_n = \frac{\text{tr}(B^n)}{X^n}, \quad (1.37)$$

so that X is the only invariant that keeps information about α . The most general low energy action for a solid is then given by

$$S = \int d^d x F(X, Y_2, \dots, Y_{d-1}), \quad (1.38)$$

where again F is a priori generic but it can be related to the equation of state of the solid. The stress energy tensor is found to be

$$T_{\mu\nu} = -2 \frac{\partial F}{\partial B^{IJ}} \partial_\mu \phi^I \partial_\nu \phi^J + \eta_{\mu\nu} F. \quad (1.39)$$

The solid phonons are parametrized as $\phi^I(x) = \alpha(x^I + \pi^I(x))$. One can again expand in small fluctuations to obtain

$$S^{(2)} = -\frac{XF_X}{d-1} \int d^d x \left\{ \dot{\vec{\pi}}^2 - c_L^2 (\partial_I \pi_L^J)^2 - c_T^2 (\partial_I \pi_T^J)^2 \right\}, \quad (1.40)$$

where now we truncated the expansion at quadratic order in the phonon fields since the interactions are rather cumbersome. We have also split the phonons in longitudinal and transverse modes. Their definition in more than three spatial dimensions is actually easier in momentum space, where they are such that $\vec{\pi}_L(\vec{k}) \propto \vec{k}$ and $\vec{\pi}_T(\vec{k}) \perp \vec{k}$. Their sounds speeds are again given in terms of background quantities:

$$c_T^2 = 1 + \frac{d-1}{XF_X} \sum_{n=2}^{d-1} \frac{\partial F}{\partial Y_n} \frac{n(n-1)}{(d-1)^n}, \quad (1.41a)$$

$$c_L^2 = 1 + \frac{2F_{XX}X^2}{(d-1)XF_X} + \frac{2(d-2)}{XF_X} \sum_{n=2}^{d-1} \frac{\partial F}{\partial Y_n} \frac{n(n-1)}{(d-1)^n}. \quad (1.41b)$$

Let us close this section by commenting on the case of a fluid. In this instance, the action needs to be invariant under all volume preserving diffs. The only possible invariant is the determinant of B , which is a very specific combination of the $d - 1$ invariants of $SO(d - 1)$. For example, in $d = 4$ and $d = 5$ we have

$$\det_4 B = \frac{1}{3!} X^3 (1 - 3Y_2 + 2Y_3), \quad (1.42a)$$

$$\det_5 B = \frac{1}{4!} X^4 (1 - 6Y_2 + 8Y_3 + 3Y_2^2 - 6Y_4). \quad (1.42b)$$

The action of a fluid is therefore much less generic than that of a solid:

$$S_{\text{fluid}} = \int d^d x F(\det B). \quad (1.43)$$

It follows that in our language a fluid is nothing but a very “tuned” solid.

The holographic duality

In 1997-98 a series of papers [34–36] had a tremendous impact on many branches of physics, both from a scientific and a sociological viewpoint (see e.g. Figure 2.1). The original papers conjectured the duality between the large N limit of $\mathcal{N} = 4$ super Yang-Mills theory in 3+1 dimensions and an $\text{AdS}_5 \times S^5$ spacetime.

This conjecture has been subject of study and improvements for the past two decades. Nowadays, it could be roughly stated as follows

$$\begin{array}{c} \text{Strongly coupled } d\text{-dimensional QFT} \\ \uparrow \\ \text{Gravitational theory in } (d+1)\text{-dimensional asymptotically AdS spacetime} \end{array}$$

This is commonly referred as the *holographic duality*, since an optical hologram encodes three dimensional information in a two dimensional object¹.

As already anticipated in the Introduction, the holographic duality was also largely employed to study condensed matter systems. In particular, the aim of this

¹Another very common name for this conjecture is *AdS/CFT correspondence*, which however does not quite describe what the duality is anymore.

The Large N limit of superconformal field theories and supergravity
 Juan Martin Maldacena (Harvard U.), Nov 1997, 21 pp.
 Published in *Int.J.Theor.Phys.* 38 (1999) 1113-1133, *Adv.Theor.Math.Phys.* 2 (1998) 231-252
 HUTP-97-A097, HUTP-98-A097
 DOI: [10.1023/A:1026654312961](https://doi.org/10.1023/A:1026654312961), [10.4310/ATMP.1998.v2.n2.a1](https://doi.org/10.4310/ATMP.1998.v2.n2.a1)
 e-Print: [hep-th/9711200](https://arxiv.org/abs/hep-th/9711200) | [PDF](https://arxiv.org/pdf/hep-th/9711200.pdf)
[References](#) | [BibTeX](#) | [LaTeX\(US\)](#) | [LaTeX\(EU\)](#) | [Harvmac](#) | [EndNote](#)
[ADS Abstract Service](#); [AMS MathSciNet](#); [OSTI.gov Server](#)

[Detailed record](#) - [Cited by 13544 records](#) (1000+)

A Model of Leptons
 Steven Weinberg (MIT, LNS), Nov 1967, 3 pp.
 Published in *Phys.Rev.Lett.* 19 (1967) 1264-1266
 DOI: [10.1103/PhysRevLett.19.1264](https://doi.org/10.1103/PhysRevLett.19.1264)
[References](#) | [BibTeX](#) | [LaTeX\(US\)](#) | [LaTeX\(EU\)](#) | [Harvmac](#) | [EndNote](#)
[ADS Abstract Service](#); [OSTI.gov Server](#); [Link to CERN Courier article](#)

[Detailed record](#) - [Cited by 11132 records](#) (1000+)

Figure 2.1: Comparison between the original paper by J. Maldacena (left panel) and the paper by S. Weinberg that presented for the first time the Standard Model of particle physics (right panel), as they appear on inSPIRE at the time of writing. Despite the unprecedented success of the Standard Model, the paper on the holographic duality presents a few thousand more citations!

“AdS/CMT” program is that of both understanding the strong dynamics of well known states of matter as well as identifying new, exotic ones. See for example [37, 38] for a review and [39, 40] for a textbook treatment.

We will devote the present chapter to the introduction of the various entries of the so-called holographic dictionary. We will mostly follow the pedagogical approach taken in [38], and present the dictionary through concrete examples.

2.1 Weak coupling is strong coupling

Let us briefly review the argument of [34], where the author considered the case of D3 branes in type IIB string theory. This will be the only section where we will employ concepts from string theory, which provides explicit examples of the duality. After that, we will forget about it forever and send it back in the box of the (many) things that the author of this thesis does not understand.

When dealing with an open string one can choose two possible boundary conditions. The first one chooses the string end point to be freely moving, and fixes its velocity. The second possibility is that of having the end point fixed at some position $X^i = \text{constant}$. The space spanned by all possible $X^i = \text{const.}$ is called a D-brane. It can be shown that the D-brane energy goes as e^{-1/g_s} , where g_s is the string coupling constant. It then follows that D-branes are nonperturbative solitons of string theory

that collect the end points of open strings. A Dp brane is an object with p spatial dimensions living in nine spatial dimensions (for the type IIB string).

Let us now consider the case of N superimposed D3 branes. It is found that the gravitational backreaction of the branes on the spacetime surrounding them becomes negligible in the limit when $\lambda \equiv 4\pi g_s N \ll 1$. Following the discussion of Section 1.1, since the D-brane clearly breaks spatial translations we expect some gapless excitations. Moreover, when we have N such solitons, their relative positions are also massless modes. It can be shown that these two kinds of degrees of freedom can be combined into an $N \times N$ bosonic matrix field. Other possible modes are those associated with the strings that extend between pairs of branes, which turn out to become massless in the limit where all the D-branes overlap. There will clearly be $N \times N$ types of such strings, which are described by a gauge field. This point is easily understood if one goes back to a more mundane kind of string: the QCD flux tube. A meson can be seen exactly as an open string extending between two quarks, and it is well known that its low energy excitations are nothing but the QCD gluons. Lastly, for the case of supersymmetric strings, one also needs to include the fermionic partners of the bosonic matrices. The low energy action for all these fluctuations turns out to be [40]

$$S_{D3} = \frac{4\pi N}{\lambda} \int d^4x \left\{ -\frac{1}{4} \text{tr}(F_{\mu\nu}F^{\mu\nu}) - \frac{1}{2} \text{tr}(D_\mu \Phi^{AB} D^\mu \Phi_{AB}) - \frac{1}{4} \text{tr}([\Phi^{AB}, \Phi^{CD}][\Phi_{AB}, \Phi_{CD}]) - i \text{tr}(\bar{\Psi}^A \gamma^\mu \partial_\mu \Psi_A) - \text{tr}(\bar{\Psi}^A [\Phi_{AB}, \Psi^B]) \right\}, \quad (2.1)$$

where $A, B = 1, \dots, 4$, $F_{\mu\nu}$ is the gauge field strength, Φ is a bosonic matrix field transforming in the adjoint of $U(N)$ and Ψ its fermionic partner. This is the action of an $\mathcal{N} = 4$ super Yang-Mills theory. One also recognizes in this a version of the 't Hooft matrix model [41, 42], with λ being the 't Hooft coupling (small in this regime).

Let us now consider the opposite case, the one where $\lambda \equiv 4\pi g_s N \gg 1$. In this

situation, the D3 branes strongly backreact on the surrounding spacetime. Indeed, they will collapse onto each other and form a black brane (not too different from a black hole), whose near horizon geometry is given by

$$ds^2 = L^2 \frac{dr^2}{r^2} + \frac{r^2}{L^2} (-dt^2 + d\vec{x}_3^2) + L^2 d\Omega_5^2, \quad (2.2)$$

which is the metric of an $\text{AdS}_5 \times S^5$ spacetime, with the horizon located at $r = 0$. The low energy excitations of the system of D3 branes will be localized very close to this horizon. The AdS radius is related to the string length, ℓ_s , and the Planck length, L_p , by

$$L = \lambda^{1/4} \ell_s = (4\pi N)^{1/4} L_p. \quad (2.3)$$

But then, for large 't Hooft coupling and for $N \gg 1$, the AdS radius is much larger than both ℓ_s and L_p , which means that the low energy excitations of the branes will simply be described by classical gravitational perturbations around the metric (2.2).

This shows that, in the large N limit, when the theory living on the D3 brane is weakly coupled, the gravitational system in which the brane lives must be described by the full quantum gravity theory (strings, in this case). On the other hand, when the theory is strongly coupled, the spacetime in the bulk is described in terms of classical weak gravity. Therefore:

Strong coupling, large N on the boundary



Weak, classical gravity in the bulk

This is the first entry of our holographic dictionary. From now on we will assume to be working in the large N limit and at strong 't Hooft coupling.

2.2 Bulk fields and boundary operators

Let us now forget about string theory. In the boundary strong coupling and large N limit, the theory in the bulk is simply Einstein's gravity. In the following sections we will show how to compute observables of the boundary theory, starting from quantities that can be extracted from the fields in the bulk.

The GKPW formula

The key quantities in any QFT are the n -point functions of the operators of the theory. If all these correlators were known, the theory would have been completely solved. Consider an operator $\mathcal{O}(x)$. All its correlators can be computed starting from the generating functional

$$Z_{\text{QFT}}[\phi_{(1)}(x)] = \left\langle e^{i \int d^d x \phi_{(1)}(x) \mathcal{O}(x)} \right\rangle. \quad (2.4)$$

Taking suitable functional derivatives with respect to the source $\phi_{(1)}(x)$ one can indeed extract all the n -point functions.

The definition of observables on the gravity side is instead a trickier business, since spacetime is dynamical. Nevertheless, asymptotically AdS spaces have a boundary where the metric is not dynamical. In particular, it is possible to set a Dirichlet problem where the value of a field in the bulk, say $\phi(r, x)$, is fixed to be $\phi_{(1)}(x)$ at the boundary. It can actually be shown that for a given boundary condition, there is a unique extension of the field towards the interior of AdS such that the field itself is regular everywhere [35]. The partition function on the bulk side can then be defined as a function of such boundary conditions, i.e.

$$Z_{\text{bulk}}[\phi_{(1)}(x)] = \int^{\phi \rightarrow \phi_{(1)}} \mathcal{D}\phi e^{iS[\phi]}. \quad (2.5)$$

Of course, in order to have a duality between the boundary QFT and the bulk gravitational theory there must be some one-to-one correspondence between their respective observables. This is exactly what is provided by the *Gubser-Klebanov-Polyakov-Witten (GKPW) formula*, which reads

$$Z_{\text{QFT}}[\phi_{(1)}(x)] = Z_{\text{bulk}}[\phi_{(1)}(x)]. \quad (2.6)$$

The previous relation is the foundation of holography. It states that given a certain field in the bulk, this field will be dual to an operator on the boundary. In particular, we have

$$\begin{array}{c} \text{Leading boundary behavior of the field in the bulk} \\ \uparrow \\ \text{Source for the dual operator of the boundary QFT} \end{array}$$

How to determine which fields are dual to which operators is a further, nontrivial problem. Before getting there, however, we will study more in depth how the properties of the boundary operator are determined by the features of the field in the bulk.

Scaling dimension of the dual operator

To make our discussion more concrete let us focus on a particular example and let us study a free massive scalar field on AdS background. The action is given by

$$S_{\text{bulk}} = \int d^{d+1}x \sqrt{-g} \left[\frac{M_p^2}{2} \left(R + \frac{d(d-1)}{L^2} \right) - \frac{1}{2} (\nabla \phi)^2 - \frac{m^2}{2} \phi^2 \right]. \quad (2.7)$$

Here R is the Ricci scalar, $2\Lambda = -d(d-1)/L^2$ is the negative cosmological constant and M_p is the Planck mass. We will work in the $M_p \rightarrow \infty$ limit, when one can neglect the backreaction of the scalar field and work on a fixed AdS background, with

a metric given by

$$ds^2 = L^2 \frac{dr^2}{r^2} + \frac{r^2}{L^2} dx_\mu dx^\mu. \quad (2.8)$$

As already pointed out, the scalar field ϕ will be associated to some operator on the boundary of AdS. The equation of motion in the bulk is given by

$$\phi'' + \frac{d+1}{r}\phi' - \frac{(mL)^2}{r^2}\phi + \frac{L^4}{r^4}\partial_\mu\partial^\mu\phi = 0, \quad (2.9)$$

which close to the boundary ($r \rightarrow \infty$) has the following solution:

$$\phi(r, x) = \phi_{(1)}(x) \left(\frac{L}{r}\right)^{d-\Delta} + \cdots + \phi_{(2)}(x) \left(\frac{L}{r}\right)^\Delta + \cdots, \quad (2.10)$$

where Δ is the largest positive solution of the equation

$$\Delta(\Delta - d) = (mL)^2. \quad (2.11)$$

Being the equation of second order there are two integration constants, $\phi_{(1)}$ and $\phi_{(2)}$, the first one being the source of the boundary operator.

Now note that the metric (2.8) is invariant under rescaling $\{t, \vec{x}, 1/r\} \rightarrow \lambda\{t, \vec{x}, 1/r\}$, and the same thing is true for Eq. (2.9). Therefore if $\phi(r)$ is a solution, then $\phi(r/\lambda)$ will be a solution as well. This means that the leading falloff transforms as $\phi_{(1)} \rightarrow \lambda^{\Delta-d}\phi_{(1)}$. But then, in order for the action in Eq. (2.4) to be invariant, the operator must transform as

$$\mathcal{O}(x) \rightarrow \lambda^{-\Delta}\mathcal{O}(x), \quad (2.12)$$

from which it follows that Δ is the *scaling dimension* of the boundary operator, which is then related to the mass of the bulk field via Eq. (2.11).

Holographic renormalization

We would now like to compute the boundary action for the background solution of Eq. (2.9). Upon integration by parts and employing the equations of motion, the on-shell action for the scalar reduces to a pure boundary term:

$$\bar{S}_{\text{bulk}} = - \int_{r \rightarrow \infty} d^d x \frac{1}{2} \sqrt{-\gamma} \phi n^M \nabla_M \phi, \quad (2.13)$$

where $\gamma_{\mu\nu}$ is the induced metric on the boundary and $n^r = r/L$ is the outward pointing unit normal vector. Using the asymptotic expression given in Eq. (2.10) one easily finds

$$\bar{S}_{\text{bulk}} = \int_{r \rightarrow \infty} d^d x \left[\frac{d - \Delta}{2L} \left(\frac{r}{L} \right)^{2\Delta-d} \phi_{(1)}^2 + \frac{d}{2L} \phi_{(1)} \phi_{(2)} \right]. \quad (2.14)$$

Given that $2\Delta > d$, the first term is infinite. Such a divergence is due to the infinite volume of the bulk spacetime, over which we have integrated.

As it happens in quantum field theory, we can get rid of the divergence by introducing a suitable counter term. From this one might infer that the radial direction of the bulk spacetime plays the role of an energy scale—in the renormalization group (RG) sense—with the near boundary region corresponding to the UV and the near horizon one to the IR. Another hint also comes from the scaling dimension of the boundary operator—see Eq. (2.12). Indeed, when the operator is *irrelevant* ($\Delta > d$) then the scalar field grows when moving towards the boundary, while when the operator is *relevant* ($\Delta < d$) it goes to zero. Moreover, one can also show that the equation of motion (2.9) corresponds precisely to the RG equation for the boundary couplings, with r playing the role of the renormalization scale (see Appendix A). We therefore found one more entry of our dictionary:

$$\begin{array}{c}
\text{Radial direction in the bulk (horizon/boundary)} \\
\uparrow \\
\text{Renormalization scale of the boundary theory (IR/UV)}
\end{array}$$

Standard quantization (the good)

Let us now introduce a counter term to cure the divergence of Eq. (2.14). The correct counter term action is given by

$$S_{\text{c.t.}} = \frac{\Delta - d}{2L} \int_{r \rightarrow \infty} d^d x \sqrt{-\gamma} \phi^2. \quad (2.15)$$

Being purely a boundary term this does not affect the equation of motion in the bulk.

There is actually another reason for which such a counter term is necessary, i.e. to fix the variational problem [43]. In fact, consider the variation of the action (2.7) (still neglecting backreaction). Again, it reduces to a boundary term given by

$$\delta S_{\text{bulk}} = \int_{r \rightarrow \infty} d^d x \delta \phi \left[\frac{d - \Delta}{L} \left(\frac{r}{L} \right)^\Delta \phi_{(1)} + \frac{\Delta}{L} \left(\frac{r}{L} \right)^{d-\Delta} \phi_{(2)} \right], \quad (2.16)$$

where $\delta \phi = \delta \phi_{(1)} (L/r)^{d-\Delta} + \delta \phi_{(2)} (L/r)^\Delta$. This is problematic. If we require for the variation to be zero for every $\delta \phi_{(1)}$ and $\delta \phi_{(2)}$, this would enforce $\phi_{(1)} = \phi_{(2)} = 0$, i.e. the trivial solution. However, if we also include the counter term the total variation is then

$$\delta S_{\text{bulk}} + \delta S_{\text{c.t.}} = \frac{2\Delta - d}{L} \int d^d x \phi_{(2)} \delta \phi_{(1)}, \quad (2.17)$$

and therefore the variational problem is well defined if $\phi_{(2)} = 0$ or $\phi_{(1)}$ = fixed.

Putting together Eqs. (2.14) and (2.15) we obtain the total on-shell action:

$$\bar{S} = \bar{S}_{\text{bulk}} + \bar{S}_{\text{c.t.}} = \frac{2\Delta - d}{2L} \int d^d x \phi_{(1)} \phi_{(2)}. \quad (2.18)$$

We are now ready to find the expectation value of the boundary operator. In particular we have (in the large N limit)

$$\begin{aligned}
\langle \mathcal{O}(x) \rangle &= \frac{-i}{Z_{\text{QFT}}[0]} \frac{\delta Z_{\text{QFT}}[\phi_{(1)}]}{\delta \phi_{(1)}(x)} = \frac{-i}{Z_{\text{bulk}}[0]} \frac{\delta Z_{\text{bulk}}[\phi_{(1)}]}{\delta \phi_{(1)}(x)} \\
&\xrightarrow{N \rightarrow \infty} \frac{\delta \bar{S}_{\text{bulk}}[\phi_{(1)}]}{\delta \phi_{(1)}(x)} = \frac{2\Delta - d}{2L} \left(\phi_{(2)}(x) + \frac{\delta \phi_{(2)}}{\delta \phi_{(1)}} \phi_{(1)}(x) \right) \\
&= \frac{2\Delta - d}{L} \phi_{(2)}(x),
\end{aligned} \tag{2.19}$$

where in the first step we employed the GKPW relation. In the last step we instead used the fact that, since the equation of motion (2.9) is linear in the bulk field, the two falloffs must be proportional to each other, i.e. it must be $\phi_{(2)}(x) = (\delta \phi_{(2)} / \delta \phi_{(1)}) \phi_{(1)}(x)$ [38, 44].

Hence, while one of the falloffs is related to the source of the dual operator, the other one is instead related to its vacuum expectation value. We just found another crucial feature of the holographic duality (for standard quantization):

$$\begin{array}{c}
\text{Subleading falloff of the bulk field} \\
\uparrow \\
\text{Expectation value of the dual operator}
\end{array}$$

Alternative quantization (the bad)

So far we have assumed that the first falloff was the one corresponding to the source of the boundary operator. This is indeed the only possible choice when the leading behavior of the field is non-normalizable. Nevertheless, if the mass of the scalar is such that

$$-\frac{d^2}{4} < (mL)^2 < -\frac{d^2}{4} + 1, \tag{2.20}$$

then both falloffs are normalizable. In particular, recall that the nature of AdS allows for fields that are slightly tachyonic. The lowest allowed mass squared is called the Breitenlohner-Freedman (BF) bound [45]. In this case we can exchange the roles of the two falloffs and consider $\phi_{(2)}$ as the source. This alternative quantization is achieved by adding one more boundary term to the action:

$$S_I = \int_{r \rightarrow \infty} d^d x \sqrt{-\gamma} \left[\frac{d - \Delta}{L} \phi^2 + \phi n^M \nabla_M \phi \right], \quad (2.21)$$

so that $S = S_{\text{bulk}} + S_{\text{c.t.}} + S_I$. With manipulations very close to the ones performed in the previous section, one can show that in this case the vev of the dual operator is given by

$$\langle \mathcal{O}(x) \rangle = \frac{d - 2\Delta}{L} \phi_{(1)}(x). \quad (2.22)$$

Mixed boundary conditions (the ugly)

The operators dual to some bulk fields are given by *single* trace operators². Just like in an ordinary QFT, even if they are absent in the far UV, *multitrace* operators will be generated by the RG flow towards the infrared—see again Appendix A.

However, multitrace operators can also be explicitly added to the spectrum of the UV theory through the so called *mixed boundary conditions* [46–48]. As we saw in the previous sections, if we consider, for example, standard quantization, this corresponds to having a term in the boundary action given by $W[\mathcal{O}] = \int d^d x \phi_{(1)}(x) \mathcal{O}(x)$. The boundary condition for the scalar field is that its leading falloffs is fixed to be $\phi_{(1)} = \phi_{(1)}(x)$. The prescription to include multitrace operators is simply that of extending this definition to W s that are nonlinear functionals of their argument. In particular,

²Single trace is here meant with respect to the global group of the boundary theory. For example, if Φ is a scalar field in the adjoint representation, then a single trace operator could be $\mathcal{O}(x) = \frac{1}{N} \text{tr}(\Phi \cdot \Phi)$. A double trace operator would be $\mathcal{O}^2(x)$ and so on.

the boundary condition for the scalar field will be

$$\phi_{(1)} = \frac{\delta W[\mathcal{O}]}{\delta \mathcal{O}} \bigg|_{\mathcal{O}=(2\Delta-d)\phi_{(2)}}. \quad (2.23)$$

From the boundary viewpoint, this boundary condition introduces a deformation in the action simply given by $\Delta S = W[\mathcal{O}]$. Since both falloffs are nonzero here, these boundary conditions can only be imposed when both of them are normalizable, i.e. for the range of masses in Eq. (2.20).

Mixed boundary conditions can trigger an RG flow that evolves from a UV fixed point with a given quantization (standard or alternative) to an IR fixed point with the other quantization [46]. Consider again the scalar field, as in Eq. (2.10), and imagine to start in the UV with alternative quantization, such that the dimension of the operator is $\dim[\mathcal{O}] = d - \Delta < d/2$, and suppose to turn on a relevant deformation, $W[\mathcal{O}] = \frac{f}{2} \int d^d x \mathcal{O}^2(x)$. The corresponding boundary condition will be $\phi_{(2)} = f\phi_{(1)}$. In the far UV $f = 0$ and indeed we have alternative quantization $\phi_{(2)} = 0$. However, in the far IR $f \rightarrow \infty$ and the boundary condition becomes $\phi_{(1)} = 0$. Therefore the multitrace operator triggers a flow between two different conformal theories, quantized in different ways.

2.3 Which symmetry?

We are finally ready to make our last crucial step. We now need to understand how to select a certain bulk theory given a boundary QFT or, of course, viceversa. Once again, we will be guided by symmetry principles. Let us make it concrete and consider the example of a $U(1)$ free photon in the bulk. The action for this gauge theory is

$$S = - \int d^{d+1} x \sqrt{-g} \frac{1}{4} F_{MN} F^{MN}, \quad (2.24)$$

with $F_{MN} = \partial_M A_N - \partial_N A_M$. The equations of motion for the gauge field are simply given by $\nabla^M F_{MN} = 0$, and close to the boundary they are solved by

$$A_\mu(r, x) = a_\mu^{(1)}(x) + \dots + j_\mu(x) \left(\frac{L}{r}\right)^{d-2} + \dots, \quad (2.25)$$

where we are working in radial gauge, $A_r = 0$, and we indicated the second falloff as j_μ for reasons that will be clear soon.

The on-shell action once again reduces to a pure boundary term³, which reads

$$\bar{S} = - \int_{r \rightarrow \infty} d^d x \sqrt{-\gamma} \frac{1}{2} n^M F_{MN} A^N = \frac{d-2}{2L} \int d^d x a_\mu^{(1)} j^\mu. \quad (2.26)$$

The theory in the bulk has a *U(1) gauge* symmetry, i.e. is invariant under $A_\mu(r, x) \rightarrow A_\mu(r, x) + \partial_\mu \lambda(r, x)$. This is true also for large gauge transformations, i.e. such that $\lambda(r, x)$ becomes constant on the boundary. But then, performing such a transformation on the on-shell bulk action above, one obtains

$$\bar{S} \rightarrow \frac{d-2}{2L} \int d^d x (a_\mu^{(1)} j^\mu + \partial_\mu \lambda j^\mu) = \bar{S} - \frac{d-2}{2L} \int d^d x \lambda \partial_\mu j^\mu. \quad (2.27)$$

In order for this to be invariant the falloff $j^\mu(x)$ must correspond to a conserved current of a *global* symmetry on the boundary, $\partial_\mu j^\mu(x) = 0$.

This teaches us that global symmetries on the boundary are gauged in the bulk. The subleading falloff of the corresponding gauge field will be the conserved current of the boundary symmetry. In the example above it will be the *U(1)* current. The subleading falloff of the bulk metric will instead be the stress energy tensor of the boundary QFT. This is because the metric of the bulk is nothing but the gauge field associated with diff invariance, which is the gauged analogue of the Poincaré invariance of the boundary. Its leading falloff is clearly the metric of the boundary

³This is a feature common to all quadratic actions.

theory, which is indeed the source for the stress energy tensor. Lastly, in Section 2.2 we saw that the falloffs of the fields are directly related to the source and vev of the dual operators. It then follows that the quantum numbers must simply match directly.

Here is the last entry of our dictionary:

$$\begin{array}{c} \text{Gauge symmetry in the bulk} \\ \uparrow \\ \text{Global symmetry of the boundary QFT} \end{array}$$

2.4 Finite temperature

Before concluding we must add one more aspect of the duality. In particular, it is rather obvious that in order to describe condensed matter systems in a complete way one must be able to turn on temperature on the boundary theory. It is well known that the thermal partition function for a certain QFT is obtained making time purely imaginary and periodic [49]. The inverse period of the imaginary time corresponds to the temperature of the system.

In the previous section we learned that the subleading falloff of the bulk metric corresponds to the boundary stress energy tensor. It follows that the leading falloff will be its source, i.e. the boundary metric itself. In other words, close to the boundary we have

$$ds^2 = L^2 \frac{dr^2}{r^2} + \frac{r^2}{L^2} h_{\mu\nu}(x) dx^\mu dx^\nu + \dots, \quad (2.28)$$

where $h_{\mu\nu}$ is precisely the (nondynamical) metric of the boundary theory. Consequently, if the boundary theory has periodic time, the bulk has it as well.

In absence of any horizon, finite temperature can be trivially introduced by compactifying time in the bulk. More interesting is the case of a black hole in the interior of AdS. The black hole metric is given by

$$ds^2 = \frac{dr^2}{g(r)} + g(r)d\tau^2 + \frac{r^2}{L^2}d\vec{x}_{d-1}^2, \quad (2.29)$$

where $g(r_+) = 0$ at some value of the radial coordinate, corresponding to the black hole horizon. Moreover, $\tau = it$ is the Euclidean time. For a nonextremal black hole, close to the horizon we can expand $g(r) = g'(r_+)(r - r_+) + \dots$, and the metric reads

$$ds^2 = \frac{dr^2}{g'(r_+)(r - r_+)} + g'(r_+)(r - r_+)d\tau^2 + \dots. \quad (2.30)$$

Let us now perform a change of coordinates such that

$$\frac{dr^2}{g'(r_+)(r - r_+)} = d\rho^2 \implies \rho = 2\sqrt{\frac{r - r_+}{g'(r_+)}}. \quad (2.31)$$

The metric then becomes $ds^2 = d\rho^2 + \rho^2 d\varphi^2 + \dots$, where $\varphi = g'(r_+)\tau/2$. This is clearly the metric of a circle and to avoid a conical singularity at $\rho = 0$ one must require that φ has period equal to 2π . But this means that the inverse period of the Euclidean time will be given by

$$T = \frac{g'(r_+)}{4\pi}. \quad (2.32)$$

Therefore, if the bulk theory has a black hole horizon the temperature of the boundary QFT will be related to the black hole radius by the above formula.

Bulk side	Boundary side
Strong/weak coupling	Weak/strong coupling
Classical gravitational theory	Large N limit
Quantum corrections	$1/N$ corrections
Falloffs of the bulk field	Source and vev of the operator (depending on the quantization)
Near boundary behavior of the falloffs	Scaling dimension of the operator
Gauge symmetry	Global symmetry
Bulk gauge field	Conserved current of global symmetry
Periodic imaginary time	Finite temperature

Table 2.1: Schematic summary of the main entries of the holographic dictionary.

2.5 Summary

Let us summarize the findings of this chapter. The holographic duality is a very powerful tool. It allows to compute the observables of a certain strongly coupled QFT using classical Einstein's gravity in a space with one additional spatial dimension. In this way one can compute observables in a regime that is not otherwise accessible with other techniques. The dictionary that brings you from one side to the other of the duality is essentially based on symmetry principles. A schematic overview is reported in Table 2.1.

Holographic superfluids

As we learned in Section 1.2 the symmetry breaking pattern of type-I superfluids is remarkably simple, since it features only one modified generator. This is probably one of the reasons why such condensed matter systems have been among the first ones to be investigated by means of the holographic duality (see for example [37, 50–59])¹.

In this chapter we will use holographic superfluids as a toy model to developed a technique that allows to explicitly compute the action of the phonons of the boundary theory starting from the fields in the bulk of AdS. Such a method will be a key ingredient in our study of holographic solids.

¹It should be noted that such systems often appear in the literature as “holographic superconductors”. The reason is that, as far as the transport properties are concerned, the charge response of a superconductor is described by superfluidity. Nevertheless, when investigating the low energy spectrum, superconductors present a gap, because of the Higgs mechanism, while superfluids do not. We will show that the systems presented in this chapter indeed have gapless modes in their spectrum.

3.1 On the previous episodes

Let us now review the features of holographic superfluids. To determine the dual of a strongly coupled superfluid one needs to use the holographic dictionary developed in Chapter 2. As seen previously, a type-I superfluid features a spontaneously broken global $U(1)$ symmetry. Global symmetries of the boundary QFT are gauge symmetries of the bulk theory. Therefore, our most minimal ingredient will be a $U(1)$ gauge field. However, this is not enough. Since the photon is not charged under the $U(1)$ group, the vev of its dual operator will not cause spontaneous breaking of the symmetry. It then follows that we will also need some kind of matter fields.

One possible realization can be found in the following way. In Section 1.2 we learned that the simplest implementation of the superfluid symmetries is through a single real scalar, $\phi(x)$, that shifts under the $U(1)$ and acquires a time dependent vev, $\langle\phi(x)\rangle = \mu t$. However, the same symmetry breaking pattern can also be realized in a more holography-friendly way, by introducing a complex scalar $\Phi(x)$ and shifting the time derivatives by the chemical potential, i.e.

$$\Phi(x) = \varphi(x) e^{i\pi(x)}, \quad \partial_0 \rightarrow \partial_0 - i\mu. \quad (3.1)$$

The complex scalar now transforms linearly under the $U(1)$ group and its phase does not acquire any vev. The chemical potential can now be considered as the temporal component of a constant gauge field. It is easy to convince oneself that the two descriptions are perfectly equivalent, if we identify $\phi(x) = \mu t + \pi(x)$.

It is now evident what a possible gravity dual is. It will be a theory of scalar QED on an asymptotically AdS background [51, 52]. The corresponding action will be

$$S = - \int d^{d+1}x \sqrt{-g} \left[|\nabla \Phi - iqA\Phi|^2 + V(|\Phi|^2) + \frac{1}{4}F_{MN}F^{MN} \right] + S_{\text{bdy}}. \quad (3.2)$$

Here S_{bdy} will be a suitable boundary term, needed to cure the ultraviolet divergences as well as to determine the quantization scheme of the boundary theory (see Section 2.2). Moreover, the scalar field potential will be generally given by

$$V(|\Phi|^2) = m^2 |\Phi|^2 + \text{interaction terms.} \quad (3.3)$$

For simplicity we will work in the so-called *probe limit*, i.e. neglecting the backreaction of the matter fields on the metric. This limit can be formally achieved by considering the limit of very large charge q [60].

Phase transition at finite temperature

One of the first features of a superfluid that one can recover holographically is its phase transition [51, 52]. In order to do that we need to turn on the temperature. As seen in Section 2.4, one way to do that is to study our scalar QED on a black hole background, i.e. considering a metric given by

$$ds^2 = L^2 \frac{dr^2}{f(r)r^2} + \frac{r^2}{L^2} \left(-f(r)dt^2 + d\vec{x}_{d-1}^2 \right). \quad (3.4)$$

where $f(r) = 1 - (r_+/r)^d$, and the horizon is located at $r = r_+$. The temperature of the system is then given by

$$T = \frac{|g'_{tt}(r_+)|}{4\pi} = \frac{d}{4\pi L^2} r_+, \quad (3.5)$$

hence the larger the black hole the hotter the superfluid.

Since we do not want to break the boundary spatial translations, we will consider ansatze for the background fields that only depend on the holographic coordinate.

From Eq. (3.1) we easily understand that the field profiles we are looking for are

$$\Phi(r, x) = \varphi(r) \quad \text{and} \quad A_M(r, x) = A(r)\delta_M^0, \quad (3.6)$$

where both φ and A are real fields. Their equations of motion are given by

$$\varphi'' + \left(\frac{d+1}{r} + \frac{f'}{f} \right) \varphi' + q^2 \left(\frac{L^2}{r^2 f} \right)^2 A^2 \varphi - \frac{L^2}{r^2 f} V'(\varphi^2) \varphi = 0, \quad (3.7a)$$

$$A'' + \frac{d-1}{r} A' - 2q^2 \frac{L^2}{r^2 f} \varphi^2 A = 0. \quad (3.7b)$$

In this section we will only consider the case of a free tachyonic scalar in $d = 2 + 1$, with a potential given by $V = -\frac{d-1}{L^2} \varphi^2$. For simplicity we also set $L = q = 1$.

As far as our boundary conditions are concerned, we require regularity throughout the whole interior of AdS. In particular, for the gauge field we must demand that close to the horizon $A(r)$ goes to zero at least as fast as $r - r_+$, to ensure that its magnitude, $A_M A^M$, which is a scalar, does not diverge. Since Eqs. (3.7a) are both of second order, these near horizon conditions will fix two of the four integration constants. The behavior of the fields near the conformal boundary is

$$\varphi(r) = \frac{\varphi_{(1)}}{r} + \frac{\varphi_{(2)}}{r^2} + \dots, \quad A(r) = \mu - \frac{\rho}{r} + \dots, \quad (3.8)$$

where μ is the chemical potential and ρ is the number density of the boundary theory. The tachyonic mass we have chosen is well within the range (2.20) and therefore both quantizations are allowed. Since we are looking for *spontaneous* breaking of the $U(1)$, our source must vanish. The two possible boundary conditions are thus either $\varphi_{(1)} = 0$ or $\varphi_{(2)} = 0$. Since we are working in $d = 2 + 1$ dimensions, in the first case (standard quantization) the scalar field will be dual to an operator \mathcal{O}_2 with scaling dimension $\Delta = 2$, while in the second case (alternative quantization) it will be dual to an operator \mathcal{O}_1 of scaling dimension $d - \Delta = 1$ [51]. Note that in this latter case,

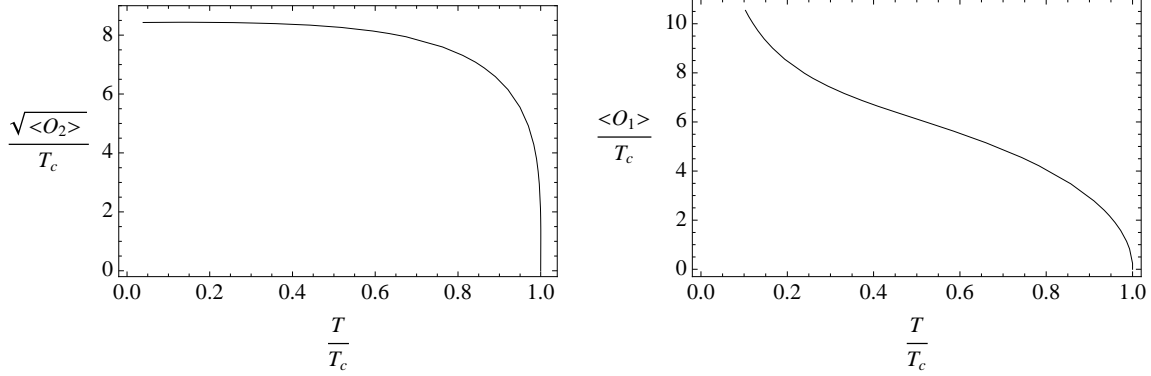


Figure 3.1: Vacuum expectation values of the dual operators in standard (left panel) and alternative (right panel) quantization as a function of temperature. Both the horizontal and vertical axes have been rescaled by the critical temperature to obtain adimensional quantities. Figures taken from [51]. The divergence at $T = 0$ of the $\langle \mathcal{O}_1 \rangle$ operator indicates that the full backreaction of the fields on the spacetime should be included at low temperatures—see e.g. [52].

the scaling dimension is such that \mathcal{O}_1^2 is also a relevant deformation and should be included on naturalness grounds. This would be done via mixed boundary conditions which were not studied in the original work [51].

Since we are imposing three boundary conditions—i.e. two at the horizon and one at the boundary—we are left with one free parameter. This corresponds precisely to the freedom of varying the chemical potential of the boundary theory.

It is now fairly easy to solve Eqs. (3.7a) numerically and extract the different falloffs as a function of temperature. The results for the two possible quantizations are reported in Figure 3.1. The interpretation is quite clear. There is a critical temperature T_c above which the scalar field is identically zero and the gauge field is exactly given by $A = \mu - \rho/r$. Such a solution does not present a condensate. Nevertheless, for $T < T_c$ the scalar field turns on, hence spontaneously breaking the $U(1)$ symmetry. This is our fluid-superfluid *phase transition*. Moreover, since we have a black hole solution both above and below the critical temperature, the entropy of our system (which is dominated by the black hole degrees of freedom) will be continuous at $T = T_c$. This is the hallmark of a second order phase transition. To confirm this

one can also fit the dependence of the condensate with temperature and show that, near the critical temperature, it exhibits a square root behavior $\langle \mathcal{O}_i \rangle \propto \sqrt{T_c - T}$ [51].

3.2 From bulk fields to boundary phonons

In the previous section we showed how one can reproduce the superfluid phase transition with holographic techniques. The literature on holographic superfluids is extremely rich (see also [53–57]) and it goes well beyond the goal of this thesis to summarize all of it.

As it is probably clear by now, the most natural question that could arise in light of the EFT viewpoint on superfluids is: what about the phonon? In other words, is it possible to gather information on the low energy spectrum of the system starting from the bulk setup? Some work in this direction has already been done [59, 60], studying in particular the behavior of first, second and fourth sounds [33] as a function of temperature². Nevertheless, to the best of our knowledge, all the available results are based on numerical analyses. In this section we will present a completely analytical method to explicitly obtain the action of the phonons of the boundary theory starting from the fields in the bulk of AdS. A first version of this technique already appeared in [61, 62], in the context of holographic fluids. Nevertheless, in that particular case, the solution to the background equations of motion is known analytically and the calculation can be carried on explicitly. Here we build on that initial result and develop a way to compute the action of the boundary phonon even if the background

²A quite interesting open problem is actually related to the behavior of second sound in holographic superfluids. At low temperatures, the speed of second sound, c_2 , should be related to that of the first sound, c_1 , by [33]:

$$\lim_{T \rightarrow 0} c_2^2 = \frac{c_1^2}{d-1},$$

where d is the number of spacetime dimensions. This behavior cannot be recovered from holography [59]. It would be interesting to try to employ the methods developed in this chapter to shed some light on the problem.

profiles are unknown. Such result has been presented in [63].

Background configuration

The relevant action for our bulk theory is still the one reported in Eq. (3.2). However, we are now solely concerned about the spectrum of first sound, i.e. zero temperature superfluids. In this case our background metric will simply be that of pure AdS, i.e.

$$ds^2 = \frac{dr^2}{r^2} + r^2 dx_\mu dx^\mu, \quad (3.9)$$

where we are setting again the AdS radius to one. Moreover, we will not need to specify our scalar field potential as in Eq. (3.3). Nevertheless, it can be shown that for several choices of such a potential, the full backreacted geometry does not exhibit conformal invariance in the infrared since it presents a mild divergence at $r = 0$ [54, 57], and hence our approximation (3.9) is a bad one. However, it can also be shown that there are choices (e.g. a free massless scalar [57] or a Mexican hat potential at large charge [53, 54]) for which our background metric is the correct one in the probe limit. We will assume to be working with potentials of this sort.

Our background fields are again given by

$$\bar{\Phi}(r, x) = \varphi(r), \quad \bar{A}_M(r, x) = \sqrt{2} r \psi(r) \delta_M^0, \quad (3.10)$$

where the definition of the profile ψ has been chosen for later convenience. For generic mass and dimension, the near boundary behavior of the fields is

$$\varphi(r) = \frac{\varphi_{(1)}}{r^{d-\Delta}} + \frac{\varphi_{(2)}}{r^\Delta} + \dots, \quad (3.11a)$$

$$\psi(r) = \frac{\mu}{\sqrt{2} r} - \frac{\rho}{\sqrt{2} r^{d-1}} + \dots. \quad (3.11b)$$

Here Δ is again defined as the largest positive solution of Eq. (2.11). For concreteness

we will work in standard quantization, imposing $\varphi_{(1)} = 0$. We recall that in this case the boundary action *for the background* is given by³

$$S_{\text{bdy}}^{\text{bkg}} = (\Delta - d) \int_{r \rightarrow \infty} d^d x \sqrt{-\gamma} \varphi^2. \quad (3.12)$$

The equations of motion for the bulk profiles are

$$\varphi'' + \frac{d+1}{r} \varphi' - \frac{V'(\varphi^2)}{r^2} \varphi + 2q^2 \frac{\psi^2}{r^2} \varphi = 0, \quad (3.13a)$$

$$\psi'' + \frac{d+1}{r} \psi' + \frac{d-1}{r^2} \psi - 2q^2 \frac{\varphi^2}{r^2} \psi = 0. \quad (3.13b)$$

Intermezzo: conformal superfluids

Before going on with our study we need to find a way to check whether or not we are indeed dealing with superfluids. In the case of a pure AdS background and of standard or alternative quantization, the boundary theory has an exact conformal invariance. What does that mean for our superfluid? A conformal theory is characterized by a traceless stress energy tensor [42]. If we require $T^\mu_\mu = 0$, Eq. (1.29) reduces to a simple equation for the dependence of the superfluid's lagrangian on the chemical potential:

$$-2XP_X(X) + dP(X) = 0 \implies P(X) \propto X^{d/2}, \quad (3.14)$$

hence completely fixing the action up to an overall constant. This also determines the speed of sound, as well as all other interaction couplings in Eq. (1.35). In particular

³Away from the background configuration the expression for the boundary action is more complicated. We will comment on that in the followings sections.

it must be

$$c_s^2 = \frac{P_X}{P_X + 2XP_X} = \frac{1}{d-1}. \quad (3.15)$$

We will show that this is exactly what we can recover from our holographic setup.

Background on-shell action

The first check we can perform is to show that the background on-shell action indeed reproduces what expected from Eq. (3.14). The argument is pleasantly simple. Consider a particular solution of Eqs. (3.13) with $\mu = 1$, and let us denote such profiles with $\hat{\varphi}(r)$ and $\hat{\psi}(r)$. Since the equations of motion are invariant under rescaling of the radial coordinate, a solution with a generic chemical potential can simply be obtained by replacing $r \rightarrow r/\mu$, i.e. $\varphi(r) = \hat{\varphi}(r/\mu)$ and $\psi(r) = \hat{\psi}(r/\mu)$.

Let us now compute the on-shell action. It is given by

$$S_{\text{bkg}} = - \int d^d x dr r^{d-1} \left[r^2 (\varphi')^2 + 2q^2 \psi^2 \varphi^2 + V(\varphi^2) - (r\psi' + \psi)^2 \right] + (\Delta - d) \int_{r \rightarrow \infty} d^d x r^d \varphi^2. \quad (3.16)$$

If we now perform a change of variable $r = \mu y$ we get

$$S_{\text{bkg}} = \mathcal{N} \int d^d x \mu^d, \quad (3.17)$$

with normalization given by

$$\mathcal{N} = - \int dy y^{d-1} \left[y^2 (\hat{\varphi}')^2 + 2q^2 \hat{\psi}^2 \hat{\varphi}^2 + V(\hat{\varphi}^2) - (y\hat{\psi}' + \hat{\psi})^2 \right] - \lim_{y \rightarrow \infty} y^d \hat{\varphi}^2, \quad (3.18)$$

which is independent of the chemical potential. If we now recall that $X = \mu^2$ at equilibrium, we can see immediately that the on-shell lagrangian at equilibrium is

indeed $P(X) = \mathcal{N}X^{d/2}$ as expected for a conformal superfluid.

O phonon, phonon, where art thou, phonon?

The previous result is an encouraging sign that we are going in the right direction. Nevertheless, one could argue that it is nothing but the consequence of dimensional analysis in a conformal theory, where the only scales available on the background are the radial coordinate and the chemical potential.

Our goal is now that of deriving the action of the superfluid phonon of the boundary theory. In order to do that it is natural to start from the fluctuations of the bulk fields, which we parametrize as

$$\Phi = (\varphi + \sigma)e^{i\pi}, \quad A_M = \bar{A}_M + \alpha_M. \quad (3.19)$$

Expanding the action (3.2) up to quadratic order in the fluctuations we get

$$\begin{aligned} S^{(2)} = - \int d^{d+1}x \sqrt{-g} \left[& \partial_M \sigma \partial^M \sigma + \varphi^2 \partial_M \pi \partial^M \pi - 4q \bar{A}^M \varphi \partial_M \pi \sigma \right. \\ & - 2q \varphi^2 \alpha^M \partial_M \pi + q^2 \bar{A}^M \bar{A}_M \sigma^2 + 4q^2 \varphi \bar{A}_M \alpha^M \sigma + q^2 \varphi^2 \alpha_M \alpha^M \\ & \left. + (V' + 2\varphi^2 V'') \sigma^2 + \frac{1}{4} f_{MN} f^{MN} \right] + S_{\text{bdy}}^{(2)}. \end{aligned} \quad (3.20)$$

Here $f_{MN} = \partial_M \alpha_N - \partial_N \alpha_M$ and $S_{\text{bdy}}^{(2)}$ are the terms of the boundary action that are quadratic in the fluctuations. Moreover, V' and V'' are computed on the background profile. Our plan of action is now the following:

1. Compute the linearized equations of motion for the fluctuations at lowest order in boundary derivatives. This will correspond to a low energy expansion for the boundary theory.
2. Solve such equations of motion for all fluctuations but the phase π .

3. Plug the solutions back into the quadratic action, to obtain the so called *partially on-shell action*.

This procedure is not too dissimilar from what presented in [61]. The main difference is that we will be able to solve the equations of motion despite the fact that the background profiles are not known analytically.

To implement the low energy expansion, we perform the following formal identifications:

$$\sigma, \alpha_\mu, \partial_r \sim O(1), \quad \partial_\mu \sim O(\epsilon), \quad \pi, \alpha_r \sim O(1/\epsilon), \quad (3.21)$$

where the last one has been done because π always appears with a boundary derivatives. The radial fluctuations of the gauge field must be of the same order for consistency with the equations. The equations of motion at lowest order in ϵ then turn out to be⁴

$$\sigma'' + \frac{d+1}{r}\sigma' - \frac{V' + 2\varphi^2 V''}{r^2}\sigma + 2\sqrt{2}q\frac{\varphi\psi}{r^3}(q\alpha_0 - \partial_0\pi) + 2q^2\frac{\psi^2}{r^2}\sigma = 0, \quad (3.22a)$$

$$(q\alpha_0 - \partial_0\pi)'' + \frac{d-1}{r}(q\alpha_0 - \partial_0\pi)' - 2q^2\frac{\varphi^2}{r^2}(q\alpha_0 - \partial_0\pi) - 4\sqrt{2}q^3\frac{\varphi\psi}{r}\sigma = 0, \quad (3.22b)$$

$$(q\alpha_i - \partial_i\pi)'' + \frac{d-1}{r}(q\alpha_i - \partial_i\pi)' - 2q^2\frac{\varphi^2}{r^2}(q\alpha_i - \partial_i\pi) = 0, \quad (3.22c)$$

$$\pi' - q\alpha_r = 0. \quad (3.22d)$$

Note that the equations for the radial mode σ and for the gauge invariant combination $q\alpha_\mu - \partial_\mu\pi$ are of second order and hence require two boundary conditions. However, the equation for the phase is only first order. In particular, if we impose that π

⁴There is small subtlety hidden here. In particular, the low energy expansion is not strictly speaking appropriate for every value of the radial coordinate since, for a region very close to $r = 0$ the coefficients of the equations could become as large as $1/\epsilon^2$. The most rigorous way to perform the expansion would that to set an IR cutoff on the radial coordinate, $r = \delta$, take the $\epsilon \rightarrow 0$ limit and then remove the cutoff once the on-shell action has been computed. It can be shown that the order of the limits does not matter.

vanishes at the center of AdS, the solution is readily found to be

$$\pi(r, x) = q \int_0^r dz \alpha_r(z, x). \quad (3.23)$$

As it will soon be clear, the phonon of the dual superfluid theory will be given by the value of π at the boundary, i.e. $\pi_B(x) \equiv \pi(r = \infty, x)$. This is the reason why we do not want to solve the equations of motion for the phase of the scalar.

Let us now solve the remaining equations. Let us start with Eq. (3.22c) and consider the change of variables $q\alpha_i - \partial_i\pi \equiv r\beta_i$. The equation then becomes

$$\beta_i'' + \frac{d+1}{r}\beta_i' + \frac{d-1}{r^2}\beta_i - 2q^2\frac{\varphi^2}{r^2}\beta_i = 0. \quad (3.24)$$

But this is precisely Eq. (3.13b) for the background profile, and hence the regular solution is $\beta_i(r, x) = b_i(x)\psi(r)$. To determine the arbitrary constant we will impose that the fluctuation α_i vanishes both in the IR and in the UV [61]. This fixes the solution to be (recall that ψ goes to zero in the IR faster than r itself)

$$\alpha_i = \frac{1}{q} \left(\partial_i\pi - \frac{\sqrt{2}}{\mu} r \psi \partial_i\pi_B \right). \quad (3.25)$$

This is the essence of our new technique, i.e. being able to determine the on-shell fluctuations as a function of the background fields, regardless of their specific functional form. Moreover, given the boundary conditions, this will be the only regular solution, as discussed in Section 2.2 and in [35].

For the remaining two fluctuations we relabel them as $\sigma \equiv -r\gamma'$ and $q\alpha_0 - \partial_0\pi \equiv -q\sqrt{2}r^2\delta'$. After that, Eqs. (3.22a) and (3.22b) become

$$\gamma''' + \frac{d+3}{r}\gamma'' + \frac{d+1}{r^2}\gamma' - \frac{V' + 2\varphi^2V''}{r^2}\gamma' + 2q^2\frac{\psi^2}{r^2}\gamma' + 4q^2\frac{\psi\varphi}{r^2}\delta' = 0, \quad (3.26a)$$

$$\delta''' + \frac{d+3}{r}\delta'' + \frac{2d}{r^2}\delta' - 2q^2\frac{\varphi^2}{r^2}\delta' - 4q^2\frac{\varphi\psi}{r^2}\gamma' = 0. \quad (3.26b)$$

One can check that these are linear combinations of Eqs. (3.13) and their derivatives and therefore admit a solution with $\gamma(r, x) = c(x)\varphi(r)$ and $\delta(r, x) = c(x)\psi(r)$, with the same proportionality factor $c(x)$. Imposing again double vanishing boundary conditions, we get

$$\sigma = \frac{\partial_0 \pi_B}{q\mu} r \varphi', \quad \text{and} \quad \alpha_0 = \frac{1}{q} \left(\partial_0 \pi + \frac{\sqrt{2}}{\mu} r^2 \psi' \partial_0 \pi_B \right). \quad (3.27)$$

It should be noted that, in order for the above solution to go to zero at the center of AdS, the derivatives of the background profiles must vanish fast enough. This is what is found, for example in [53, 57].

If now we plug the solutions found so far into the quadratic action (3.20) and use the equations of motion for the background, we find that the action reduces to a purely boundary term given by

$$S^{(2)} = \frac{(d-1)(d-2)\rho}{2q^2\mu} \int d^d x \left[\dot{\pi}_B^2 - \frac{1}{d-1} (\vec{\nabla} \pi_B)^2 \right] + S_{\text{bdy}}^{(2)}. \quad (3.28)$$

As one can see, we are almost done. Unfortunately, for a complex field, the boundary term S_{bdy} does not have a universal expression valid for all dimensions. Nevertheless, we will now argue that it cannot contribute to the above action. At lowest order in boundary derivatives, the most general boundary action can be written as

$$S_{\text{bdy}} = \int_{r \rightarrow \infty} d^d x \mathcal{L}_{\text{bdy}} [\Phi, D_M \Phi, F_{MN}], \quad (3.29)$$

where \mathcal{L}_{bdy} is an analytic function of gauge and diff invariant combinations of its arguments and their derivatives.

For the sake of our argument, it is more convenient to redefine the radial coordinate as $r = 1/u$, so that all the metric components are on equal footing, $g^{MN} \sim u^2$.

In this coordinates the boundary is at $u = 0$. Now notice that pairs of indices can be contracted with g^{MN} , while a single radial index can also be contracted with the vector normal to the boundary $n^M \sim u$. It then follows that each free covariant index carries a factor of u . Close to the boundary the fields and their derivatives will then behave as

$$\Phi \sim u^\Delta, \quad D_u \Phi \sim u^\Delta, \quad D_\mu \Phi \sim u^{\Delta+1}, \quad F_{u\mu} \sim u^{d-1}, \quad (3.30)$$

while, instead, $F_{\mu\nu}$ is of higher order in boundary derivatives. One can easily check that the above scalings are correct for both the background fields and their fluctuations. The most general gauge and diff invariant lagrangian term can be written schematically as

$$\sqrt{-\gamma} \Phi^n (D_M \Phi)^m (F_{MN})^\ell \sim u^{-d+(n+m)\Delta+\ell(d-1)}, \quad (3.31)$$

where the free indices should be thought of as being contracted with either g^{MN} or n^M . The estimate above is the most conservative one (lowest possible power of u for $u \rightarrow 0$).

Gauge invariance imposes that the boundary term includes an equal number of Φ and Φ^* fields. This means that $n + m = 2\kappa$, with $\kappa \geq 0$. But then the combination (3.31) always vanishes at the boundary. In fact, since $\Delta > d/2$ we have

$$-d + 2\kappa\Delta + \ell(d-1) > (\kappa-1)d + \ell(d-1) \geq 0, \quad (3.32)$$

for $d > 2$. Moreover, in the case when $\kappa = 0$, diff invariance forces $\ell \geq 2$ and again $-d + \ell(d-1) > 0$.

Now that we have proved that the boundary term does not contribute to the

on-shell action, Eq. (3.28) finally reduces to

$$S^{(2)} = \frac{(d-1)(d-2)\rho}{2q^2\mu} \int d^d x \left[\dot{\pi}_B^2 - \frac{1}{d-1} (\vec{\nabla} \pi_B)^2 \right], \quad (3.33)$$

which is indeed the action for the phonon of a conformal superfluid, with sound speed $c_s^2 = 1/(d-1)$, as expected from Eq. (3.15).

Note that, with our conventions, $\rho/\mu > 0$, hence ensuring that for $d > 2$ the overall coefficient is positive and the Goldstone bosons are not ghost-like. Moreover, our argument does not hold for $d = 2$ since the asymptotic behavior of the fields is not regular anymore. However, in this particular case we do not expect Goldstone modes in the first place, in compliance with Coleman's theorem [64, 65].

Moreover, it should be pointed out that the boundary Goldstone is here nothing but the Wilson line of the radial component of the gauge field fluctuation—see Eq. (3.23). This same result is also found in several different contexts as, for example, a bulk Einstein-Maxwell theory [62], holographic fluids [61] and pions in holographic QCD [66].

3.3 Summary

In this chapter we have provided an explicit, analytical proof that a theory of scalar QED in AdS is dual to a superfluid on the conformal boundary. In particular, we have done that by explicitly solving the equations of motion for all the bulk fluctuations except for the the only gapless one, i.e. the scalar phase π .

Of course, given the vast number of other proofs developed during the years, no sane person would have argued the opposite. The relevance of our proof actually lies in the technique employed to derive it. In order to find the on-shell fluctuations we did not need the detailed knowledge of the background profile. This comes as a blessing given that, in most of the interesting cases, the background equations of

motion are nonlinear and an analytic solution is rarely available.

As we will see in the next chapter, thanks to the experience gained with this toy model, we will be able to employ the same method to derive the gravity dual of a solid, which is a true novelty.

Holographic solids

As explained in the previous chapters, the holographic duality is a powerful statement that has been used to explore (among other things) a great variety of condensed matter systems, many of which are quite exotic. Nevertheless, one, very simple class of systems have been essentially lacking from the literature: solids. The gravity dual of a theory in a solid state has never been found (or essentially looked for) so far. Some attempts in this direction have been made in [67–70], where the authors try to describe a solid state on the boundary theory via a theory of massive gravity in the bulk. The approach is rather interesting and indeed reproduces some properties of the boundary theory that closely resemble those expected from a solid. However, it is rather unclear whether the rigorous application of the holographic dictionary would tell that massive gravity corresponds to a dual theory with the right symmetries to describe a solid. Furthermore, beyond some interesting indications, no actual proof of the duality has been presented.

In this chapter we will exhibit a clear gravity dual for a solid in d spacetime dimensions, providing an analytical proof of the duality. We will find that the corre-

sponding theory on the gravity side is that of an $SO(d)$ magnetic monopole coupled to a scalar field in the fundamental representation. It would be a missed opportunity not to dub such a configuration *solidon*. Some hints of this duality could have been found in the results reported in [71, 72]. We will also compute the free energy of our solidon and show that indeed the boundary system undergoes a first order solid-to-liquid phase transition as expected. This work has been presented in [73].

4.1 Conformal solids and solids on a sphere

How does the holographic dictionary apply to the symmetries of a solid? In Chapter 1 we explained that the symmetry breaking pattern of a solid in d spacetime dimensions requires an internal $ISO(d-1)$ group. The holographic duality would tell us to take this global symmetry and gauge it in the bulk. However, one quickly realizes that it is not such an easy task. In particular, $ISO(d-1)$ is a noncompact group (because of the shifts) which is nonlinearly realized, and to find its gauged, Yang-Mills version is not a trivial task. In Appendix B we show how to build linear representations of the Euclidean group and to deduce the gauged version of our $ISO(d-1)$ symmetry. Nevertheless, in this chapter laziness wins over cleverness and we take a different approach. In particular, we will consider at first a solid on a sphere¹. In this case, the original shifts compactify and become additional rotations, and the symmetry group becomes $SO(d)$. The Yang-Mills theory for such a symmetry is very standard and allows us to readily deduce the gravity dual. Once this is done, we can focus our attention to a region close to the pole of our sphere and recover a flat solid.

Given the program spelled out above, we need to take two preliminary steps. First of all, we have to understand what to expect from a conformal solid, and secondly, we have to write down the effective theory for a solid on a sphere.

¹Note that this is not a spherical solid, like a marble, but rather a solid living on a spherical manifold, like a spherical thin shell.

Conformal solids

Just like we did for holographic superfluids, we now want to check what the implications of conformal symmetry are for a solid. This will again be our way to check whether or not we are doing everything correctly. Whether or not there exist CFTs that admit a solid state is still an open question. Note also that people familiar with crystalline structures might find the idea of a conformal solid rather unusual, given the natural length scale provided by the microscopic lattice spacing. However, for a solid with an underlying lattice, conformal symmetry would simply imply that all possible lattice spacings are allowed.

If we assume that we have a CFT in a solid state, then conformal invariance forces the stress tensor to be traceless. From Eq. (1.39) one deduces

$$\begin{aligned}
T_{\mu}^{\mu} &= -2 \frac{\partial F}{\partial B^{IJ}} B^{IJ} + dF = -2F_X \frac{\partial X}{\partial B^{IJ}} B^{IJ} - 2 \sum_{n=2}^{d-1} \frac{\partial F}{\partial Y_n} \frac{\partial Y_n}{\partial B^{IJ}} B^{IJ} + dF \\
&= -2XF_X - 2 \sum_{n=2}^{d-1} \frac{\partial F}{\partial Y_n} \left(\frac{n(B^{n-1})_{IJ}}{X^n} - \frac{nY_n}{X} \delta^{IJ} \right) B^{IJ} + dF \\
&= -2XF_X + dF = 0,
\end{aligned} \tag{4.1}$$

which fixes the dependence of the lagrangian on X for every field configuration, i.e.

$$F = X^{d/2} f(Y_2, \dots, Y_{d-1}). \tag{4.2}$$

As for the case of the superfluid, this has consequences for the sound speeds. In particular, from equations (1.41) one easily finds that the longitudinal and transverse speeds must be related to each other:

$$c_L^2 = \frac{1}{d-1} + 2 \frac{d-2}{d-1} c_T^2. \tag{4.3}$$

In the absence of transverse modes ($c_T^2 = 0$) one recovers the sound speed of conformal

fluids and superfluids. In what follows we will treat this relation as the hallmark of conformal solids.

It is interesting to note that in the absence of instabilities or superluminalities, Eq. (4.3) implies that for a conformal solid

$$0 \leq c_T^2 \leq 1/2 \quad \text{and} \quad \frac{1}{d-1} \leq c_L^2 \leq 1. \quad (4.4)$$

Consequently, a conformal solid is always a relativistic system, hence hardly realizable in the lab. This is also confirmed by the fact that the vanishing of the trace for the stress energy tensor implies that pressure and energy density are of the same order of magnitude. From a certain viewpoint, a conformal solid is closer to a fluid than the solids we are used to in everyday life. The reason is that for common solids one can have a nonzero density but zero pressure (e.g. your seat is not expanding underneath you). For a conformal solid that is not possible.

EFT for solids on a sphere

Let us now work out the effective theory for solids on a sphere. In order for this effective theory to make sense we must consider a sphere with a radius much larger than the UV cutoff, otherwise there would be no range of energies for which we could actually talk about collective modes. Moreover, if our solid presents an underlying crystalline structure, dislocations will arise because of the curvature of the manifold. We assume that we can ignore such effects if they are fairly sparse and homogeneously distributed.

The internal symmetry group is now $SO(d)$. The comoving coordinates, ϕ^I will now be $d - 1$ angles that, at equilibrium, can be chosen to coincide with the physical

angles, i.e.

$$\langle \phi^I \rangle = \theta^I. \quad (4.5)$$

Exactly as for a flat solid, this vacuum expectation value breaks the isometries of the sphere and the internal $SO(d)$ (as well as the usual boosts) down to the diagonal subgroup. The main difference with respect to a solid in flat space is the absence of the free parameter α —see below Eq. (1.36). Such freedom is due to the fact that a flat, homogeneous and isotropic solid can be compressed, dilated or sheared, which corresponds to varying continuously α or turning it into a matrix. For a solid on a sphere this cannot be done without spoiling homogeneity. For example, if we want to compress one pole we would end up stretching the opposite one.

An effective action for the ϕ^I fields that is invariant under $SO(d)$ can again be written in terms of the matrix $B^{IJ} = \partial_\mu \phi^I \partial^\mu \phi^J$. In this case, spacetime indices are contracted with the metric for $\mathbb{R} \times S^{d-1}$, while the internal ones are contracted with the following metric in field space:

$$g_{IJ}(\phi) = \text{diag} \left(1, \sin^2 \phi_1, \dots, \prod_{n=1}^{d-2} \sin^2 \phi_n \right). \quad (4.6)$$

The most general action will again be a function of the invariants built out of B^{IJ} .

However, as far as the application of the holographic dictionary is concerned, the most transparent way of writing down the EFT is to think about the $(d-1)$ -dimensional sphere as being embedded in a d -dimensional flat space. One can then introduce a real multiplet $\vec{\Phi}(x)$ in the fundamental representation of $SO(d)$. This scalar will acquire a vev in the radial direction, that we can parametrize as

$$\langle \vec{\Phi} \rangle = \Phi_0 R(\theta) \cdot \hat{x}_d, \quad (4.7)$$

with \hat{x}_d being the normal vector pointing along the x_d -axis. Let us now replace the angles θ^I with the comoving coordinates ϕ^I . Then the traces of powers of the matrix $\mathcal{B}^{IJ} = \partial_\mu \Phi^I \partial^\mu \Phi^J$ are invariant under $SO(d)$, which is realized linearly on $\vec{\Phi}$ and nonlinearly on the ϕ 's. The most general effective action is then

$$S = \mathcal{R}^{d-1} \int dt d\Omega_{d-1} F(X, Y_2, \dots, Y_{d-2}), \quad (4.8)$$

where X and Y_n are defined as in Eq. (1.37) but now using \mathcal{B}^{IJ} , and \mathcal{R} is the radius of the sphere.

To recover the EFT for flat solids, one can look at a patch of the sphere with size much smaller than the sphere radius, i.e. such that $\theta^I = x^I/\mathcal{R}$, with $|x^I| \ll \mathcal{R}$. For an observer who only has access to momenta $k \gg 1/\mathcal{R}$, it is impossible to probe the global properties of the manifold. For such an observer $\alpha \equiv 1/\mathcal{R}$ effectively plays the role of a free parameter, to be eventually determined by boundary conditions. In this limit we indeed find again that $\langle \phi^I \rangle = \alpha x^I$.

4.2 Meet the solidon

In this section we will describe our gravity dual. We will start at first with the case of AdS space with a spherical boundary but then we will focus our attention on a small patch of such a boundary, to recover the EFT of flat solids.

Setup

The holographic dictionary tells us to take the global symmetries of the boundary theory and gauge them in the bulk. In light of what discussed in the previous section, we will consider the following action for an $SO(d)$ Yang-Mills theory coupled to a

real scalar in the fundamental representation, i.e.

$$S = - \int d^{d+1}x \sqrt{-g} \left[\frac{1}{2} D_M \vec{\Phi} \cdot D^M \vec{\Phi} + V(|\vec{\Phi}|^2) + \frac{1}{8} F_{MN}^{AB} F^{AB MN} \right] + S_{\text{bdy}}, \quad (4.9)$$

where, as in Chapter 3, the scalar potential is kept generally of the form

$$V(|\vec{\Phi}|^2) = \frac{m^2}{2} |\vec{\Phi}|^2 + \text{interaction terms}. \quad (4.10)$$

Although we will keep the interaction terms unspecified, later on in our analysis we will restrict the range of masses. For later convenience, we also choose to work in the notation where $A, B, \dots = 1, \dots, d$ are indices in the fundamental representation. With this choice, the real generators of the fundamental representation are given by

$$T_{IJ}^{AB} = \delta_J^A \delta_I^B - \delta_I^A \delta_J^B. \quad (4.11)$$

The group algebra is

$$[T^{AB}, T^{CD}] = \frac{1}{2} f^{ABCDEF} T^{EF}, \quad (4.12)$$

where the structure constants are

$$\begin{aligned} f^{ABCDEF} = & \delta^{AC} \delta^{BE} \delta^{DF} + \delta^{AE} \delta^{BD} \delta^{CF} \\ & - \delta^{AD} \delta^{BE} \delta^{CF} - \delta^{AE} \delta^{BC} \delta^{DF} - (E \leftrightarrow F). \end{aligned} \quad (4.13)$$

Moreover, from now we will use $i, j, \dots = 1, \dots, d-1$. Although a bit heavier than the usual notation with indices in the adjoint representation, this will allow an easier classification of the quantum numbers of our fluctuations.

In order to study the spectrum of the phonons we will neglect backreaction and consider the zero temperature case. Thus we take our background metric in global

coordinates to be

$$ds^2 = - (1 + \rho^2) d\tau^2 + \frac{d\rho^2}{1 + \rho^2} + \rho^2 d\Omega_{d-1}^2, \quad (4.14)$$

where we set again $L = 1$. Again, we will assume to be working with scalar field potentials that are consistent with this approximation—see discussion below Eq. (3.9).

We now have to select our ansatze for the background fields. The scalar field profile is simply inspired by the discussion done in the previous section, Eq. (4.7), while for the gauge field we consider a generalization of the ‘t Hooft-Polyakov monopole [74].

In particular

$$\vec{\Phi} = \varphi(\rho)\hat{\rho}, \quad A_M^{AB} = \rho\psi(\rho)\partial_M\hat{\rho} \cdot T^{AB} \cdot \hat{\rho}, \quad (4.15)$$

where $\hat{\rho}$ is a unit vector pointing towards the boundary of AdS. The corresponding equations of motion are given by

$$\varphi'' + \frac{(d-1) + (d+1)\rho^2}{\rho(1+\rho^2)}\varphi' - \frac{2V'(\varphi^2)}{1+\rho^2}\varphi - (d-1)\frac{(1+q\rho\psi)^2}{\rho^2(1+\rho^2)}\varphi = 0, \quad (4.16a)$$

$$\begin{aligned} \psi'' + \frac{(d-1) + (d+1)\rho^2}{\rho(1+\rho^2)}\psi' + \frac{(d-3) + (d-1)\rho^2}{\rho^2(1+\rho^2)}\psi \\ - (d-2)\frac{(1+q\rho\psi)(2+q\rho\psi)}{\rho^2(1+\rho^2)}\psi - q\frac{1+q\rho\psi}{\rho(1+\rho^2)}\varphi^2 = 0. \end{aligned} \quad (4.16b)$$

Close to the boundary we again have

$$\varphi = \frac{\varphi_{(1)}}{\rho^{d-\Delta}} + \frac{\varphi_{(2)}}{\rho^\Delta} + \dots, \quad \psi = \frac{\psi_{(1)}}{\rho} + \frac{\psi_{(2)}}{\rho^{d-1}} + \dots \quad (4.17)$$

What about boundary conditions? We are looking for spontaneous breaking of our symmetry, which means that the sources associated with charged operators must vanish. While in the superfluid case the $U(1)$ photon did not carry charge, here the nonabelian gauge field does. It then follows that we must impose $\psi_{(1)} = 0$. For

the scalar field the situation is a bit more subtle. In particular, in the absence of a temporal component for the gauge field, which provides an effective negative mass square, the scalar field cannot condense by itself. This essentially means that the only solution consistent with either $\varphi_{(1)} = 0$ or $\varphi_{(2)} = 0$ is the trivial one, as it can be checked numerically.

We are therefore forced to introduce mixed boundary conditions, where both falloffs are nonzero. This means that both falloffs must be normalizable and hence the allowed range of masses is $-d^2/4 < m^2 < -d^2/4 + 1$. The source of the dual operator will be given by $J_\Phi \propto \varphi_{(2)} - f|\varphi_{(1)}|^{\nu-1}\varphi_{(1)}$, where ν is some number and f is the coupling associated with the multitrace operator (see Section 2.2). Our boundary conditions will then be $J_\Phi = 0$. In particular, for $\nu = \Delta/(d - \Delta)$ they will preserve conformal symmetry on the boundary. These boundary conditions correspond to deforming the QFT with the following operator

$$\Delta S[\mathcal{O}] = f \int d^d x |\vec{\mathcal{O}}(x)|^{\nu+1}. \quad (4.18)$$

In general, this deformation should be analytic in the operator $\vec{\mathcal{O}}$, in order for the conformal vacuum $\langle \vec{\mathcal{O}} \rangle = 0$ to exist, so that it is indeed possible to regard the boundary theory as a UV completion of our EFT for solids. This forces ν to be an odd positive integer. Nevertheless, as long as we are interested in states that are far away from the conformal vacuum (as for the study of phonons) we can keep it general.

The boundary conditions described above are achieved with the following boundary term

$$S_{\text{bdy}} = -\frac{d - \Delta}{2} \int_{\rho \rightarrow \infty} d^d x \sqrt{-\gamma} |\vec{\Phi}|^2 - \frac{2\Delta - d}{\nu + 1} f \int d^d x |\vec{\Phi}_{(1)}|^{\nu+1} + O(\partial_\mu^2), \quad (4.19)$$

where again $\gamma_{\mu\nu}$ is the induced metric on the boundary, and $O(\partial_\mu^2)$ stands for higher order terms. Such terms can always be neglected in our analysis because the back-

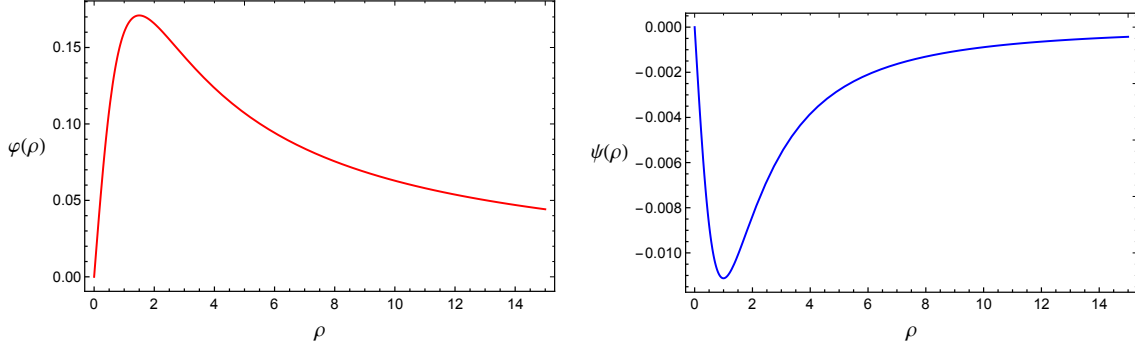


Figure 4.1: Background profiles for the scalar (left panel) and gauge (right panel) fields. The solution is obtained for $d = 3$, $V(\varphi^2) = -\varphi^2$ and $q = 1$. The gauge field satisfies $\psi_{(1)} = 0$, while the scalar satisfies $\varphi_{(2)} = f\varphi_{(1)}$ with $f = -1.8$.

ground will not depend on the boundary coordinates x_μ , while for the fluctuations we will be implementing a low energy expansion. The first falloff is defined as $\vec{\Phi}_{(1)} = \lim_{\rho \rightarrow \infty} \rho^{d-\Delta} \vec{\Phi}$.

The equations of motion (4.16) are both of second order and therefore we need four integration constants. Again, we will impose regularity in the interior of AdS, which fixes two of them. The remaining two are fixed by setting to zero the sources associated with the scalar and gauge field. This means that, for a given coupling of the multitrace operator, our theory will have no free parameters. This is in line with the absence of free parameters in the EFT for solids on a sphere (see Eq. (4.5)).

In Figure 4.1 we report an example of solutions for the background profiles.

A convenient gauge transformation

In the next section we want to restrict our attention only to a region close to a pole of our sphere, in order to recover the results for a flat solid. Before doing that, it is convenient to perform a gauge transformation in the bulk. The radial vector can be obtained starting from \hat{x}_d as $\hat{\rho} = R \cdot \hat{x}_d$, with $R = \prod_{i=1}^{d-1} \exp \left[\left(\theta_i - \frac{\pi}{2} \right) T^{id} \right]$. At this point we can perform a gauge transformation on the profiles (4.15) with element R^{-1} .

The resulting profiles are

$$\vec{\Phi} = \varphi(\rho) \hat{x}_d, \quad (4.20a)$$

$$A_M^{AB} = \rho \psi(\rho) (R^{-1} \cdot \partial_M R \cdot \hat{x}_d)^T \cdot T^{AB} \cdot \hat{x}_d - \frac{1}{2q} \text{tr} (R^{-1} \cdot \partial_M R \cdot T^{AB}). \quad (4.20b)$$

This is nothing but the gauge transformation that brings from a 't Hooft-Polyakov solution in the so called hedgehog gauge to a Dirac monopole [74].

Flat limit

We can now finally take the flat limit and study our solidon in a small region close to one of the poles. In order to do so we need to change from global coordinates to Poincaré patch coordinates. This can be achieved with the following change of variables:

$$\rho = \mathcal{R} r, \quad \tau = t/\mathcal{R}, \quad \theta_i = \frac{\pi}{2} - \frac{x_i}{\mathcal{R}}, \quad (4.21)$$

and by taking the large \mathcal{R} limit [71]. This corresponds to zooming in close to the x_d -axis. Indeed, the metric becomes

$$ds^2 = -r^2 dt^2 + \frac{dr^2}{r^2} + r^2 d\vec{x}_{d-1}^2 + O(\mathcal{R}^{-2}), \quad (4.22)$$

and the matter fields become

$$\vec{\Phi} = \varphi(r) \hat{x}_d, \quad A_M^{AB} = r \psi(r) T_{id}^{AB} \delta_M^i + O(\mathcal{R}^{-2}). \quad (4.23)$$

Note that, with a little abuse of notation, we have relabeled the background profiles as $\varphi(\mathcal{R}r) \rightarrow \varphi(r)$ and $r\psi(\mathcal{R}r) - \frac{1}{\mathcal{R}q} \rightarrow r\psi(r)$. In particular, now the gauge field does not vanish at the boundary anymore but it goes to a constant, $\psi_{(1)} \equiv 1/(\mathcal{R}q)$, which now

plays the role of a free parameter, very much like the chemical potential of holographic superfluids. As already mentioned, there is actually a smarter way to deduce the ansatze (4.23) in Poincaré patch. Nevertheless, we believe the derivation presented here is more pedagogical. The alternative derivation can be found in Appendix B.

In Poincaré patch the equations of motion for the background fields are considerably simpler. They are given by

$$\varphi'' + \frac{d+1}{r}\varphi' - (d-1)\frac{q^2\psi^2}{r^2}\varphi - 2\frac{V'(\varphi^2)}{r^2}\varphi = 0, \quad (4.24a)$$

$$\psi'' + \frac{d+1}{r}\psi' + \frac{d-1}{r^2}\psi - \frac{q^2\varphi^2}{r^2}\psi - (d-2)\frac{q^2\psi^3}{r^2} = 0. \quad (4.24b)$$

As for the superfluid, an analytical solution to these nonlinear equations is not available. Nevertheless, we will be able to solve for the fluctuations of the bulk fields as a function of the previous profiles and we will be able to find the partially on-shell action anyway.

4.3 Phonons of the boundary theory

Let us now introduce the fluctuations of the bulk fields. We will parametrize them as a global $SO(d)$ modulation of the symmetry breaking vev but with local transformation parameters [12]. In particular, we have

$$\vec{\Phi} = (\varphi + \sigma)\mathcal{M} \cdot \hat{x}_d, \quad A_M = \mathcal{M} \cdot (\bar{A}_M + \alpha_M) \cdot \mathcal{M}^{-1}, \quad (4.25)$$

where the $SO(d)$ element is $\mathcal{M} = \exp(-\pi^i T^{id})$. The gauge field is here represented as a matrix in the adjoint representation.

Similarly to what we have done for the background profiles, we also perform a gauge transformation on the fields in Eq. (4.25). We choose the transformation

element to be precisely \mathcal{M}^{-1} , in order to obtain

$$\vec{\Phi} = (\varphi + \sigma)\hat{x}_d, \quad A_M^{AB} = \bar{A}_M^{AB} + \delta A_M^{AB}. \quad (4.26)$$

This is a much more convenient parametrization, since we embedded both the gauge field and the angular perturbations in a single field. Indeed, at linear order $\delta A_M^{AB} = \alpha_M^{AB} - \frac{1}{q}\partial_M\pi^{AB}$, with $\pi^{id} = -\pi^{di} \equiv \pi^i$ and $\pi^{ij} = \pi^{dd} = 0$. At this point we still have the residual gauge freedom of applying a transformation generated by the T^{ij} only, under which the scalar field is invariant. We use this to also fix the fluctuations so that $\delta A_r^{ij} = 0$.

We are now ready to compute the partially on-shell action. We will again follow the procedure outlined below Eq. (3.20), with the low energy expansion implemented in the following way:

$$\sigma, \delta A_\mu^{AB}, \partial_r \sim O(1), \quad \partial_\mu \sim O(\epsilon), \quad \delta A_r^{id} \sim O(1/\epsilon). \quad (4.27)$$

At lowest order in energy, the linearized equations for the fluctuations read

$$\sigma'' + \frac{d+1}{r}\sigma' - (d-1)\frac{q^2\psi^2}{r^2}\sigma - 2\frac{V' + 2\varphi^2V''}{r^2}\sigma + 2\frac{q^2\varphi\psi}{r^3}\delta A_i^{id} = 0, \quad (4.28a)$$

$$\begin{aligned} \delta A_j^{id''} + \frac{d-1}{r}\delta A_j^{id'} + \frac{q^2\psi^2}{r^2} & \left[\delta A_i^{jd} - (d-3)\delta A_j^{id} - 2\delta_j^i\delta A_k^{kd} \right] \\ & - \frac{q^2\varphi^2}{r^2}\delta A_j^{id} + 2\frac{q^2\varphi\psi}{r}\delta_j^i\sigma = 0, \end{aligned} \quad (4.28b)$$

$$\delta A_t^{id''} + \frac{d-1}{r}\delta A_t^{id'} - (d-2)\frac{q^2\psi^2}{r^2}\delta A_t^{id} - \frac{q^2\varphi^2}{r^2}\delta A_t^{id} = 0, \quad (4.28c)$$

$$\delta A_r^{id} = 0. \quad (4.28d)$$

Eq. (4.28d) once again tells us that the gapless fluctuation is given by the Wilson line

of the radial component of the gauge field, i.e.

$$\pi^i = q \int_0^r dz \alpha_r^{id}(z). \quad (4.29)$$

Just like for the superfluid we will find that $\pi_B^i(x) \equiv \pi^i(r = \infty, x)$ will correspond to the Goldstone modes of the boundary theory.

Once again we will be able to rewrite the equations of motion for the fluctuations in terms of those for the background profiles, and their derivatives. Here δA_t^{id} is decoupled from all other fluctuations, and it is easy to show that the regular solution is given by $\delta A_t^{id} = c_t^i(x)r\psi$, with generic c_t^i . Indeed, plugging this into Eq. (4.28c), one gets back the background equation (4.24b). Imposing double vanishing boundary conditions both at the center and at the boundary of AdS we obtain

$$\delta A_t^{id} = -\frac{\partial_t \pi_B^i}{q\psi_{(1)}} r\psi(r). \quad (4.30)$$

This is again the only regular solution for our boundary conditions.

To solve for the other components is a much trickier business, given the complicated tensor structure. First of all let us decompose the fluctuations in irreducible representations of $SO(d)$, i.e.

$$\delta A_j^{id} = \frac{1}{d-1} \delta_j^i \delta A_k^{kd} + \frac{1}{2} \mathcal{A}_j^i + \frac{1}{2} \mathcal{T}_j^i, \quad (4.31)$$

where \mathcal{A}_j^i is antisymmetric and \mathcal{T}_j^i is symmetric and traceless. In this way, the equations of motion for the three combinations decouple from each other.

It is easy to show that the solution for the antisymmetric part is given by $\mathcal{A}_j^i = a_j^i(x)r\psi$, with generic a_j^i . Imposing the boundary conditions it becomes

$$\mathcal{A}_j^i = -\frac{\partial_j \pi_B^i - \partial_i \pi_B^j}{q\psi_{(1)}} r\psi(r). \quad (4.32)$$

Let us now turn to the trace part of Eq. (4.31). Since it is invariant under $SO(d)$, it has the same quantum numbers as the scalar fluctuation σ and, in fact, their equations are coupled. If one writes $\sigma = c(x)r\varphi'$ and $\delta A_i^{id} = -c(x)r^2\psi'/(d-1)$, the equations for these two fields reduce to a combination of Eqs. (4.24) and their derivatives. Thus, the two solutions are

$$\delta A_i^{id} = \frac{\partial_i \pi_B^i}{q\psi_{(1)}} r^2 \psi'(r), \quad \sigma = -(d-1) \frac{\partial_i \pi_B^i}{q\psi_{(1)}} r \varphi'(r). \quad (4.33)$$

We should now deal with the traceless symmetric part, \mathcal{T}_j^i . Unfortunately we will not be able to solve its equations of motion. Nevertheless, we will still constrain its behavior close to the conformal boundary. The corresponding equation of motion reads

$$\mathcal{T}_j^{i''} + \frac{d-1}{r} \mathcal{T}_j^{i'} - \frac{q^2 \varphi^2}{r^2} \mathcal{T}_j^i - (d-4) \frac{q^2 \psi^2}{r^2} \mathcal{T}_j^i = 0, \quad (4.34)$$

which cannot be rewritten in terms of background equations. However, we know that the most general expression close to the boundary will be

$$\mathcal{T}^{ij} = -\frac{\partial^{\{i} \pi_B^{j\}}}{q} + \frac{\mathcal{T}_{(2)}^{ij}(x_\mu)}{r^{d-2}} + \dots, \quad (4.35)$$

where the first falloff has been fixed by the boundary condition at $r = \infty$. With $\{\dots\}$ we represent the symmetric traceless combination of indices. Now, note that the tensor structure of Eq. (4.35) is trivial, i.e. all the components obey the same equation. Moreover, the equation only involves derivatives with respect to the holographic coordinate and the x_μ dependences do not couple. It then follows that Eq. (4.35) is just a second-order ordinary differential equation (ODE) for the radial dependence of each component of the tensor. Given its linearity, the second falloff must be proportional

to the first one. Hence we can write

$$\mathcal{T}_{(2)}^{ij} = -\frac{\psi_{(2)}}{q\psi_{(1)}} \lambda \partial^{\{i} \pi_B^{j\}} , \quad (4.36)$$

where the prefactor has been chosen for later convenience. Here λ is an integration constant that should be determined from the exact solution to the equation of motion. Its value will in general depend on the particular form of the background profiles.

We are almost at the end of our program. Once the on-shell fluctuations have been found (all but π^i), we can write down the partially on-shell action. Upon using the equations of motion, the quadratic action reduces to a purely boundary term given by

$$S^{(2)} = - \int_{r \rightarrow \infty} d^d x \sqrt{-g} g^{rr} \left[g^{\mu\nu} \frac{1}{2} \delta A_\mu^{id'} \delta A_\nu^{id} + g^{\mu\nu} \frac{1}{4} \delta A_\mu^{ij'} \delta A_\nu^{ij} + \frac{1}{2} \sigma \sigma' \right] + S_{\text{bdy}}^{(2)} , \quad (4.37)$$

with $S_{\text{bdy}}^{(2)}$ given by the terms in the boundary action (4.19) that are quadratic in the fluctuations.

The second term in square brackets does not contribute to the phonon action since $\pi^{ij} = 0$, and we can thus neglect it. The scalar fluctuation instead enters both the last term in square brackets and the boundary term. Together they give a contribution that is proportional to the following dimensionless quantity:

$$\Sigma \equiv \frac{(d-1)^2(d-\Delta)^2(2\Delta-d)}{d-2} \left[\frac{\Delta}{d-\Delta} - \nu \right] \frac{f|\varphi_{(1)}|^{\nu+1}}{\psi_{(1)}\psi_{(2)}} , \quad (4.38)$$

which vanishes exactly when the boundary conditions preserve the conformal invariance of the boundary theory, i.e. for $\nu = \Delta/(d-\Delta)$ —see Section 4.2. Using the solutions in Eqs. (4.30), (4.32), (4.33) and (4.34) we finally obtain the action for the

boundary phonons

$$S^{(2)} = -\frac{d-2}{2} \frac{\psi_{(2)}}{q^2 \psi_{(1)}} \int d^d x \left\{ \dot{\pi}_B^2 - (\partial_k \pi_B^k)^2 - \frac{1}{2} [(\partial_j \pi_B^i)^2 - (\partial_k \pi_B^k)^2] - \frac{\lambda}{2} \left[(\partial_j \pi_B^i)^2 + \frac{d-3}{d-1} (\partial_k \pi_B^k)^2 \right] - \Sigma (\partial_k \pi_B^k)^2 \right\} \quad (4.39a)$$

$$= -\frac{d-2}{2} \frac{\psi_{(2)}}{q^2 \psi_{(1)}} \int d^d x \left\{ \dot{\pi}_L^2 + \dot{\pi}_T^2 - \left[1 + \lambda \frac{d-2}{d-1} + \Sigma \right] (\partial_j \pi_L^i)^2 - \frac{\lambda+1}{2} (\partial_j \pi_T^i)^2 \right\}, \quad (4.39b)$$

where the phonon field has been split into a longitudinal and a transverse component, $\vec{\pi}_B = \vec{\pi}_L + \vec{\pi}_T$. Our numerical analysis shows that the two gauge field falloffs, $\psi_{(1)}$ and $\psi_{(2)}$, have opposite sign, and hence, at least for some potentials, the Goldstones are not ghost-like.

The two sound speeds can be readily obtained from Eq. (4.39b). They are

$$c_T^2 = \frac{\lambda+1}{2}, \quad \text{and} \quad c_L^2 = 1 + \lambda \frac{d-2}{d-1} + \Sigma. \quad (4.40)$$

Their values will depend in a complicated way on the particular bulk theory under consideration. This is because both the integration constant λ and the parameter Σ depend on the background field profiles, and hence on the scalar potential. However, in the conformal case, $\Sigma = 0$, the speeds of sound are related to each other by

$$c_L^2 = \frac{1}{d-1} + 2 \frac{d-2}{d-1} c_T^2, \quad (4.41)$$

for *any* value of λ . This is precisely the relation anticipated in Section 4.1 for conformal solids. We interpret this as an analytical proof that our gravity dual is indeed the right one.

4.4 Melting the solidon

We just argued that our solidon is indeed dual to a solid on the boundary of AdS. A very natural question that one might want to answer is then: does our solid melt? To answer it we need to turn on temperature, but there are first a few subtleties to be addressed. First of all we will move back to global coordinates, where we are confident that the global properties of our fields are well defined. Secondly, since now we want to look for a transition between a spontaneously broken phase, $\langle \vec{\mathcal{O}} \rangle \neq 0$, and the conformal vacuum, $\langle \vec{\mathcal{O}} \rangle = 0$, we need to introduce in our theory a multitrace deformation that is analytic in $\vec{\mathcal{O}}$. This means that the boundary conditions must be $\varphi_{(2)} = f\varphi_{(1)}^\nu$ with ν odd. In particular, we will choose $d = 3$ and $\nu = 1$, in which case the deformation is *relevant*.

At this stage we reintroduce backreaction. We parametrize the metric as

$$ds^2 = -(1 + \rho^2)h(\rho)g(\rho)dt^2 + \frac{h(\rho)}{g(\rho)} \frac{d\rho^2}{1 + \rho^2} + \rho^2 d\Omega_2^2. \quad (4.42)$$

We also consider the case of a free scalar with $m^2 = -2$, which is safely above the Breitenlohner-Freedman bound [45]. Lastly, we set $q = 1$ for simplicity. The equations of motion for the background profiles now read

$$\varphi'' + \left(\frac{2 + 4\rho^2}{\rho(1 + \rho^2)} + \frac{g'}{g} \right) \varphi' + \frac{2h}{(1 + \rho^2)g} \varphi - \frac{2h(1 + \rho\psi)^2}{g\rho^2(1 + \rho^2)} \varphi = 0, \quad (4.43a)$$

$$\begin{aligned} \psi'' + \left(\frac{2 + 4\rho^2}{\rho(1 + \rho^2)} + \frac{g'}{g} \right) \psi' + \left(\frac{2}{1 + \rho^2} + \frac{g'}{\rho g} \right) \psi - \frac{h(1 + \rho\psi)(2 + \rho\psi)}{g\rho^2(1 + \rho^2)} \psi \\ - \frac{h(1 + \rho\psi)}{g\rho(1 + \rho^2)} \varphi^2 = 0. \end{aligned} \quad (4.43b)$$

Einstein's equations can instead be combined to yield the following first order equa-

tions for h and g :

$$g' + \frac{1+3\rho^2}{\rho(1+\rho^2)}g - \frac{1+3\rho^2}{\rho(1+\rho^2)}h + \frac{\psi^2(2+\rho\psi)^2 + 2\varphi^2(1-\rho^2 + 2\rho\psi + \rho^2\psi^2)}{2\rho(1+\rho^2)}h = 0, \quad (4.44a)$$

$$h' - \left(\frac{\rho}{2}\varphi'^2 + \frac{(\psi + \rho\psi')^2}{\rho} \right)h = 0. \quad (4.44b)$$

Einstein's equations also present a second order one which, however, can be derived from the ones above. Note that we again set $L = 1$ as well as $M_p = 1$. This can be done by an appropriate rescaling of the fields as well as of the Planck mass, the AdS radius and the couplings q and f (see [73]).

In Section 2.4 we learned that there are two possible ways to introduce temperature in the bulk. We could either compactify the Euclidean time (a so called *thermal soliton*) for our solidon configuration, or place the solidon on a black hole background. It can be shown numerically that, for every fixed f , there is always a minimum temperature below which the black hole solution ceases to exist—i.e. there are no solutions with the prescribed boundary conditions—which is in contrast with the fact that solids at zero temperature do exist. We will therefore simply consider the case of a thermal solidon.

Let us now solve the equations in the bulk. Regularity fixes three out six free parameters, and the remaining ones can be taken to be $\varphi'(0)$, $\psi'(0)$ and $g(0)$. Close to the boundary, the asymptotic behaviors are

$$\varphi = \frac{\varphi_{(1)}}{\rho} + \frac{\varphi_{(2)}}{\rho^2} + \dots, \quad (4.45a)$$

$$\psi = \frac{\psi_{(1)}}{\rho} + \frac{\psi_{(2)}}{\rho^2} + \dots, \quad (4.45b)$$

$$g = g_{(0)} + \frac{g_{(0)}\varphi_{(1)}^2}{4\rho^2} + \frac{g_{(3)}}{\rho^3} + \dots, \quad (4.45c)$$

$$h = g_{(0)} - \frac{g_{(0)}\varphi_{(1)}^2}{4\rho^2} - \frac{2g_{(0)}\varphi_{(1)}\varphi_{(2)}}{3\rho^3} + \dots. \quad (4.45d)$$

As anticipated, we will use the three free parameters to impose $g_{(0)} = 1$, $\psi_{(1)} = 0$ and $\varphi_{(2)} = f\varphi_{(1)}$. Our life can be made easier by noticing that the equations of motion exhibit the following scaling symmetry

$$t \rightarrow t/a, \quad g \rightarrow ag, \quad h \rightarrow ah. \quad (4.46)$$

This can always be used to rescale a particular solution in order to achieve $g_{(0)} = 1$. The two free parameters left are $\varphi'(0)$ and $\psi'(0)$, and they can be used in a shooting algorithm to impose the two remaining boundary conditions.

It is well known that the free energy of the boundary theory is given by the on-shell Euclidean action of the bulk side, $F = TS_E$ (see e.g. [38, 40]), where the temperature is the inverse of the periodicity of time. Notice that our background does not depend on time, and hence we can set our system to any temperature we want. The complete on-shell Euclidean action is given by

$$S_E = - \int d^4x_E \sqrt{g_E} \left[\frac{R}{2} + 3 + \mathcal{L}_m \right] + S_E^{\text{GH}} + S_E^{\text{c.t.}} + S_E^{\text{bdy}}. \quad (4.47)$$

Here \mathcal{L}_m is the lagrangian for the matter fields, R is the Ricci scalar for the bulk spacetime, and S_E^{bdy} is the Euclidean analogue of the action in Eq. (4.19). Moreover, S_E^{GH} and $S_E^{\text{c.t.}}$ are the Gibbons-Hawking [75] and counterterm [76] actions, which are needed to fix the variational problem and cure the divergences of the gravity part of the action. In our case, they are given by

$$S_E^{\text{GH}} = - \int_{\rho \rightarrow \infty} d^3x_E \sqrt{\gamma_E} K, \quad (4.48)$$

$$S_E^{\text{c.t.}} = \frac{1}{2} \int_{\rho \rightarrow \infty} d^3x_E \sqrt{\gamma_E} \left[4 + \mathcal{R} + \mathcal{R}^{\mu\nu} \mathcal{R}_{\mu\nu} - \frac{3}{8} \mathcal{R}^2 \right]. \quad (4.49)$$

Here, $K = n^\rho \partial_\rho \log \sqrt{\gamma_E}$ is the scalar extrinsic curvature of the boundary, γ_E the Euclidean induced metric, $n^\rho = 1/\sqrt{g_{\rho\rho}}$ the ρ -component of the vector normal to the

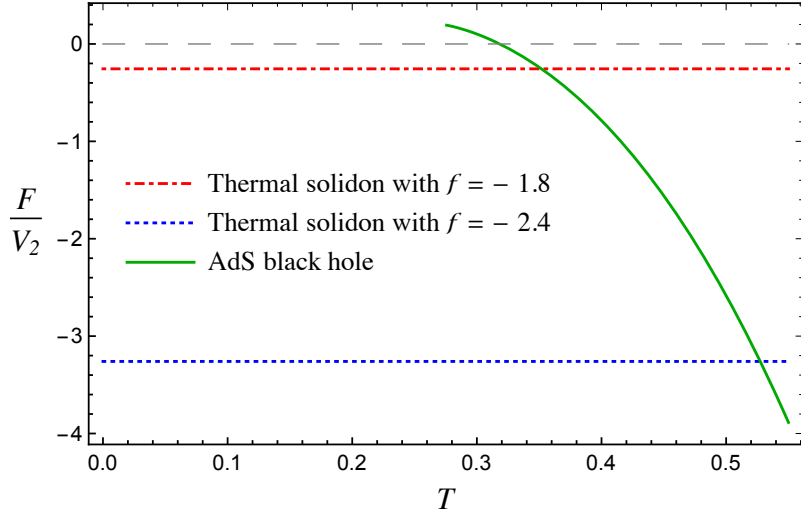


Figure 4.2: Comparison between the free energies of the solidon for two different values of the double trace coupling, and the free energy of SAdS. Below $T = \sqrt{3}/2\pi$ the black hole ceases to exist. The gray dashed line corresponds to pure AdS.

boundary, and $\mathcal{R}_{\mu\nu}$ the Ricci tensor built out of the induced metric.

The melting of our solid will correspond to a transition between a spontaneously broken phase and an unbroken one. We therefore need to compare the free energy of the solidon with that of a solution with $\varphi = 0$. Given that the source of the gauge field is set to zero as well, it turns out that the only possibility is the one for which $\psi = 0$ as well. Consequently we consider the simple Schwarzschild-AdS (SAdS) black hole. This is also very reasonable given that such a solution is well known to be dual to a fluid.

The result of this comparison is reported in Figure 4.2. It is evident that below a certain critical temperature our solidon is the preferred configuration. Moreover, the derivative of the free energy presents a discontinuity at the critical temperature, which is the hallmark of a first order phase transition. Indeed, the dual interpretation is that of a solid-to-liquid phase transition. Moreover, the fact that the free energy approaches a constant value at zero temperature is consistent with what expected from a solid [77].

Two comments are in order. First of all, it should be noticed that we ignored

the contribution of phonons to the free energy, since we are working solely with the background profiles. Phonons are expected to contribute with an additive term, $F_\pi \propto 2 \times T^3$, with 2 being the number of polarizations in $d = 3$ dimensions [77]. At low temperatures this contribution will be smaller than the constant term. Even though a more accurate analysis should include such a factor, unless the speed of sound is very small, we expect the large N_c^2 factor of the black hole free energy to ensure for the phase transition to happen anyway.

Secondly, one should be careful to make sure that the parameters of the solutions we are considering are such that they indeed allow for a large separation between the IR and UV cutoffs (see discussion in Section 4.1). Our IR cutoff is simply the inverse radius of the sphere, while the UV one is set by the energy density of our solution $\langle T_{00} \rangle$. Taking into account the fact that $1/N_c$ here plays the role of a coupling, the criterion to have a parametric separation between these cutoff is $\langle |T_{00}| \rangle / N_c^2 \gg 1/\mathcal{R}^3$. It can be checked that our results actually do not satisfy this requirement. Nevertheless, we showed in [73] that the results can be easily extrapolated to the correct regime, and that the conclusions remain unchanged.

4.5 Summary

In this chapter we have derived the gravity dual of a solid in d spacetime dimensions, which turned out to be an $SO(d)$ magnetic monopole coupled to a scalar in the fundamental representation. Such a solution can only be achieved with mixed boundary conditions, and we called it a *solidon*. The operators dual to the bulk fields realize precisely the symmetry breaking pattern of a solid, as explained in Chapter 1. To prove that this is indeed the case, we employed the techniques developed in Chapter 3 for holographic superfluids and we explicitly computed the action for the phonons of the boundary theory. We showed that in the conformal case we recover what is expected

from the EFT approach.

Moreover, we studied the melting of our solid: as the temperature is raised our solid undergoes a first order solid-to-liquid phase transition. The dual interpretation of this is a transition between the solidon and an SAdS solution. It is rather interesting to note that this happens for temperatures that are *larger* than the one at which the Hawking-Page phase transition occurs [78]. This seems to suggest that there might be strongly coupled theories that, at low temperatures, undergo a transition to a solid state rather than a confined one.

Our results have the nice feature of not only filling a gap in the zoology of holographic states of matters, but also of making explicit contact between the holographic language and the EFT one.

Lastly, we are not aware of any evident connection between our results and those presented in [67–70].

Vortex lines in superfluids

The developments of the previous chapters were mostly formal, given that the main goal was to recover the known EFT formulation from the holographic approach. The aim of this chapter is instead rather different and, at least to the very personal opinion of the author, more relevant. Here we try to convince the reader that the effective theory approach to condensed matter is now mature enough to be more than an interesting theoretical formulation of some well known problems. We will show that it can be used successfully as a powerful tool to describe the real world and that, in certain circumstances, it presents several advantages over more traditional methods. We will do so through a specific example, by studying the precession of a straight vortex in a confined superfluid. Such a phenomenon is well known and it has been the object of intense theoretical study [79–85]. Nevertheless, the EFT formulation will provide a particularly transparent explanation for it, and will allow us to derive it in a very simple and general way.

In order to do that, we will present an effective string theory for vortex lines in superfluids, and then explore its consequences in the presence of some external

trapping that spatially confines the system. Of course, writing down such an EFT is not an easy task, and it requires a fair amount of work and theoretical understanding. Nevertheless, it can be done once and for all. After the theory has been written down it can be used in a variety of contexts, and it often makes the theorist's life much easier.

The results of this chapter were presented in [86].

5.1 Vortices and their precession

Let us now summarize the main properties of vortices in superfluids, and describe the phenomenon of their precession in confined ultra cold atoms. Explaining this phenomenon will be the ultimate goal of this chapter.

A brief introduction to vortex lines

The vorticity of a superfluid is identically zero, given that its velocity field can be expressed as the gradient of a scalar, $\vec{v} = \vec{\nabla}\phi/m$, where m is the mass of the microscopic component of the superfluid. The possible motions of the condensate are therefore quite limited. One possibility is that of vortices [20, 87], i.e. string-like objects of atomic thickness, where the $U(1)$ symmetry is locally restored. They are the only degrees of freedom that can carry vorticity (which is localized on the line), and the velocity field around them is irrotational but nontrivial. For example, for a straight vortex configuration the velocity field away from the vortex has a $1/r$ profile. The circulation around the vortex line is quantized. In particular

$$\Gamma = \oint d\vec{\ell} \cdot \vec{v} = \frac{2\pi\gamma}{m}, \quad (5.1)$$

where γ is an integer. The possibility of quantized circulation was first introduced by Onsager in [88] and Feynman in [89].

The first indirect evidences for the existence of these objects were already obtained half a century ago in superfluid He-4 [90, 91], and they were later followed by several direct observations (see e.g. [92–96]).

Vortex precession

When a vortex is created off-axis in a confined superfluid (i.e. of finite size), it spontaneously starts orbiting around the axis of the cloud. Moreover, at least for vortices close enough to the center of the superfluid, if the cloud is circular, so is the orbit of the vortex line. If the cloud is elliptical the orbit will be elliptical as well, with the same aspect ratio. It is also interesting to note that to trigger the rotation no initial “push” is required. The simple fact that the vortex is located away from the center of the superfluid will force it to rotate. The explanation of this will be clear in the next section. The first observation of such a phenomenon (the so called *precession*) was made in [97] using a nearly spherical condensate of ^{87}Rb . A more recent analysis was instead reported in [98], where the authors studied the trajectory and precession frequency of a vortex line in an elliptical cloud of ^6Li . A representation of this phenomenon is reported in Figure 5.1.

An interesting peculiarity of this phenomenon is given by the magnitude of the precession frequency when the system is confined by an harmonic trapping. Suppose that the atom cloud is confined by some effective potential of the form

$$V(\vec{x}_\perp) = \frac{m}{2} (\omega_x^2 x^2 + \omega_y^2 y^2). \quad (5.2)$$

It can be shown that in this situation the precession frequency for a straight vortex

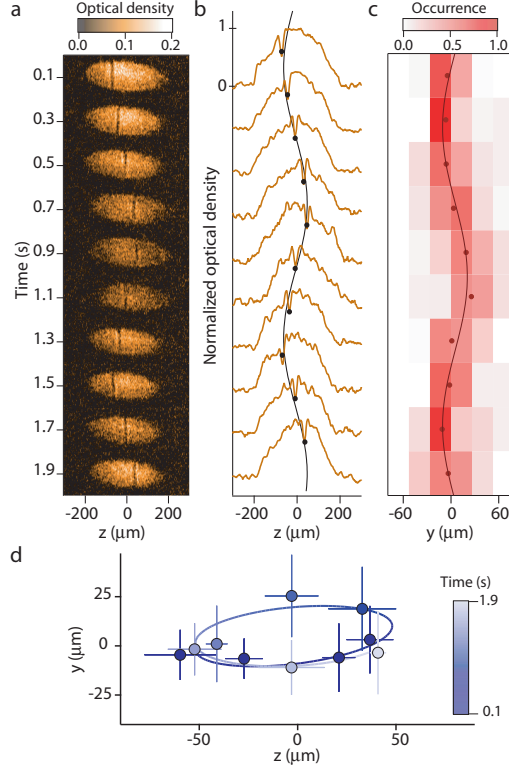


Figure 5.1: Experimental observation of the vortex precession as reported in [98]. (a) Tomographic image of a slice of the superfluid cloud along a direction parallel to the vortex line. The oscillatory motion of the vortex is evident. (b) Density profile of the cloud. The depletion corresponds to the position of the vortex, which is fitted by the black solid line. (c) Average vortex oscillation as seen in a plane perpendicular to the vortex axis. The average has been computed by repeating the experiment ~ 7 times for each slice in the y direction. (d) Vortex trajectory on the plane perpendicular to itself as a function of time. Note that, in this plot, the x axis has been labeled z . We prefer to keep our xy labeling for clarity with the following analysis.

is given by

$$\omega_p = \frac{3}{4} \frac{\omega_x \omega_y}{\mu} \log \left(\frac{R_\perp}{\xi} \right), \quad (5.3)$$

where μ is the chemical potential, R_\perp is the typical transverse size of the cloud, and ξ is the so called *healing length* [20], which can be thought of as the microscopic size of the vortex core. Given that $R_\perp \gg \xi$, the precession frequency is quite larger than the typical frequency of the system, which is set by either ω_x or ω_y . Such an enhancement is indeed observed experimentally [98].

It should be noted that different traditional approaches often disagree on the exact expression for Eq. (5.3) (see e.g. [79, 81, 82] and [83]). The experimental analyses are now refined enough to be able to discriminate between the different possibilities. We will show that our EFT approach easily recovers Eq. (5.3). As we will show, the vortex precession is due to long distance physics, rather than the microscopic one. This means that it follows essentially from the symmetries of the confined superfluid. In this cases the EFT methods are the most suitable ones, since they do not depend on the assumptions and approximations made for the microscopic dynamics.

5.2 One more EFT: vortex lines in superfluids

Let us now describe the effective theory for vortex lines in superfluids. The vortex thickness is comparable to the typical atomic scales; at much longer distances, the vortex can be described as a string coupled to the superfluid modes [99]. The development of such an EFT is an interesting topic per se, but to present it in all its details goes beyond the goal of this work. In the next few sections we will present those aspects that are of importance for the vortex precession. For all the other details the reader should refer to [99] (see also [100]).

An alternative action for the superfluid modes

As mentioned above, we will effectively describe the vortex line as a classical string. However, if we describe the superfluid modes with the single scalar ϕ presented in Section 1.4 we run into complications. In particular, in the presence of a vortex, the scalar field becomes the winding number around the vortex and it is therefore not single valued. This means that the leading coupling between ϕ and the string will contain at least one derivative. This is because derivatives of ϕ are single valued and can hence be used to write down local couplings.

Nevertheless, in $3 + 1$ dimensions, a theory of a scalar field with shift invariance always admits a dual description in terms of a 2-form field $\mathcal{A}_{\mu\nu}$ whose action is now invariant under the following gauge transformation [101, 102]:

$$\mathcal{A}_{\mu\nu} \rightarrow \mathcal{A}_{\mu\nu} + \partial_\mu \theta_\nu - \partial_\nu \theta_\mu. \quad (5.4)$$

The most general effective action for such a field, at lowest order in derivatives is given by

$$S = \int d^4x G(Y), \quad \text{with:} \quad Y = -F_\mu F^\mu \quad \text{and} \quad F^\mu = \frac{1}{2}\epsilon^{\mu\nu\rho\sigma}\partial_\nu\mathcal{A}_{\rho\sigma}, \quad (5.5)$$

where again $G(Y)$ is an a priori generic function. In Appendix C we show how to go from the scalar to the 2-form formulation of the system.

The action (5.5) describes the dynamics of the superfluid modes. In particular, the energy density, pressure and four-velocity are given by

$$\rho = -G(Y), \quad p = G(Y) - 2YG'(Y) \quad \text{and} \quad u_\mu = -\frac{F_\mu}{\sqrt{Y}}, \quad (5.6)$$

while $n = \sqrt{Y}$ is the superfluid number density.

The relation between F_μ and the old ϕ is given by $\partial_\mu\phi/\sqrt{X} = F_\mu/\sqrt{Y}$. From this relation we deduce that, on the background, it must be

$$\frac{1}{2}\epsilon^{ijk}\partial_i\langle\mathcal{A}_{jk}\rangle = -\bar{n}, \quad \frac{1}{2}\epsilon^{ijk}(2\partial_j\langle\mathcal{A}_{0k}\rangle - \partial_0\langle\mathcal{A}_{jk}\rangle) = 0, \quad (5.7)$$

which are solved, up to gauge transformations, by

$$\langle\mathcal{A}_{0i}\rangle = 0 \quad \text{and} \quad \langle\mathcal{A}_{ij}\rangle = -\frac{1}{3}\bar{n}\epsilon_{ijk}x^k. \quad (5.8)$$

This background profiles implement the superfluid symmetry breaking pattern in

the dual description. The fluctuations of the 2-form around equilibrium can be parametrized using two 3-vectors, \vec{A} and \vec{B} :

$$\mathcal{A}_{0i}(x) = \frac{\bar{n}}{c} A_i(x), \quad \mathcal{A}_{ij}(x) = \bar{n} \epsilon_{ijk} \left(-\frac{1}{3} x^k + B^k(x) \right), \quad (5.9)$$

where we have explicitly reintroduced the speed of light, c , to facilitate the nonrelativistic (NR) limit later on. The quadratic action for these fields now reads

$$S^{(2)} = \frac{\bar{w}}{c^2} \int d^3x dt \left\{ \frac{1}{2} (\vec{\nabla} \times \vec{A})^2 + \frac{1}{2} \left[\dot{\vec{B}}^2 - c_s^2 (\vec{\nabla} \cdot \vec{B})^2 \right] - \dot{\vec{B}} \cdot (\vec{\nabla} \times \vec{B}) \right. \\ \left. - \frac{1}{2\xi} (\vec{\nabla} \times \vec{B})^2 + \frac{1}{2\xi} (\vec{\nabla} \cdot \vec{A})^2 \right\}. \quad (5.10)$$

Here $\bar{w} = \bar{\rho} + \bar{p} = -2\bar{n}^2 G'(\bar{n}^2)$ is the background (relativistic) enthalpy density, while the sound speed is given by $c_s^2 = (2YG'' + G')/G'$, evaluated on the background as well. We also introduced the following gauge fixing term

$$S_{\text{g.f.}} = -\frac{\bar{w}}{\bar{n}^2} \int d^3x dt \frac{1}{2\xi} (\partial_i \mathcal{A}^{i\mu})^2. \quad (5.11)$$

From now on we will also work in the Landau gauge, $\xi \rightarrow 0$, which imposes $\partial_i \mathcal{A}^{i\mu} = 0$. This forces the \vec{A} field to be purely transverse, $\vec{\nabla} \cdot \vec{A} = 0$, and the \vec{B} field to be purely longitudinal, $\vec{\nabla} \times \vec{B} = 0$. In this gauge the mixing terms disappear from Eq. (5.10), and the two propagators are easily found to be

$$G_A^{ij}(k) = \frac{c^2}{\bar{w}} \frac{i(\delta^{ij} - \hat{k}^i \hat{k}^j)}{k^2}, \quad G_B^{ij}(k) = \frac{c^2}{\bar{w}} \frac{i \hat{k}^i \hat{k}^j}{\omega^2 - c_s^2 k^2}. \quad (5.12)$$

From here we can easily understand the physical meaning of these two new fields. The \vec{B} field describes a longitudinal mode that propagates at the speed of sound, i.e. nothing but the superfluid phonon. The \vec{A} field instead does not propagate any additional degree of freedom (there is no ω in its propagator), but can mediate long

distance interactions. It is very similar to the static Coulomb potential, and for this reason it is dubbed *hydraphoton* [103].

The action for the vortex line

The action in Eq. (5.5) describes the dynamics of the superfluid bulk modes, in the absence of any vortex line. In this section we introduce our string-like object, as well as its interactions with the \vec{A} and \vec{B} fields.

As already mentioned, when we are only interested in long distance phenomena, the vortex line can effectively be treated as a string, described by an embedding position $X^\mu(\tau, \sigma)$, where σ is a coordinate along the string itself. It is well known that the action for the string alone is given by a Nambu-Goto term [104], i.e.

$$S_{\text{NG}'} \propto \int d\sigma d\tau \sqrt{-\det(G_{\mu\nu}(X) \partial_\alpha X^\mu \partial_\beta X^\nu)}. \quad (5.13)$$

From now on α, β, \dots run over the worldsheet coordinates τ and σ . Here $G_{\mu\nu}(X)$ is *any* tensor that could play the role of a spacetime metric. In vacuum this can only be $G_{\mu\nu} = \eta_{\mu\nu}$, but in a Lorentz-violating background as ours we have different possibilities. In particular, there is now another gauge invariant object that can carry a Lorentz index, i.e. the superfluid four-velocity in Eq. (5.6). A perfectly valid metric could be any linear combination of $\eta_{\mu\nu}$ and $u_\mu u_\nu$, with coefficients that can in principle also depend on Y . One can at this point borrow a result from bi-gravity theories [105], i.e. that given two metrics, $g_{\alpha\beta}$ and $h_{\alpha\beta}$, the most general action that is diff invariant and with no derivatives is

$$\int d^d x \sqrt{-\det g} f((g^{-1} \cdot h)^\alpha_\beta), \quad (5.14)$$

where $f(M_\beta^\alpha)$ is a generic function¹.

For our worldsheet, the two possible metric tensors can be taken to be

$$g_{\alpha\beta} = \eta_{\mu\nu} \partial_\alpha X^\mu \partial_\beta X^\nu, \quad \text{and} \quad h_{\alpha\beta} = u_\mu u_\nu \partial_\alpha X^\mu \partial_\beta X^\nu. \quad (5.15)$$

It turns out that there is only one independent invariant that can be built out of these two tensors [99], i.e. the trace $g^{\alpha\beta} h_{\alpha\beta}$. Moreover, we can also include a generic dependence on the gauge invariant quantity Y . The action for a free string in the superfluid is then given by

$$S_{\text{NG}'} = - \int d\tau d\sigma \sqrt{-\det g} \mathcal{T}(g^{\alpha\beta} h_{\alpha\beta}, Y). \quad (5.16)$$

The function \mathcal{T} is essentially a generalization of the standard string tension.

This is not the end of the story. There is one more term that is gauge, Lorentz and reparametrization invariant², i.e. the direct coupling between the string and the bulk modes:

$$S_{\text{KR}} = \lambda \int d\tau d\sigma \mathcal{A}_{\mu\nu} \partial_\tau X^\mu \partial_\sigma X^\nu, \quad (5.17)$$

where the 2-form is computed on the string worldsheet, and KR stands for “Kalb-Ramond”. Here λ is an effective coupling which is related to the vortex circulation by $\lambda = \bar{w}\Gamma/\bar{n}$. The possibility to build the direct interaction (5.17) is the reason why we introduced the 2-form language in the first place. The same interaction written in terms of the scalar field ϕ will look highly nonlocal [100].

There are of course also higher derivative terms which, however, are negligible in our long distance regime.

¹To be more precise, the only requirement on f is that $f(M) = f(S \cdot M \cdot S^{-1})$ for any S .

²The invariance under reparametrizations corresponds to the freedom of redefining the worldsheet coordinates, $\tau \rightarrow \tau'(\tau, \sigma)$ and $\sigma \rightarrow \sigma'(\tau, \sigma)$.

Expanding the action

The complete action for a vortex line in a superfluid is given by Eqs. (5.5), (5.13) and (5.17). We are interested in expanding it for small fluctuations and small derivatives. Before doing so one must notice that, in order for the effective theory to be valid, the velocity of the vortex must be much smaller than the speed of sound³. To see that, recall that the velocity of the superfluid at a distance r from the vortex is of order $v \sim \Gamma/r$ (see Eq. (5.1)). Since this must be smaller than the sound speed up to distances of the order of the vortex core, ξ , we must have $\Gamma \lesssim c_s \xi$. Now imagine that the string is perturbed around a straight configuration by a distortion of typical length ℓ . The typical vortex velocity will be [106]

$$\partial_t \vec{X} \sim \Gamma/\ell \ll c_s, \quad (5.18)$$

given that the vortex core must be much smaller than ℓ .

Our expansion will therefore be an expansion in small fluctuations around equilibrium, small derivatives of the \vec{A} and \vec{B} fields, and small string velocities. Note that the Kalb-Ramond coupling starts at first order in $\partial_t \vec{X}$. The final result is

$$S \rightarrow \frac{\bar{w}}{c^2} \int d^3x dt \left[\frac{1}{2} (\vec{\nabla} \times \vec{A})^2 + \frac{1}{2} (\dot{\vec{B}}^2 - c_s^2 (\vec{\nabla} \cdot \vec{B})^2) \right. \quad (5.19a)$$

$$\left. + \frac{1}{2} \left(1 - \frac{c_s^2}{c^2} \right) \vec{\nabla} \cdot \vec{B} (\dot{\vec{B}} - \vec{\nabla} \times \vec{A})^2 \right]$$

$$- \int dt d\sigma \left[\frac{1}{3} \bar{n} \lambda \epsilon_{ijk} X^k \partial_t X^i \partial_\sigma X^j + T_{(00)} |\partial_\sigma \vec{X}| \right] \quad (5.19b)$$

$$+ \int dt d\sigma \left[\bar{n} \lambda (A_i \partial_\sigma X^i + \epsilon_{ijk} B^k \partial_t X^i \partial_\sigma X^j) \right. \quad (5.19c)$$

$$\left. + |\partial_\sigma \vec{X}| \left(2T_{(01)} \vec{\nabla} \cdot \vec{B} + 2T_{(10)} (\dot{\vec{B}} - \vec{\nabla} \times \vec{A}) \cdot \frac{\vec{v}_\perp}{c^2} \right) \right],$$

where \vec{v}_\perp is the local superfluid velocity perpendicular to the string, and the T s are

³This is *not* a NR limit, given that the sound speed c_s can still be comparable to the speed of light.

effective couplings obtained from the generalized tension by

$$T_{(mn)} = a^m b^n \frac{\partial^m}{\partial a^m} \frac{\partial^n}{\partial b^n} \mathcal{T}(a, b), \quad (5.20)$$

evaluated on the background. For the sake of brevity we only included one cubic term, which is already known to contribute to the renormalization of $T_{(01)}$ coupling [99], and will be crucial for our analysis as well.

We can already note a very interesting feature of Eq. (5.19a). The kinetic term for the vortex is only of *first order* in time derivatives. This means that to determine the vortex trajectory one only needs to provide one initial condition, e.g. its position. This is why the vortex precession does not require an initial “push” to the vortex itself, as mentioned in Section 5.1.

The terms in Eq. (5.19a) describe the interaction of the bulk modes in the absence of a vortex, those in Eq. (5.19b) describe the dynamics of the string moving in the superfluid at equilibrium, and those in Eq. (5.19c) describe the coupling between the vortex line and the superfluid modes.

5.3 Trapping the superfluid

The superfluid considered in the previous section clearly has no boundaries. However, if we want to apply the EFT we just developed to a real experiment we need to be able to describe the spatial confinement of the superfluid. Let us forget for a moment about the presence of the vortex and, once again, let symmetry be our guiding principle. Of course the trapping term will have to explicitly depend on position, and its most general form will be [86]

$$S_{\text{tr}} = - \int d^3x dt \mathcal{E}(\sqrt{Y}, \vec{u}, \vec{x}), \quad (5.21)$$

where \mathcal{E} is for now a generic function with dimensions of an energy density. In terms of the fluctuations, Y and \vec{u} are readily found to be

$$Y = \bar{n}^2 \left[(1 - \vec{\nabla} \cdot \vec{B})^2 - \frac{1}{c^2} (\dot{\vec{B}} - \vec{\nabla} \times \vec{B})^2 \right], \quad \vec{u} = \frac{\dot{\vec{B}} - \vec{\nabla} \times \vec{A}}{1 - \vec{\nabla} \cdot \vec{B}}. \quad (5.22)$$

The trapping term therefore provides new interactions for the superfluid bulk modes:

$$S_{\text{tr}} \rightarrow \int d^3x dt \left\{ \bar{n}V(\vec{x}) \left[\vec{\nabla} \cdot \vec{B} + \frac{1}{2c^2} (\dot{\vec{B}} - \vec{\nabla} \times \vec{A})^2 \right] - \frac{1}{2} \rho_{ij}(\vec{x}) (\dot{\vec{B}} - \vec{\nabla} \times \vec{A})^i (\dot{\vec{B}} - \vec{\nabla} \times \vec{A})^j \right\}, \quad (5.23)$$

where

$$V(\vec{x}) \equiv \frac{\partial \mathcal{E}}{\partial \sqrt{Y}}, \quad \rho_{ij}(\vec{x}) \equiv \frac{\partial^2 \mathcal{E}}{\partial u^i \partial u^j}, \quad (5.24)$$

both evaluated on the background, $Y = \bar{n}^2$ and $\vec{u} = 0$. Here we have assumed that the trapping mechanism does not involve any breaking of time-reversal symmetry. If such a breaking is present (e.g. for magnetic trapping of charged particles) then one should also allow for a term linear in \vec{u} . The truncation done in Eq. (5.23) is all we need for our purposes.

It should be noted that in the standard Gross-Pitaevskii approach [20, 22] the spatial confinement of the superfluid happens through a direct coupling between the *trapping potential*, $V_{\text{tr}}(\vec{x})$, and the superfluid number density. This corresponds to a particular case of our more general formula. In particular, it corresponds to $\mathcal{E}(\sqrt{Y}, \vec{u}, \vec{x}) = V_{\text{tr}}(\vec{x})\sqrt{Y}$. If we neglect the dependence on the superfluid velocity, the two approaches coincide at lowest order in perturbation theory.

The action (5.23) provides an external source for the phonon field, i.e.

$$\vec{J}_B(x) = -\bar{n} \vec{\nabla} V(\vec{x}). \quad (5.25)$$

Such an external source will modify the superfluid background. In particular, the new expectation value for the phonon field can be computed with standard Green's functions techniques:

$$\langle B^i(x) \rangle = \int \frac{d^3 k d\omega}{(2\pi)^4} i G_B^{ij}(k) J_B^j(k) e^{ik \cdot x}, \quad (5.26)$$

from which it immediately follows that

$$\langle \vec{\nabla} \cdot \vec{B} \rangle = \frac{\bar{n}c^2}{\bar{w}c_s^2} V(\vec{x}). \quad (5.27)$$

Since there are no external sources for \vec{A} , and the vev in Eq. (5.26) is time-independent, it follows from Eq. (5.22) that the superfluid density in the presence of a weak external trap is given by

$$n(\vec{x}) = \sqrt{Y} = \bar{n} \left(1 - \frac{\bar{n}c^2}{\bar{w}c_s^2} V(\vec{x}) \right). \quad (5.28)$$

This result is completely relativistic and true for *any* fairly regular trapping potential. In the NR limit the enthalpy density is dominated by the mass density, and therefore $\bar{w} \simeq m\bar{n}c^2$. The local number density then reduces to

$$n(\vec{x}) \rightarrow \bar{n} \left(1 - \frac{V(\vec{x})}{mc_s^2} \right), \quad (5.29)$$

which is the standard result obtained in the Thomas-Fermi approximation⁴ [20].

It is also quite interesting to note that the dependence of the superfluid density on the trapping potential is completely local, i.e. the density at position \vec{x} only depends on the value of the trap at the same point. This is not what one would have expected.

⁴To make better contact with the more standard language the reader might want to recall that, in the Gross-Pitaevskii approximation of weak coupling, one has $c_s^2 = \mu/m$ and $\mu = nU_0$, where μ is the chemical potential and U_0 is the coupling of the nonlinear terms in the equation.

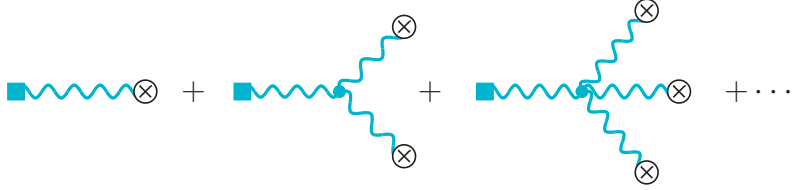


Figure 5.2: Resummation of the nonlinear corrections to Eqs. (5.28) and (5.29). The crossed circles represent the trapping potential V , the squares the density and the wavy lines the \vec{B} propagator.

In fact, integrating out gapless modes as in this case typically results in non-local interactions. What is happening here is that the number of spatial derivatives acting on \vec{B} in the expression for the density and in the interaction term cancel exactly the powers of momentum that appear in the denominator of the propagator of \vec{B} .

The EFT language we are using here also allows us to perform one more step forward. Eq. (5.29) is true to first order in the trapping potential. Nevertheless, since the superfluid density will eventually go to zero far enough from the center of the cloud, this approximation must break down close to the edge. Nevertheless, the spatial position around which we are performing the expansion is clearly arbitrary. In other words, we can always redefine \bar{n} to be the density of the superfluid at a point different from the center of the cloud. It follows that we are truly expanding in small *variations* of the potential. We can thus transform Eq. (5.29) into a differential RG-type equation [86]:

$$c_s^2(n) \frac{dn}{n} = -\frac{dV}{m} . \quad (5.30)$$

The solution to this will give the density to all orders in the trapping potential, and corresponds to a resummation of tree level diagrams as in Figure 5.2. This is another advantage over the traditional approach. In fact, one typically assumes the naïve equation of state $c_s^2 \propto n$, in which case Eq. (5.29) is true to all orders in V . For more general (and realistic) equations of state, the nonlinear corrections might be relevant.

5.4 Vortex precession in 2D

Let us now consider a superfluid only confined in the $\vec{x}_\perp = (x, y)$ plane, which corresponds to a trapping potential constant along the z direction. We will work in a gauge for the string worldsheet such that $\tau = t$, and we will restrict ourselves to a straight vortex, along the z -axis, i.e. $\vec{X}(t, z) = (X(t), Y(t), z)$. We also assume that $|\vec{X}| \ll R_\perp$, where R_\perp is the typical transverse size of the cloud. Moreover, to make the comparison with experiment more direct, we will take the nonrelativistic limit from the beginning, i.e. considering $c \rightarrow \infty$. To this end, we treat ρ_{ij} in Eq. (5.23) as a relativistic correction as well, assuming that it is secretly suppressed by inverse powers of c . Indeed, the direct coupling to the superfluid velocity can be achieved experimentally from Doppler-like effects [107]. The inclusion of relativistic corrections is quite straightforward and it is reported in Appendix D.

The vortex effective action

From the action (5.19c) we see that the vortex line as well provides additional external sources for the superfluid modes. In particular, for $c \rightarrow \infty$, such sources are easily found to be

$$\vec{J}_A(x) = \bar{n}\lambda\delta^2(\vec{x}_\perp - \vec{X})\hat{z}, \quad (5.31a)$$

$$\vec{J}_B(x) = \left[\left(\bar{n}\lambda\epsilon_{ab}\dot{X}^b - 2T_{(01)}\partial_a \right) \delta^2(\vec{x}_\perp - \vec{X}) - \bar{n}\partial_a V(\vec{x}_\perp) \right] \hat{x}_\perp^a, \quad (5.31b)$$

where, from now on, $a, b = 1, 2$.

What should we do now? Our final goal is that of describing the motion of the vortex line. To this end, the procedure we will follow is the standard one for effective theories:

1. Solve the equations of motion for the \vec{A} and \vec{B} fields in the presence of the

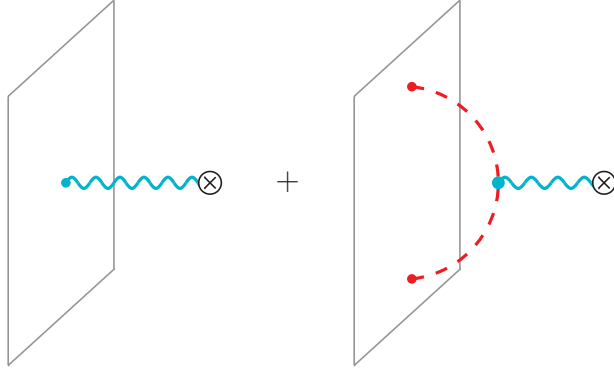


Figure 5.3: Feynman diagrams representing the nonrelativistic interactions between the worldsheet of the vortex line and the trapping potential (crossed circle). The interaction can be mediated by phonons (wavy blue line) or hydrophotons (dashed red line). The cubic term in Eq. (5.19a) can be thought of as a correction to the hydrophoton propagator.

sources reported above.

2. Plug such solutions back into the original action to find the effective action for the vortex only. This amounts to integrating out the gapless modes on-shell.
3. Once the effective action is known, finding the trajectory of the vortex reduces to a simple point particle problem.

Integrating out the \vec{A} and \vec{B} modes at lowest order will result in the following additional term to the string action

$$S_{\text{eff}}[\vec{X}] \supset \int \frac{d^3 k d\omega}{(2\pi)^4} [J_A^i(-k) i G_A^{ij}(k) J_A^j(k) + J_B^i(-k) i G_B^{ij}(k) J_B^j(k)]. \quad (5.32)$$

Inspecting the sources in Eqs. (5.31), it is clear that these correction will contain mixed terms describing the interaction between the vortex line and the trapping potential, mediated by the superfluid modes. This corresponds to computing the Feynman diagrams in Figure 5.3.

The free action for the string already contains a kinetic term and therefore every correction to it coming from the interaction with V will be subleading. On the other hand, it does not feature any space-dependent potential. Hence, every “force”

acting on the vortex will necessarily arise from the interaction with V . Based on these considerations, we can neglect the first term in the source (5.31b), which is proportional to a time derivative and will result in a correction to the vortex kinetic term.

The term due to the interaction mediated by a phonon is easily found to be (recall that in the NR limit $\bar{w} \simeq m\bar{n}c^2$)

$$S_{\text{eff}}^{(B)}[\vec{X}] \supset \frac{2T_{(01)}}{mc_s^2} \int dt dz V(\vec{X}) . \quad (5.33)$$

This is again completely local in the potential, for the same reasons explained around Eq. (5.29). The contribution from the hydrophoton is instead

$$S_{\text{eff}}^{(A)}[\vec{X}] \supset \frac{\bar{n}^3 \lambda^2 c^4}{8\pi^2 \bar{w}^2 c_s^2} \left(1 - \frac{c_s^2}{c^2}\right) \int dt dz d^2 x_\perp \frac{V(\vec{x}_\perp + \vec{X})}{x_\perp^2} , \quad (5.34)$$

which is instead nonlocal in the sense that it depends on the value of the potential away from the position of the vortex. The complete effective action for the vortex line in the nonrelativistic approximation is then given by

$$S_{\text{eff}}^{(\text{NR})}[\vec{X}] = \int dt dz \left[\frac{\bar{n}\lambda}{3} \epsilon_{ab} X^a \dot{X}^b + \frac{2T_{(01)}}{mc_s^2} V(\vec{X}) + \frac{\bar{n}\lambda^2}{8\pi^2 m^2 c_s^2} \int d^2 x_\perp \frac{V(\vec{x}_\perp + \vec{X})}{x_\perp^2} \right] . \quad (5.35)$$

This result is very powerful. It allows us to describe the vortex motion for any regular trapping potential, as long as the vortex is located at a position where perturbation theory in the small trap does not break down.

As promised, finding the equations of motion for the position of the string is now just a point particle problem. In particular, they are given by

$$\frac{2\bar{n}\lambda}{3} \epsilon_{ab} \dot{X}^b - \partial_a V_{\text{eff}}(\vec{X}) = 0 , \quad (5.36)$$

where the effective potential, for vortex lines close to the center of the cloud, can be approximated by

$$V_{\text{eff}}(\vec{X}) \simeq -\frac{1}{2}X^aX^b \left[\frac{2T_{(01)}}{mc_s^2} \partial_a \partial_b V(0) + \frac{\bar{n}\lambda^2}{8\pi^2 m^2 c_s^2} \int d^2 x_\perp \frac{\partial_a \partial_b V(\vec{x}_\perp)}{x_\perp^2} \right], \quad (5.37)$$

where we have assumed that the potential and its gradient vanish at the center of the cloud, $V(0) = \vec{\nabla}V(0) = 0$, which is what defined the “center”. It is important to stress that the result in Eqs. (5.36) and (5.37) is valid whether the microscopic theory is weakly coupled or not.

This could in principle be the end of the story. However, to reproduce the experimental results we will now specify the form of the trapping potential. In particular, there will be two qualitatively different regimes: harmonic traps for which $\partial_a \partial_b V(0) \neq 0$, and anharmonic traps for which $\partial_a \partial_b V(0) = 0$.

Harmonic traps — $\partial_a \partial_b V(0) \neq 0$

If the second derivative of the trapping potential does not vanish near the center of the cloud the integral in Eq. (5.37) will be logarithmic divergent close to $\vec{x}_\perp = 0$. In particular, one can write

$$\int d^2 x_\perp \frac{\partial_a \partial_b V(\vec{x}_\perp)}{x_\perp^2} = \partial_a \partial_b V(0) 2\pi \log(R_\perp/a) + \dots, \quad (5.38)$$

where a is some UV cutoff and the dots stand for terms that are finite for $a \rightarrow 0$. As it happens in any QFT, the UV cutoff must appear in the log together with an IR scale for dimensional reasons. In our case the IR scale will be set by the typical transverse size of the cloud. Note that, in the EFT language the cutoff a does not represent any physical scale but it is just a regulator for the UV divergences and, as such, it must be removed.

Following standard RG logic, we can get rid of the cutoff by allowing for a running

of the $T_{(01)}$ coupling. In particular, the renormalized effective potential will be given by

$$V_{\text{eff}}(\vec{X}) \simeq -\frac{T_{(01)}(1/R_{\perp})}{mc_s^2} \partial_a \partial_b V(0) X^a X^b, \quad (5.39)$$

where the running coupling is

$$T_{(01)}(q) = -\frac{\bar{n}\lambda^2}{8\pi m} \log(q\ell). \quad (5.40)$$

The length scale ℓ is now a true microscopic scale. The effective theory is unable to determine its value, which should be extracted from data. The running of the generalized tension coupling $T_{(01)}$ matches exactly the one already found in [99]. This is a somewhat peculiar result, given that such a running arises at the classical level (no quantum mechanics has been considered so far).

The standard parametrization for harmonic trappings is (see e.g. [98])

$$V(\vec{x}_{\perp}) = \frac{m}{2} (\omega_x^2 x^2 + \omega_y^2 y^2) + O(r^4), \quad (5.41)$$

in which case the equations of motion for the vortex line are simply

$$\dot{X}(t) = \omega_p \frac{\omega_y}{\omega_x} Y(t), \quad \dot{Y}(t) = -\omega_p \frac{\omega_x}{\omega_y} X(t). \quad (5.42)$$

These equations describe exactly an elliptical trajectory with the same orientation and aspect ratio as the potential. Moreover, the precession frequency is readily found to be

$$\omega_p \equiv \frac{3\Gamma}{8\pi c_s^2} \omega_x \omega_y \log(R_{\perp}/\ell), \quad (5.43)$$

where we used $\lambda = m\Gamma$ in the NR limit. When the Gross-Pitaevskii equation ap-

plies $c_s^2 = \mu/m$ [20], and this reduces exactly to the result reported in Eq. (5.3). Nevertheless, since our approach does not assume anything about the microscopic dynamics of the superfluid, we emphasize that it is more general than what derived in the Gross-Pitaevskii approximation (i.e. weak, contact interactions). In particular, if c_s is known in all regimes, then Eq. (5.43) is valid also at strong coupling as, for example, at the BEC-BCS crossover [98].

As already explained, the microscopic scale ℓ should be determined from experiment. However, one can make one further step and consider the precession frequency for two different traps, say ‘1’ and ‘2’ and define $\chi \equiv \omega_p/\omega_x\omega_y$ for each of them. In this case one has

$$\chi_1 - \chi_2 = \frac{3\Gamma}{8\pi c_s^2} \log(R_{\perp,1}/R_{\perp,2}), \quad (5.44)$$

which is independent of ℓ and hence completely predictive.

Just for fun, we have compared our predictions with the data reported in [98] for the precession frequency as a function of the trapping frequency. The results and details are reported in Figure 5.4. The agreement between Eq. (5.43) (in the weak coupling limit) and the experimental data is quite good. The discrepancies are most likely due to the fact that, in the experimental setup, the logarithmic enhancement is actually just $\log(R_{\perp}/\xi) \simeq 2 - 5$ and hence next to leading log corrections should be included. Moreover, at the crossover between the BCS (when the condensate is formed by the Cooper pairs) and the BEC (when the condensate is formed by the Li molecules) regimes, the system is strongly coupled and to apply our prediction we should know the superfluid sound speed, which was not provided in the experimental paper. It should however be noted that the fit has only one free parameter.

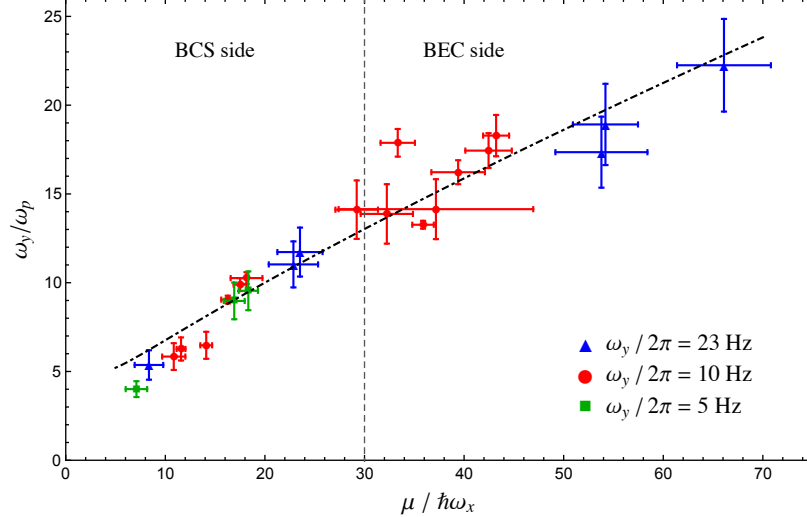


Figure 5.4: Comparison between the experimental data measured in [98] and our result Eq. (5.43). On the vertical axis we report the ratio of the trapping frequency in the y -direction over the precession frequency, while on the horizontal axis we report the chemical potential normalized to the trapping frequency along the x -direction. The vertical dashed line separates the data taken in the BEC regime from those taken in the BCS regime. Our model, in the weak coupling regime, is given by $\omega_y/\omega_p = \frac{4}{3} \frac{\mu}{\hbar\omega_x} \frac{1}{\log(\mu/(\hbar\omega_x\alpha))}$, with α being our only free parameter. The maximum likelihood estimator for it gives $\alpha = 1.391 \pm 0.077$, at 1σ C.L.. The result of the fit is the black, dot-dashed line. The agreement is good but not excellent, with $\chi^2/\text{d.o.f.} = 1.4$. The reason is probably twofold. First of all, the logarithmic enhancement is actually quite mild for the experimental setup under consideration [98], and higher order corrections are likely relevant. Secondly, at the crossover between BEC and BCS regimes, the system is strongly coupled and our fitting function does not apply anymore. To employ our prediction (5.43) correctly one would need the value of the speed of sound for each point. Unfortunately that was not provided in [98].

Anharmonic traps — $\partial_a \partial_b V(0) = 0$

The other situation we can consider is that of anharmonic traps, i.e. $\partial_a \partial_b V(0) = 0$. This regime became of phenomenological interest very recently, given that the authors of [108–110] managed to produce a trapping potential which resembles a perfect box with very good approximation. This essentially means that the density is roughly constant inside the cloud, decreasing to zero very fast near the edge of the superfluid. For later convenience, let us parametrize the potential as $V(\vec{x}_\perp) = mc_s^2 f(\vec{x}_\perp/R_\perp)$, where f is a dimensionless function varying between zero and $O(1)$, when moving

from the center to the edge of the cloud. The first term in Eq. (5.37) is now zero, and the second one is convergent. It will be given generically by

$$\int d^2x_\perp \frac{\partial_a \partial_b V(\vec{x}_\perp)}{x_\perp^2} = \frac{mc_s^2}{R_\perp^2} f_{ab} , \quad (5.45)$$

where f_{ab} is a constant symmetric tensor with order-one entries. If we align our axes with its eigenvectors then the equations of motion for the vortex line are given by

$$\dot{X}(t) = \omega_p \sqrt{\frac{f_{yy}}{f_{xx}}} Y(t) , \quad \dot{Y}(t) = -\omega_p \sqrt{\frac{f_{xx}}{f_{yy}}} X(t) . \quad (5.46)$$

These again describe elliptical orbits with aspect ratio $\sqrt{f_{yy}/f_{xx}}$, and precession frequency

$$\omega_p = \frac{3}{16\pi^2} \frac{\Gamma}{R_\perp^2} \sqrt{f_{xx}f_{yy}} . \quad (5.47)$$

Interestingly, the logarithmic enhancement of Eq. (5.43) is now gone. This is in line with what found in [111] with standard techniques. Moreover, given that no microscopic scale is now present, the above equation is already completely predictive.

5.5 Summary

In this chapter we have presented an effective string theory that describes vortex lines in a superfluid, and we have employed it to describe the experimental results obtained, for example, in [98]. This is an important step. It shows that the EFT approach to condensed matter can indeed be used in real experimental problems and that it can offer several advantages over more standard methods.

Here are some of the steps forward that our EFT allowed:

- We were able to study the trajectory of a vortex line in a confined superfluid

for any fairly regular trapping potential. This is not what typically happens. Most of the literature is forced to study the motion of the vortex case by case, for each given trap.

- Our results are general for any superfluid. The vortex precession turn out to be a phenomenon due solely to long distance/low energy physics. The results obtained here are therefore universal, regardless of the microscopic features of the system. In particular, they go beyond the standard Gross-Pitasevskii approach [20], which is valid in the weak coupling regime.
- The physics behind the vortex precession is always the same for all kinds of trapping potential. In particular, it is due to the interaction between the vortex line and the trap, mediated by the superfluid gapless modes. Such a unifying picture seem to be lacking from the literature (see for example the discussion in [112]).

It is also interesting to note that the potential in Eq. (5.35) is negative definite (the coupling $T_{(01)}$ is expected to be positive [99]). This means that the interaction with phonons (for example at finite temperatures) is expected to cause the vortex line to drift towards the edge of the cloud until it disappears—see e.g. [81].

Lastly, although common experiments are highly nonrelativistic, the relativistic corrections to the vortex action (see Appendix D) might be relevant, for example, for neutron star physics. It has in fact been conjectured that the dynamics of vortices in the superfluid core of the neutron stars might be the explanation for some observed “glitches” in their rotational frequency [113].

Conclusion

It is always very exciting when two seemingly distant fields of physics find some unexpected and fruitful overlap. This is the case for certain high energy theory methods and some problems in low energy physics, which found a common ground in the last fifteen years or so.

In this thesis we mainly presented two of them: the effective field theory approach and the holographic duality. Both of them have been successful in providing a new viewpoint for some condensed matter problems, as well as helping identifying new possible directions to investigate. On the one hand, the EFT approach provides a beautifully simple unifying viewpoint of the condensed matter world. As often happens, effective theories constitute a useful calculation tool and help describe phenomena in a remarkably simple way. In this case, this is done by isolating the universal low energy/long distance properties of condensed matter systems from their complicated microscopic structure, which is instead different from case to case.

On the other hand, the holographic duality offers a very powerful tool. It allows to perform calculations in a nonperturbative regime that is hardly accessible with more standard techniques. This is possible thanks to the surprising connection between certain strongly coupled field theories and certain theories of gravity.

The more formal achievement of this thesis is that of having exhibited an explicit relation between the EFT language and the holographic one. Being the holographic duality specifically designed to improve the understanding of the microscopic under-

lying theory, the focus on the long distance physics was often secondary. Here we showed that, of course, one can recover the latter starting from the former. This also helped us determining the gravity dual of a common solid, which was, surprisingly, lacking from the literature.

From a phenomenological viewpoint, we instead successfully applied the EFT for vortex lines in superfluids to explain the phenomenon of vortex precession in confined ultra cold gases. The simplicity of EFTs allowed us to reproduce the known results, as well as to perform several steps forward in the understanding of the phenomenon. More broadly, we can consider this as a proof that the effective theories for condensed matter are not just a theorist's game. They can be used to describe real experimental data in a way that, sometimes, is much simpler than the more traditional techniques.

The future of this field is bright. There is a huge variety of low energy problems that would benefit from a high energy perspective and viceversa. Much work still has to be done on holographic solids. For example, it would be interesting to study their transport properties and dissipative behavior [114]. Beside being of interest for the phenomenology of holographic solids, this problem can also shed some light on questions related to the holographic duality per se as, for example, how dissipation arises in the absence of a black hole horizon.

Another interesting line of research concerns the following question: what happens when a phonon is coupled to gravity? Does it float or does it sink? In a recent paper it has been showed that superfluid phonons indeed float [115]. Since this is true in the nonrelativistic limit as well, it is not related to the statement that mass and energy are equivalent. Rather, it means that phonons truly transport negative gravitational mass, in the most mundane Newtonian sense. To the best of our knowledge, the common lore is instead that collective excitations should only transport energy. One can then try to show the same thing for fluids and solids as well, using both EFT methods as well as standard hydrodynamical equations [116]. Beside being quite fun,

this realization has intriguing experimental consequences. In fact, cold atom trapping could be used to simulate a much stronger gravity, possibly allowing for the direct observation of the floating of phonons.

Lastly, a very promising idea is that of employing our EFT methods to provide new ideas for the detection of sub-GeV dark matter particles, for which there are currently no experimental constraints [117]. Ideas in this direction have already been developed [118, 119], where superfluid helium-4 was proposed as a possible material to detect dark matter particles with masses down to some keV. The EFT viewpoint can definitely help improve these ideas, as well as propose new possible signatures. One promising possibility is that of detecting the emission of Čerenkov sound following the interaction of a dark matter particle with one of the nuclei of the superfluid helium [120]. This possibility, which seems possible with the current available technology, would have the great advantage of providing an optimal way of discriminating the dark matter event from the overwhelming thermal background.

These are just few of the questions that could be addressed employing high energy ideas applied to condensed matter. It is an exciting feeling to have such a novel and powerful tool at one's disposal. There is a whole world of possibilities, and the fun has just begun.

Bibliography

- [1] A. Esposito et al. “A Mechanism for Hadron Molecule Production in $p\bar{p}(p)$ Collisions.” In: *J. Mod. Phys.* 4 (2013), pp. 1569–1573. DOI: [10.4236/jmp.2013.412193](https://doi.org/10.4236/jmp.2013.412193). arXiv: [1305.0527](https://arxiv.org/abs/1305.0527) [hep-ph].
- [2] A. Esposito et al. “Observation of light nuclei at ALICE and the $X(3872)$ conundrum.” In: *Phys. Rev.* D92.3 (2015), p. 034028. DOI: [10.1103/PhysRevD.92.034028](https://doi.org/10.1103/PhysRevD.92.034028). arXiv: [1508.00295](https://arxiv.org/abs/1508.00295) [hep-ph].
- [3] A. Esposito et al. “Doubly charmed tetraquarks in B_c and Ξ_{bc} decays.” In: *Phys. Rev.* D88.5 (2013), p. 054029. DOI: [10.1103/PhysRevD.88.054029](https://doi.org/10.1103/PhysRevD.88.054029). arXiv: [1307.2873](https://arxiv.org/abs/1307.2873) [hep-ph].
- [4] A. Esposito, A. L. Guerrieri, and A. Pilloni. “Probing the nature of $Z_c^{(\prime)}$ states via the $\eta_c\rho$ decay.” In: *Phys. Lett.* B746 (2015), pp. 194–201. DOI: [10.1016/j.physletb.2015.04.057](https://doi.org/10.1016/j.physletb.2015.04.057). arXiv: [1409.3551](https://arxiv.org/abs/1409.3551) [hep-ph].
- [5] A. Esposito, A. Pilloni, and A. D. Polosa. “Hybridized Tetraquarks.” In: *Phys. Lett.* B758 (2016), pp. 292–295. DOI: [10.1016/j.physletb.2016.05.028](https://doi.org/10.1016/j.physletb.2016.05.028). arXiv: [1603.07667](https://arxiv.org/abs/1603.07667) [hep-ph].
- [6] A. Esposito, A. Pilloni, and A. D. Polosa. “Multiquark Resonances.” In: *Phys. Rept.* 668 (2016), pp. 1–97. DOI: [10.1016/j.physrep.2016.11.002](https://doi.org/10.1016/j.physrep.2016.11.002). arXiv: [1611.07920](https://arxiv.org/abs/1611.07920) [hep-ph].
- [7] A. Esposito et al. “Four-Quark Hadrons: an Updated Review.” In: *Int. J. Mod. Phys.* A30 (2015), p. 1530002. DOI: [10.1142/S0217751X15300021](https://doi.org/10.1142/S0217751X15300021). arXiv: [1411.5997](https://arxiv.org/abs/1411.5997) [hep-ph].
- [8] A. Esposito and M. Gyulassy. “Hadronization scheme dependence of long-range azimuthal harmonics in high energy $p + A$ reactions.” In: *Phys. Lett.* B747 (2015), pp. 433–440. DOI: [10.1016/j.physletb.2015.06.037](https://doi.org/10.1016/j.physletb.2015.06.037). arXiv: [1505.03734](https://arxiv.org/abs/1505.03734) [hep-ph].

[9] B. Horn, L. Hui, and X. Xiao. “Soft-Pion Theorems for Large Scale Structure.” In: *JCAP* 1409.09 (2014), p. 044. DOI: [10.1088/1475-7516/2014/09/044](https://doi.org/10.1088/1475-7516/2014/09/044). arXiv: [1406.0842](https://arxiv.org/abs/1406.0842) [hep-th].

[10] A. Esposito, L. Hui, and R.. Scoccimarro. *To appear*.

[11] A. Nicolis et al. “Zoology of condensed matter: Framids, ordinary stuff, extraordinary stuff.” In: *JHEP* 06 (2015), p. 155. DOI: [10.1007/JHEP06\(2015\)155](https://doi.org/10.1007/JHEP06(2015)155). arXiv: [1501.03845](https://arxiv.org/abs/1501.03845) [hep-th].

[12] S. Weinberg. *The Quantum Theory of Fields*. Vol. 2. Cambridge University Press, 1995.

[13] A. Nicolis et al. “More on gapped Goldstones at finite density: More gapped Goldstones.” In: *JHEP* 11 (2013), p. 055. DOI: [10.1007/JHEP11\(2013\)055](https://doi.org/10.1007/JHEP11(2013)055). arXiv: [1306.1240](https://arxiv.org/abs/1306.1240) [hep-th].

[14] E. A. Ivanov and V. I. Ogievetsky. “The Inverse Higgs Phenomenon in Nonlinear Realizations.” In: *Teor. Mat. Fiz.* 25 (1975), pp. 164–177. DOI: [10.1007/BF01028947](https://doi.org/10.1007/BF01028947).

[15] I. Low and A. V. Manohar. “Spontaneously broken space-time symmetries and Goldstone’s theorem.” In: *Phys. Rev. Lett.* 88 (2002), p. 101602. DOI: [10.1103/PhysRevLett.88.101602](https://doi.org/10.1103/PhysRevLett.88.101602). arXiv: [hep-th/0110285](https://arxiv.org/abs/hep-th/0110285) [hep-th].

[16] I. N. McArthur. “Nonlinear realizations of symmetries and unphysical Goldstone bosons.” In: *JHEP* 11 (2010), p. 140. DOI: [10.1007/JHEP11\(2010\)140](https://doi.org/10.1007/JHEP11(2010)140). arXiv: [1009.3696](https://arxiv.org/abs/1009.3696) [hep-th].

[17] J. P. Gauntlett, K. Itoh, and P. K. Townsend. “Superparticle With Extrinsic Curvature.” In: *Phys. Lett.* B238 (1990), pp. 65–74. DOI: [10.1016/0370-2693\(90\)92101-N](https://doi.org/10.1016/0370-2693(90)92101-N).

[18] S. Endlich, A. Nicolis, and R. Penco. “Ultraviolet completion without symmetry restoration.” In: *Phys. Rev.* D89.6 (2014), p. 065006. DOI: [10.1103/PhysRevD.89.065006](https://doi.org/10.1103/PhysRevD.89.065006). arXiv: [1311.6491](https://arxiv.org/abs/1311.6491) [hep-th].

[19] A. Nicolis and F. Piazza. “Implications of Relativity on Nonrelativistic Goldstone Theorems: Gapped Excitations at Finite Charge Density.” In: *Phys. Rev. Lett.* 110.1 (2013). [Addendum: *Phys. Rev. Lett.* 110,039901(2013)], p. 011602. DOI: [10.1103/PhysRevLett.110.011602](https://doi.org/10.1103/PhysRevLett.110.011602), [10.1103/PhysRevLett.110.039901](https://doi.org/10.1103/PhysRevLett.110.039901). arXiv: [1204.1570](https://arxiv.org/abs/1204.1570) [hep-th].

[20] C. J. Pethick and H. Smith. *Bose-Einstein Condensation in Dilute Gases*. Cambridge University Press, 2008.

- [21] D. T. Son. “Low-energy quantum effective action for relativistic superfluids.” In: (2002). arXiv: [hep-ph/0204199 \[hep-ph\]](#).
- [22] A. J. Leggett. *Quantum Liquids: Bose Condensation and Cooper Pairing in Condensed-matter Systems*. OUP Oxford, 2006.
- [23] A. Nicolis, R. Rattazzi, and E. Trincherini. “The Galileon as a local modification of gravity.” In: *Phys. Rev.* D79 (2009), p. 064036. DOI: [10.1103/PhysRevD.79.064036](#). arXiv: [0811.2197 \[hep-th\]](#).
- [24] D. Vollhardt and P. Wolfle. *The Superfluid Phases of Helium 3*. Dover Books on Physics. Dover Publications, 2013. ISBN: 9780486315881.
- [25] R. Jackiw et al. “Perfect fluid theory and its extensions.” In: *J. Phys.* A37 (2004), R327–R432. DOI: [10.1088/0305-4470/37/42/R01](#). arXiv: [hep-ph/0407101 \[hep-ph\]](#).
- [26] S. Dubovsky et al. “Null energy condition and superluminal propagation.” In: *JHEP* 03 (2006), p. 025. DOI: [10.1088/1126-6708/2006/03/025](#). arXiv: [hep-th/0512260 \[hep-th\]](#).
- [27] S. Endlich et al. “The Quantum mechanics of perfect fluids.” In: *JHEP* 04 (2011), p. 102. DOI: [10.1007/JHEP04\(2011\)102](#). arXiv: [1011.6396 \[hep-th\]](#).
- [28] D. T. Son. “Effective Lagrangian and topological interactions in supersolids.” In: *Phys. Rev. Lett.* 94 (2005), p. 175301. DOI: [10.1103/PhysRevLett.94.175301](#). arXiv: [cond-mat/0501658 \[cond-mat\]](#).
- [29] J. Léonard et al. “Supersolid formation in a quantum gas breaking a continuous translational symmetry.” In: *Nature* 543 (Mar. 2017), p. 87. arXiv: [1609.09053 \[cond-mat.quant-gas\]](#).
- [30] J. Léonard et al. “Monitoring and manipulating Higgs and Goldstone modes in a supersolid quantum gas.” In: *Science* 358.6369 (2017), pp. 1415–1418. arXiv: [1704.05803 \[cond-mat.quant-gas\]](#).
- [31] G. Goon et al. “Galileons as Wess-Zumino Terms.” In: *JHEP* 06 (2012), p. 004. DOI: [10.1007/JHEP06\(2012\)004](#). arXiv: [1203.3191 \[hep-th\]](#).
- [32] A. Nicolis. “Low-energy effective field theory for finite-temperature relativistic superfluids.” In: (2011). arXiv: [1108.2513 \[hep-th\]](#).
- [33] L. D. Landau and E. M. Lifshitz. *Fluid Mechanics*. v. 6. Elsevier Science, 2013. ISBN: 9781483140506.

[34] J. M. Maldacena. “The Large N limit of superconformal field theories and supergravity.” In: *Int. J. Theor. Phys.* 38 (1999). [Adv. Theor. Math. Phys.2,231(1998)], pp. 1113–1133. DOI: 10.1023/A:1026654312961. arXiv: [hep-th/9711200](https://arxiv.org/abs/hep-th/9711200) [hep-th].

[35] E. Witten. “Anti-de Sitter space and holography.” In: *Adv. Theor. Math. Phys.* 2 (1998), pp. 253–291. arXiv: [hep-th/9802150](https://arxiv.org/abs/hep-th/9802150) [hep-th].

[36] S. S. Gubser, I. R. Klebanov, and A. M. Polyakov. “Gauge theory correlators from noncritical string theory.” In: *Phys. Lett.* B428 (1998), pp. 105–114. DOI: 10.1016/S0370-2693(98)00377-3. arXiv: [hep-th/9802109](https://arxiv.org/abs/hep-th/9802109) [hep-th].

[37] S. A. Hartnoll. “Lectures on holographic methods for condensed matter physics.” In: *Class. Quant. Grav.* 26 (2009), p. 224002. DOI: 10.1088/0264-9381/26/22/224002. arXiv: [0903.3246](https://arxiv.org/abs/0903.3246) [hep-th].

[38] S. A. Hartnoll, A. Lucas, and S. Sachdev. “Holographic quantum matter.” In: (2016). arXiv: [1612.07324](https://arxiv.org/abs/1612.07324) [hep-th].

[39] M. Natsuume. *AdS/CFT Duality User Guide*. Lecture Notes in Physics. Springer Japan, 2015. ISBN: 9784431554417.

[40] J. Zaanen et al. *Holographic Duality in Condensed Matter Physics*. Cambridge University Press, 2015. ISBN: 9781107080089.

[41] G. ’t Hooft. “A Planar Diagram Theory for Strong Interactions.” In: *Nucl. Phys.* B72 (1974), p. 461. DOI: 10.1016/0550-3213(74)90154-0.

[42] S. Coleman. *Aspects of Symmetry: Selected Erice Lectures*. Cambridge University Press, 1988. ISBN: 9780521318273.

[43] F. Denef. *Private communication*.

[44] D. T. Son and A. O. Starinets. “Minkowski space correlators in AdS / CFT correspondence: Recipe and applications.” In: *JHEP* 09 (2002), p. 042. DOI: 10.1088/1126-6708/2002/09/042. arXiv: [hep-th/0205051](https://arxiv.org/abs/hep-th/0205051) [hep-th].

[45] P. Breitenlohner and D. Z. Freedman. “Stability in Gauged Extended Supergravity.” In: *Annals Phys.* 144 (1982), p. 249. DOI: 10.1016/0003-4916(82)90116-6.

[46] E. Witten. “Multitrace operators, boundary conditions, and AdS / CFT correspondence.” In: (2001). arXiv: [hep-th/0112258](https://arxiv.org/abs/hep-th/0112258) [hep-th].

[47] I. Papadimitriou. “Multi-Trace Deformations in AdS/CFT: Exploring the Vacuum Structure of the Deformed CFT.” In: *JHEP* 05 (2007), p. 075. DOI: 10.1088/1126-6708/2007/05/075. arXiv: hep-th/0703152 [hep-th].

[48] D. Marolf and S. F. Ross. “Boundary Conditions and New Dualities: Vector Fields in AdS/CFT.” In: *JHEP* 11 (2006), p. 085. DOI: 10.1088/1126-6708/2006/11/085. arXiv: hep-th/0606113 [hep-th].

[49] J. Zinn-Justin. *Quantum Field Theory and Critical Phenomena*. International series of monographs on physics. Clarendon Press, 2002. ISBN: 9780198509233.

[50] G. T. Horowitz. “Introduction to Holographic Superconductors.” In: *Lect. Notes Phys.* 828 (2011), pp. 313–347. DOI: 10.1007/978-3-642-04864-7_10. arXiv: 1002.1722 [hep-th].

[51] S. A. Hartnoll, C. P. Herzog, and G. T. Horowitz. “Building a Holographic Superconductor.” In: *Phys. Rev. Lett.* 101 (2008), p. 031601. DOI: 10.1103/PhysRevLett.101.031601. arXiv: 0803.3295 [hep-th].

[52] S. A. Hartnoll, C. P. Herzog, and G. T. Horowitz. “Holographic Superconductors.” In: *JHEP* 12 (2008), p. 015. DOI: 10.1088/1126-6708/2008/12/015. arXiv: 0810.1563 [hep-th].

[53] S. S. Gubser and F. D. Rocha. “The gravity dual to a quantum critical point with spontaneous symmetry breaking.” In: *Phys. Rev. Lett.* 102 (2009), p. 061601. DOI: 10.1103/PhysRevLett.102.061601. arXiv: 0807.1737 [hep-th].

[54] S. S. Gubser and A. Nellore. “Ground states of holographic superconductors.” In: *Phys. Rev.* D80 (2009), p. 105007. DOI: 10.1103/PhysRevD.80.105007. arXiv: 0908.1972 [hep-th].

[55] S. S. Gubser. “Breaking an Abelian gauge symmetry near a black hole horizon.” In: *Phys. Rev.* D78 (2008), p. 065034. DOI: 10.1103/PhysRevD.78.065034. arXiv: 0801.2977 [hep-th].

[56] S. S. Gubser and A. Nellore. “Low-temperature behavior of the Abelian Higgs model in anti-de Sitter space.” In: *JHEP* 04 (2009), p. 008. DOI: 10.1088/1126-6708/2009/04/008. arXiv: 0810.4554 [hep-th].

[57] G. T. Horowitz and M. M. Roberts. “Zero Temperature Limit of Holographic Superconductors.” In: *JHEP* 11 (2009), p. 015. DOI: 10.1088/1126-6708/2009/11/015. arXiv: 0908.3677 [hep-th].

[58] G. T. Horowitz and B. Way. “Complete Phase Diagrams for a Holographic Superconductor/Insulator System.” In: *JHEP* 11 (2010), p. 011. DOI: 10.1007/JHEP11(2010)011. arXiv: 1007.3714 [hep-th].

[59] C. P. Herzog and A. Yarom. “Sound modes in holographic superfluids.” In: *Phys. Rev.* D80 (2009), p. 106002. DOI: 10.1103/PhysRevD.80.106002. arXiv: 0906.4810 [hep-th].

[60] A. Yarom. “Fourth sound of holographic superfluids.” In: *JHEP* 07 (2009), p. 070. DOI: 10.1088/1126-6708/2009/07/070. arXiv: 0903.1353 [hep-th].

[61] J. de Boer, M. P. Heller, and N. Pinzani-Fokeeva. “Effective actions for relativistic fluids from holography.” In: *JHEP* 08 (2015), p. 086. DOI: 10.1007/JHEP08(2015)086. arXiv: 1504.07616 [hep-th].

[62] D. Nickel and D. T. Son. “Deconstructing holographic liquids.” In: *New J. Phys.* 13 (2011), p. 075010. DOI: 10.1088/1367-2630/13/7/075010. arXiv: 1009.3094 [hep-th].

[63] A. Esposito, S. Garcia-Saenz, and R. Penco. “First sound in holographic superfluids at zero temperature.” In: *JHEP* 12 (2016), p. 136. DOI: 10.1007/JHEP12(2016)136. arXiv: 1606.03104 [hep-th].

[64] S. R. Coleman. “There are no Goldstone bosons in two-dimensions.” In: *Commun. Math. Phys.* 31 (1973), pp. 259–264. DOI: 10.1007/BF01646487.

[65] D. Anninos, S. A. Hartnoll, and N. Iqbal. “Holography and the Coleman-Mermin-Wagner theorem.” In: *Phys. Rev.* D82 (2010), p. 066008. DOI: 10.1103/PhysRevD.82.066008. arXiv: 1005.1973 [hep-th].

[66] T. Sakai and S. Sugimoto. “Low energy hadron physics in holographic QCD.” In: *Prog. Theor. Phys.* 113 (2005), pp. 843–882. DOI: 10.1143/PTP.113.843. arXiv: hep-th/0412141 [hep-th].

[67] L. Alberte et al. “Solid Holography and Massive Gravity.” In: *JHEP* 02 (2016), p. 114. DOI: 10.1007/JHEP02(2016)114. arXiv: 1510.09089 [hep-th].

[68] L. Alberte, M. Baggioli, and O. Pujolas. “Viscosity bound violation in holographic solids and the viscoelastic response.” In: *JHEP* 07 (2016), p. 074. DOI: 10.1007/JHEP07(2016)074. arXiv: 1601.03384 [hep-th].

[69] L. Alberte et al. “Black hole elasticity and gapped transverse phonons in holography.” In: *JHEP* 01 (2018), p. 129. DOI: 10.1007/JHEP01(2018)129. arXiv: 1708.08477 [hep-th].

[70] L. Alberte et al. “Holographic Phonons.” In: (2017). arXiv: 1711 . 03100 [hep-th].

[71] S. Bolognesi and D. Tong. “Monopoles and Holography.” In: *JHEP* 01 (2011), p. 153. DOI: 10.1007/JHEP01(2011)153. arXiv: 1010.4178 [hep-th].

[72] P. Sutcliffe. “Monopoles in AdS.” In: *JHEP* 08 (2011), p. 032. DOI: 10.1007/JHEP08(2011)032. arXiv: 1104.1888 [hep-th].

[73] A. Esposito et al. “Conformal solids and holography.” In: *JHEP* 12 (2017), p. 113. DOI: 10.1007/JHEP12(2017)113. arXiv: 1708.09391 [hep-th].

[74] E. J. Weinberg. *Classical Solutions in Quantum Field Theory: Solitons and Instantons in High Energy Physics*. Cambridge Monographs on Mathematical Physics. Cambridge University Press, 2012.

[75] G. W. Gibbons and S. W. Hawking. “Action Integrals and Partition Functions in Quantum Gravity.” In: *Phys. Rev.* D15 (1977), pp. 2752–2756. DOI: 10.1103/PhysRevD.15.2752.

[76] M. Bianchi, D. Z. Freedman, and K. Skenderis. “Holographic renormalization.” In: *Nucl. Phys.* B631 (2002), pp. 159–194. DOI: 10.1016/S0550-3213(02)00179-7. arXiv: hep-th/0112119 [hep-th].

[77] L. D. Landau and E. M. Lifshitz. *Statistical Physics*. v. 5. Elsevier Science, 2013. ISBN: 9780080570464.

[78] S. W. Hawking and Don N. Page. “Thermodynamics of Black Holes in anti-De Sitter Space.” In: *Commun. Math. Phys.* 87 (1983), p. 577. DOI: 10.1007/BF01208266.

[79] B. Jackson, J. F. McCann, and C. S. Adams. “Vortex line and ring dynamics in trapped Bose-Einstein condensates.” In: *Phys. Rev. A* 61.1 (1999), p. 013604. DOI: 10.1103/PhysRevA.61.013604.

[80] J. Tempere and J.T. Devreese. “Vortex dynamics in a parabolically confined Bose-Einstein condensate.” In: *Solid State Commun.* 113.8 (2000), pp. 471 – 474. ISSN: 0038-1098.

[81] E. Lundh and P. Ao. “Hydrodynamic approach to vortex lifetimes in trapped Bose condensates.” In: *Phys. Rev. A* 61.6 (6 2000), p. 063612. DOI: 10.1103/PhysRevA.61.063612.

[82] A. A. Svidzinsky and A. L. Fetter. “Stability of a Vortex in a Trapped Bose-Einstein Condensate.” In: *Phys. Rev. Lett.* 84 (26 2000), pp. 5919–5923. DOI: [10.1103/PhysRevLett.84.5919](https://doi.org/10.1103/PhysRevLett.84.5919).

[83] A. L. Fetter and J.-k. Kim. “Vortex Precession in a Rotating Nonaxisymmetric Trapped Bose-Einstein Condensate.” In: *J. Low Temp. Phys.* 125.5 (2001), pp. 239–248. ISSN: 1573-7357. DOI: [10.1023/A:1012919924475](https://doi.org/10.1023/A:1012919924475).

[84] S. A. McGee and M. J. Holland. “Rotational dynamics of vortices in confined Bose-Einstein condensates.” In: *Phys. Rev. A* 63.4 (2001), p. 043608. DOI: [10.1103/PhysRevA.63.043608](https://doi.org/10.1103/PhysRevA.63.043608).

[85] D. L. Feder et al. “Anomalous Modes Drive Vortex Dynamics in Confined Bose-Einstein Condensates.” In: *Phys. Rev. Lett.* 86.4 (2001), pp. 564–567. DOI: [10.1103/PhysRevLett.86.564](https://doi.org/10.1103/PhysRevLett.86.564).

[86] A. Esposito, R. Krichevsky, and A. Nicolis. “Vortex precession in trapped superfluids from effective field theory.” In: *Phys. Rev. A* 96.3 (2017), p. 033615. DOI: [10.1103/PhysRevA.96.033615](https://doi.org/10.1103/PhysRevA.96.033615). arXiv: [1704.08267 \[hep-th\]](https://arxiv.org/abs/1704.08267).

[87] A. M. J. Schakel. *Boulevard of Broken Symmetries: Effective Field Theories of Condensed Matter*. World Scientific, 2008. ISBN: 9789812813909.

[88] L. Onsager. In: *Nuovo Cimento* 6 (1949), p. 249.

[89] R. P. Feynman. *Progress in low temperature physics*. Vol. 1. North-Holland, Amsterdam, 1955.

[90] H. E. Hall and W. F. Vinen. “The Rotation of Liquid Helium II. I. Experiments on the Propagation of Second Sound in Uniformly Rotating Helium II.” In: *Proc. R. Soc. Lond. A* 238.1213 (1956), pp. 204–214.

[91] W. F. Vinen. “The Detection of Single Quanta of Circulation in Liquid Helium II.” In: *Proc. R. Soc. Lond. A* 260.1301 (1961), pp. 218–236.

[92] G. A. Williams and R. E. Packard. “Photographs of Quantized Vortex Lines in Rotating He II.” In: *Phys. Rev. Lett.* 33.5 (1974), pp. 280–283. DOI: [10.1103/PhysRevLett.33.280](https://doi.org/10.1103/PhysRevLett.33.280).

[93] E. J. Yarmchuk, M. J. V. Gordon, and R. E. Packard. “Observation of Stationary Vortex Arrays in Rotating Superfluid Helium.” In: *Phys. Rev. Lett.* 43.3 (1979), pp. 214–217. DOI: [10.1103/PhysRevLett.43.214](https://doi.org/10.1103/PhysRevLett.43.214).

[94] D. V. Freilich et al. “Real-Time Dynamics of Single Vortex Lines and Vortex Dipoles in a Bose-Einstein Condensate.” In: *Science* 329.5996 (2010), pp. 1182–1185.

[95] M. R. Matthews et al. “Vortices in a Bose-Einstein Condensate.” In: *Phys. Rev. Lett.* 83.13 (1999), pp. 2498–2501. DOI: 10.1103/PhysRevLett.83.2498.

[96] K. W. Madison et al. “Vortex Formation in a Stirred Bose-Einstein Condensate.” In: *Phys. Rev. Lett.* 84.5 (2000), pp. 806–809. DOI: 10.1103/PhysRevLett.84.806.

[97] B. P. Anderson et al. “Vortex Precession in Bose-Einstein Condensates: Observations with Filled and Empty Cores.” In: *Phys. Rev. Lett.* 85.14 (2000), pp. 2857–2860. DOI: 10.1103/PhysRevLett.85.2857.

[98] M. J. H. Ku et al. “Motion of a Solitonic Vortex in the BEC-BCS Crossover.” In: *Phys. Rev. Lett.* 113.6 (2014). DOI: 10.1103/PhysRevLett.113.065301.

[99] B. Horn, A. Nicolis, and R. Penco. “Effective string theory for vortex lines in fluids and superfluids.” In: *JHEP* 10 (2015), p. 153. DOI: 10.1007/JHEP10(2015)153. arXiv: 1507.05635 [hep-th].

[100] S. Garcia-Saenz, E. Mitsou, and A. Nicolis. “A multipole-expanded effective field theory for vortex ring-sound interactions.” In: *JHEP* 02 (2018), p. 022. DOI: 10.1007/JHEP02(2018)022. arXiv: 1709.01927 [hep-th].

[101] E. Cremmer and J. Scherk. “Spontaneous dynamical breaking of gauge symmetry in dual models.” In: *Nucl. Phys.* B72 (1974), pp. 117–124. DOI: 10.1016/0550-3213(74)90224-7.

[102] A. Zee. “Vortex strings and the antisymmetric gauge potential.” In: *Nucl. Phys.* B421 (1994), pp. 111–124. DOI: 10.1016/0550-3213(94)90226-7.

[103] S. Endlich and A. Nicolis. “The incompressible fluid revisited: vortex-sound interactions.” In: (2013). arXiv: 1303.3289 [hep-th].

[104] J. Polchinski. *String Theory: Volume 1, An Introduction to the Bosonic String*. Cambridge Monographs on Mathematical Physics. Cambridge University Press, 1998. ISBN: 9781139457408.

[105] S. F. Hassan and R. A. Rosen. “Bimetric Gravity from Ghost-free Massive Gravity.” In: *JHEP* 02 (2012), p. 126. DOI: 10.1007/JHEP02(2012)126. arXiv: 1109.3515 [hep-th].

[106] R. J. Donnelly. *Quantized Vortices in Helium II*. Cambridge Studies in American Literature and Culture v. 2. Cambridge University Press, 1991. ISBN: 9780521324007.

[107] S. Will. *Private communication*.

[108] A. L. Gaunt et al. “Bose-Einstein Condensation of Atoms in a Uniform Potential.” In: *Phys. Rev. Lett.* 110.20 (2013). DOI: 10.1103/PhysRevLett.110.200406.

[109] L. Chomaz et al. “Emergence of coherence via transverse condensation in a uniform quasi-two-dimensional Bose gas.” In: *Nature Communications* 6 (2015).

[110] B. Mukherjee et al. “Homogeneous Atomic Fermi Gases.” In: *Phys. Rev. Lett.* 118.12 (2017). DOI: 10.1103/PhysRevLett.118.123401.

[111] P. G. Kevrekidis et al. “Vortex precession dynamics in general radially symmetric potential traps in two-dimensional atomic Bose-Einstein condensates.” In: *Phys. Rev. A* 96 (2017). arXiv: 1706.07137 [cond-mat].

[112] A. J. Groszek et al. “Motion of vortices in inhomogeneous Bose-Einstein condensates.” In: *Phys. Rev. A* 97 (2018). arXiv: 1708.09202 [cond-mat].

[113] P. W. Anderson and N. Itoh. “Pulsar glitches and restlessness as a hard superfluidity phenomenon.” In: *Nature* 256 (1975).

[114] A. Esposito, S. Garcia-Saenz, and R. Penco. *To appear*.

[115] A. Nicolis and R. Penco. “Mutual Interactions of Phonons, Rotons, and Gravity.” In: (2017). arXiv: 1705.08914 [hep-th].

[116] A. Esposito, R. Krichevsky, and A. Nicolis. *To appear*.

[117] J. Alexander et al. “Dark Sectors 2016 Workshop: Community Report.” In: 2016. arXiv: 1608.08632 [hep-ph].

[118] K. Schutz and K. M. Zurek. “Detectability of Light Dark Matter with Superfluid Helium.” In: *Phys. Rev. Lett.* 117.12 (2016), p. 121302. DOI: 10.1103/PhysRevLett.117.121302. arXiv: 1604.08206 [hep-ph].

[119] S. Knapen, T. Lin, and K. M. Zurek. “Light Dark Matter in Superfluid Helium: Detection with Multi-excitation Production.” In: *Phys. Rev. D* 95.5 (2017), p. 056019. DOI: 10.1103/PhysRevD.95.056019. arXiv: 1611.06228 [hep-ph].

[120] A. Esposito, A. Nicolis, and A. D. Polosa. *To appear*.

- [121] J. de Boer, E. P. Verlinde, and H. L. Verlinde. “On the holographic renormalization group.” In: *JHEP* 08 (2000), p. 003. DOI: [10.1088/1126-6708/2000/08/003](https://doi.org/10.1088/1126-6708/2000/08/003). arXiv: [hep-th/9912012](https://arxiv.org/abs/hep-th/9912012) [hep-th].
- [122] I. Heemskerk and J. Polchinski. “Holographic and Wilsonian Renormalization Groups.” In: *JHEP* 06 (2011), p. 031. DOI: [10.1007/JHEP06\(2011\)031](https://doi.org/10.1007/JHEP06(2011)031). arXiv: [1010.1264](https://arxiv.org/abs/1010.1264) [hep-th].
- [123] T. Faulkner, H. Liu, and M. Rangamani. “Integrating out geometry: Holographic Wilsonian RG and the membrane paradigm.” In: *JHEP* 08 (2011), p. 051. DOI: [10.1007/JHEP08\(2011\)051](https://doi.org/10.1007/JHEP08(2011)051). arXiv: [1010.4036](https://arxiv.org/abs/1010.4036) [hep-th].
- [124] E. Inonu and E. P. Wigner. “On the contraction of groups and their representations.” In: *Proceedings of the National Academy of Sciences* 39 (1953).

Appendix A: From bulk equations to RG flow

In this appendix we will show how to derive the renormalization group (RG) flow for the operators of the boundary theory starting from the bulk of AdS [121–123]. In particular, it will become clear that the radial coordinate plays exactly the role of an energy scale of the dual theory.

Let us look at the bulk theory and introduce a radial cutoff at $r = \mathcal{R}$, close to the boundary. The bulk action will then be written as

$$S = \int_0^{\mathcal{R}} dr \int d^d x \sqrt{-g} \mathcal{L}[\phi, \partial_M \phi] + S_{\text{bdy}}[\phi, \mathcal{R}]. \quad (48)$$

As we explained in Section 2.2, S_{bdy} fixes the boundary conditions of our field at $r = \mathcal{R}$. Let us again consider a scalar field with lagrangian density

$$\mathcal{L} = -\frac{1}{2} \partial_M \phi \partial^M \phi - V(\phi). \quad (49)$$

By varying the action one finds the boundary conditions at $r = \mathcal{R}$, which are given by

$$\frac{\delta S_{\text{bdy}}}{\delta \phi} = \sqrt{-g} g^{rr} \phi' = -\Pi_r, \quad (50)$$

where we have noticed that the right hand side is nothing but (minus) the conjugate momentum for the flow along r .

Since the choice of UV cutoff is arbitrary, the on-shell action cannot depend on it. From this it follows that

$$\frac{dS}{d\mathcal{R}} = 0 = \int_{r=\mathcal{R}} d^d x \sqrt{-g} \mathcal{L}[\phi, \partial_M \phi] + \int_{r=\mathcal{R}} d^d x \frac{\delta S_{\text{bdy}}}{\delta \phi} \phi' + \partial_{\mathcal{R}} S_{\text{bdy}}[\phi, \mathcal{R}]. \quad (51)$$

This is an equation for how the boundary action changes with the UV cutoff. In

particular

$$\begin{aligned}\sqrt{g^{rr}} \partial_{\mathcal{R}} S_{\text{bdy}}[\phi, \mathcal{R}] &= \int_{r=\mathcal{R}} d^d x \left[-\Pi_r \phi' + \sqrt{-g} \mathcal{L} \right] \\ &= \int_{r=\mathcal{R}} d^d x \sqrt{-\gamma} \left[\frac{1}{2\gamma} \Pi_r^2 + \frac{1}{2} \partial_M \phi \partial^M \phi + V(\phi) \right].\end{aligned}\quad (52)$$

Here $\gamma = gg^{rr}$ is again the determinant of the induced metric at $r = \mathcal{R}$. This is the RG equation we were looking for. We have learned that, once the boundary conditions are fixed, the field ϕ at $r = \mathcal{R}$ can be written in terms of its dual operator \mathcal{O} . The boundary action can be expanded in powers of such operator, i.e.

$$S_{\text{bdy}} = \sum_n \int d^d x \sqrt{-\gamma} \lambda_n(x, \mathcal{R}) \mathcal{O}^n(x). \quad (53)$$

If we plug this expression in Eq. (52) one can compute the β -functions for the couplings λ_n .

Appendix B: Linear representations of the Euclidean group

Because of its shift part the Euclidean group, $ISO(d-1)$, is typically presented with its nonlinear realizations. Here we show how to build its linear representations, which can be useful when determining how to gauge such a group—see Section 4.2. To build these representations we will employ the so called Wigner-Inonu contraction [124].

Consider the algebra of $SO(d)$, and let us separate its generators into irreducible representations of the $SO(d-1)$ group that leave the d -direction invariant. There are those that transform as a vector, T^{id} , and those that transform as a tensor, T^{ij} . Their commutation relations read

$$[T^{ij}, T^{km}] = \delta^{ik}T^{jm} + \delta^{jm}T^{ik} - \delta^{im}T^{jk} - \delta^{jk}T^{im}, \quad (54a)$$

$$[T^{ij}, T^{kd}] = \delta^{ik}T^{jd} - \delta^{jk}T^{id}, \quad (54b)$$

$$[T^{id}, T^{jd}] = T^{ij}. \quad (54c)$$

It is easy to show that if we define some new generators such that $P^{ij} = T^{ij}$ and $P^i = \frac{1}{\zeta}T^{id}$, these satisfy the $ISO(d-1)$ algebra in the $\zeta \rightarrow \infty$ limit, with the P s playing the role of the generators of translations.

To build a proper representation we now need to look at the states. Consider an $SO(d)$ multiplet in the fundamental representation, $\tilde{\psi}$. Under an infinitesimal transformation generated by the P s, the multiplet transforms as

$$\delta\psi^i = \frac{1}{2}\theta^{ij}\psi_j + \frac{1}{\zeta}\theta^{id}\psi_d, \quad \text{and} \quad \delta\psi_d = \frac{1}{\zeta}\theta^{id}\psi_i. \quad (55)$$

Now rescale the components of the multiplet as well. In particular, we choose $\psi_i = \tilde{\psi}_i$ and $\psi_d = \zeta\tilde{\psi}_d$, such that the “tilde” fields stay finite in the $\zeta \rightarrow \infty$ limit. After the contraction we have that

$$\delta\tilde{\psi}^i = \frac{1}{2}\theta^{ij}\tilde{\psi}_j + \theta^{id}\tilde{\psi}_d, \quad \text{and} \quad \delta\tilde{\psi}_d = 0. \quad (56)$$

The above transformations are clearly linear and one can easily show that the corresponding generators satisfy the algebra of $ISO(d-1)$. Interestingly, from this

viewpoint, the fact that translations are usually nonlinearly realized can be seen as a consequence of the spontaneous breaking of $SO(d)$ due to the large vev acquired by ψ_d .

Now imagine to set $\psi_d = \zeta h(x)$ such that $\langle h(x) \rangle = 1$. From Eq. (56) we understand that the $\psi_i = \phi_i$ transform exactly as our comoving coordinates in Eq. (1.36), so that $\langle \phi^i(x) \rangle = \alpha x^i$ realizes the symmetry breaking pattern of a solid. The full $\vec{\psi}$ multiplet can then be parametrized as

$$\vec{\psi}(x) = \mathcal{O}(x) \vec{\Phi} = (\phi_1(x), \dots, \phi_{d-1}(x), \zeta h(x))^T, \quad (57)$$

with

$$\vec{\Phi} = \zeta h(x) \hat{x}_d, \quad \mathcal{O}(x) = \exp\left(-\frac{\phi_i(x)}{h(x)} P^i\right). \quad (58)$$

Note that Eq. (57) is true in the $\zeta \rightarrow \infty$ limit. It is the flat space analogue of Eq. (4.7). The solid lagrangian could now be written in terms of the invariants build out of the matrix $B^{ij} = \partial_\mu \phi^i \partial^\mu \phi^j$. However, we can also write

$$\partial_\mu \vec{\psi} = \mathcal{O} \partial_\mu \Phi + \partial_\mu \mathcal{O} \Phi = \mathcal{O} (\partial_\mu \Phi + \mathcal{O}^{-1} \partial_\mu \mathcal{O} \Phi) \equiv \mathcal{O} D_\mu \Phi. \quad (59)$$

It follows that the same theory can also be written in terms of the invariants built out of $\tilde{B}^{ij} = (D_\mu \Phi)^i (D^\mu \Phi)^j$. On the background the covariant derivative reduces to

$$\langle D_\mu \vec{\Phi} \rangle = \langle \mathcal{O}^{-1} \partial_\mu \mathcal{O} \vec{\Phi} \rangle = \alpha \delta_\mu^i P^i \vec{\Phi} = \alpha \delta_\mu^i T^{id} \hat{x}_d. \quad (60)$$

Which means that the theory for our solid can also be expressed in terms of a single scalar field with a vacuum expectation value $\langle \vec{\Phi} \rangle \propto \hat{x}_d$, and a constant gauge field $A_i^{AB} = \alpha T_{id}^{AB}$. This is indeed the ansatz found in Eq. (4.23) in the Poincaré patch limit.

Appendix C: How to go from the scalar to the 2-form and back

In Chapter 1 we presented the simplest realization of the type-I superfluid symmetry breaking pattern, i.e. the one involving a single real scalar ϕ . On the other hand, in Chapter 5 we argued that, in order to couple the superfluid modes to vortex lines, a dual 2-form description is more convenient. Let us show how one can go from one to the other.

The two descriptions are related to each other by a Legendre transform. Consider in fact the following action involving the 2-form, $\mathcal{A}_{\mu\nu}$, and a 1-form, H_μ [100]:

$$S[H, \mathcal{A}] = \int d^4x [P(X) - F^\mu H_\mu], \quad X = -H_\mu H^\mu, \quad F^\mu = \frac{1}{2}\epsilon^{\mu\nu\rho\sigma}\partial_\nu\mathcal{A}_{\rho\sigma}. \quad (61)$$

The 2-form only appears linearly and can thus be considered as a Lagrange multiplier. Varying with respect to it leads to the equation $\partial_\nu H_\mu - \partial_\mu H_\nu = 0$, which is solved by $H_\mu = -\partial_\mu\phi$, for any scalar field ϕ . The action for ϕ then reduces to

$$\begin{aligned} S[\phi] &= \int d^4x \left[P(X) - \frac{1}{2}\epsilon^{\mu\nu\rho\sigma}\partial_\nu\mathcal{A}_{\rho\sigma}\partial_\mu\phi \right] \\ &= \int d^4x P(X) - \frac{1}{2}\epsilon^{\mu\nu\rho\sigma} \oint d\Sigma_\mu \partial_\nu\mathcal{A}_{\rho\sigma}\phi. \end{aligned} \quad (62)$$

This is exactly the action (1.27), up to a boundary term that does not affect the bulk dynamics.

Let us now instead vary the action (61) with respect to H_μ . The corresponding equations of motion are $2P_X(X)H^\mu = -F^\mu$. From its square we get

$$2\sqrt{X}P_X(X) = \sqrt{-F^\mu F_\mu} \equiv \sqrt{Y}, \quad (63)$$

which we know is the superfluid number density—see Section 5.2. After integrating out the 1-form, we obtain

$$S[\mathcal{A}] = \int d^4x [P(X) - 2XP(X)] = - \int d^4x \rho(Y) \equiv \int d^4x G(Y), \quad (64)$$

which is instead the action in Eq. (5.5), with G equals minus the energy density.

Appendix D: Relativistic corrections to the vortex action

In Chapter 5 we found more convenient to take the nonrelativistic limit right from the beginning of our calculation. Nevertheless, one of the advantages of the EFT formulation of the problem is that it allows for a fully relativistic analysis. Although the experiments performed in lab always have sound speeds much smaller than the speed of light, there might be instances (e.g. in the interior of neutron stars) where relativistic corrections are relevant.

With respect to the analysis of Section 5.4, there are three relativistic corrections: the correction to the second line of Eq. (5.19a), the last term in Eq. (5.19c), and the ρ_{ij} term in Eq. (5.23). To include the first one we simply keep all corrections in Eq. (5.34). The second correction can instead be neglected all together. It is in fact proportional to a time derivative and will provide a negligible correction to the string kinetic term (see again discussion in Section 5.4). The only new term in the action then comes from the relativistic corrections to the trapping action, i.e. [86]

$$S \supset \int d^3x dt \frac{\bar{n}}{2c^2} U_{ij}(\vec{x}_\perp) (\vec{\nabla} \times \vec{A})^i (\vec{\nabla} \times \vec{A})^j , \quad (65)$$

where $U_{ij}(\vec{x}_\perp) \equiv V(\vec{x}_\perp)\delta_{ij} - V_{ij}(\vec{x}_\perp)$, and $\rho_{ij} = \frac{\bar{n}}{c^2} V_{ij}$. This term provides an interaction between the external trap and the vortex line, mediated by the hydrophoton—see Figure 1. The new contribution to the vortex effective action is easily found to be

$$\begin{aligned} S_{\text{eff}}[\vec{X}] &\supset -\frac{\bar{n}^3 \lambda^2 c^2}{2\bar{w}^2} \int d^3x dt \epsilon^{ab} \epsilon^{cd} U_{ac}(\vec{x}_\perp + \vec{X}) \int \frac{d^2 p_\perp d^2 q_\perp}{(2\pi)^4} e^{-i(\vec{p}_\perp + \vec{q}_\perp) \cdot \vec{x}_\perp} \frac{p_\perp^b q_\perp^d}{p_\perp^2 q_\perp^2} \\ &= \frac{\bar{n}^3 \lambda^2 c^2}{8\pi^2 \bar{w}^2} \int dt d\sigma \int d^2 x_\perp \epsilon^{ab} \epsilon^{cd} U_{ac}(\vec{x}_\perp + \vec{X}) \frac{x_\perp^b x_\perp^d}{x_\perp^4} . \end{aligned} \quad (66)$$

We can now consider Eq. (5.35) and replace $m \rightarrow \bar{w}/\bar{n}c^2$. Putting the two terms

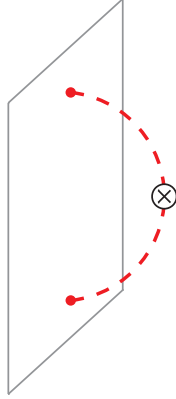


Figure 1: Leading relativistic vortex/trap interaction.

together we obtain the fully relativistic vortex action [86]:

$$\begin{aligned}
 S_{\text{eff}}[\vec{X}] = & \int dt d\sigma \left[\frac{\bar{n}\lambda}{3} \epsilon_{ab} X^a \dot{X}^b + \frac{2T_{(01)}\bar{n}c^2}{\bar{w}c_s^2} V(\vec{X}) + \frac{\bar{n}^3 \lambda^2 c^4}{8\pi^2 \bar{w}^2 c_s^2} \int d^2 x_\perp \frac{V(\vec{x}_\perp + \vec{X})}{x_\perp^2} \right. \\
 & \left. - \frac{\bar{n}^3 \lambda^2 c^2}{8\pi^2 \bar{w}^2} \int d^2 x_\perp \epsilon^{ab} \epsilon^{cd} V_{ac}(\vec{x}_\perp + \vec{X}) \frac{x_\perp^b x_\perp^d}{x_\perp^4} \right]. \tag{67}
 \end{aligned}$$

Again, the motion of the vortex line is now a simple point particle problem.